Available online at www.sciencedirect.com
SCIENCE DIRECT®
Coordination Chemistry Reviews 242 (2003) 159–201
COORDINATION CHEMISTRY REVIEWS
www.elsevier.com/locate/ccr

Chiral thioether ligands: coordination chemistry and asymmetric catalysis

Anna M. Masdeu-Bultó [a,*], Montserrat Diéguez [a], Erika Martin [b,*], Montserrat Gómez [c]

[a] *Departament de Química Física i Inorgànica, Universitat Rovira i Virgili, Plaça Imperial Tàrraco, 1, E-43005 Tarragona, Spain*
[b] *Departamento de Química Inorgánica, Facultad de Química, Universidad Nacional Autónoma de Mexico, Cd. Universitaria, 04510 Mexico DF, Mexico*
[c] *Departament de Química Inorgànica, Universitat de Barcelona, Martí i Franquès, 1-11, E-08028 Barcelona, Spain*

Contents

* Corresponding authors. Tel.: +34-977-55-9572; fax: +34-977-55-9563 (A.M.M.B.). Tel.: +52-5-622-3720; fax: +52-5-622-3531 (E.M.).
E-mail addresses: masdeu@quimica.urv.es (A.M. Masdeu-Bultó), erikam@servidor.unam.mx (E. Martin).

0010-8545/03/$ - see front matter
doi:10.1016/S0010-8545(03)00106-1

Abstract

This review covers the recent applications of chiral thioether ligands in asymmetric catalysis with transition metal complexes. S,S-Homo and S,X-heterodonor ligands are considered with special emphasis to their coordination chemistry. The results obtained with metal/thioether containing catalytic systems in asymmetric allylic substitution, hydrogenation, transfer hydrogenation, hydrosilylation, Michael addition, 1,4-conjugate addition and copolymerization reactions are reviewed including mechanistic considerations.

Keywords: Chiral thioether; Asymmetric catalysis; Transition metal complexes; Homogeneous catalysis

1. Introduction

Transition metal complexes with thioether donor ligands have been prepared since the beginning of the development of coordination chemistry [1,2]. Neutral thioethers coordinate to the metals through one (terminal) or both (bridging) of the lone pairs this latter being less common (Scheme 1a and b). They usually form strong bonds with *soft* metals and more rarely with *hard* ones. They are considered both poor σ-donor and poor π-acceptor ligands, the latter involving the σ* orbitals of the S–X bonds [3]. This π-acceptor character can contribute to the M–S bond strength. In addition, their *trans* influence is considered to be lower than that of phosphines and higher than that of primary amines [1,4,5].

Upon coordination to the metal, disymmetric substituted thioethers generate a new stereocentre on the sulphur atom, but the configuration at sulphur can be reversed easily by pyramidal inversion due to the low barrier (10–15 kcal mol^{-1}) associated with this intramolecular process (Scheme 1c). Moreover, when the thioether forms part of a chelating ligand, conformational changes in the ring may also take place [6,7]. The formation of sulphur stereocentres generates diastereomeric species if other stereogenic units are present in the molecule.

Sulphur donor ligands have been used much less than phosphorus donor ligands in homogeneous catalysis [8–10] although in recent decades, the number of studies with sulphur containing catalytic systems has increased notably [11,12]. As stated above, compared to phosphorus, sulphur has less both donor and acceptor character. In addition to these electronic considerations, the sulphur atom in thioether ligands has only two substituents, which can create a less hindered environment than trivalent phosphorus. The formation of mixtures of diastereomeric thioether complexes and the difficulty to control their interconversion in solution have also been regarded as a problem for asymmetric induction in catalytic reactions. Nevertheless, in recent years, bidentate S-donor ligands have proven to be as useful as other classical asymmetric ligands, specially when combined with other donor atoms [13–18]. For this reason, we decided to focus on the examples reported for the metal-catalyzed asymmetric reactions using thioether ligands. The specific structural complexity inherent to the thioether coordination means that special attention must be paid to structural information and the reactivity of the metal–thioether complexes.

This review covers the literature reports on transition metal complexes with chiral thioether ligands from 1995 through June 2002. In the first part, transition metal complexes with chiral thioether ligands are described regardless of whether they have been applied as catalysts. The second part compiles the catalytic systems containing chiral thioether ligands that have been applied in asymmetric homogeneous catalysis. Mechanistic aspects are also discussed when reported. Only chiral non-racemic ligands have been considered. The thioether ligands (**1**–**80**) mentioned in this review are shown in Figs. 1–7.

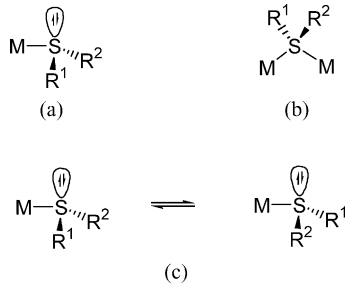

Scheme 1. Coordination of thioethers (a) terminal and (b) bridge; (c) pyramidal inversion in thioether ligands.

2. Complexes with chiral thioether ligands

Chiral thioether ligands have been obtained with a stereogenic backbone, or with stereogenic units on sulphur substituents and/or heteroatom substituents in heterodonor ligands (S,X-) (X = N, P, Se...). Examples of all these cases are described in this review.

2.1. S,S-Dithioethers

2.1.1. Ligand design

Most of the homodonor chiral S,S-dithioether ligands reported in the literature were prepared for use in asymmetric homogeneous catalysis (Fig. 1). For this reason they are usually sulphur analogous to chiral diphosphines such as 4,5-bis(diphenylphosphinomethyl)-2,2-dimethyl-1,3-dioxolane (DIOP) [19], 2,2′-bis(diphenylphosphino)-1,1′-binaphthyl [20–23], 2,4-bis(diphenylphosphino)pentane [24], 1,2-*O*-isopropylidene-3,5-bis-diphenylphosphane-α-D-xylofuranose (XY-

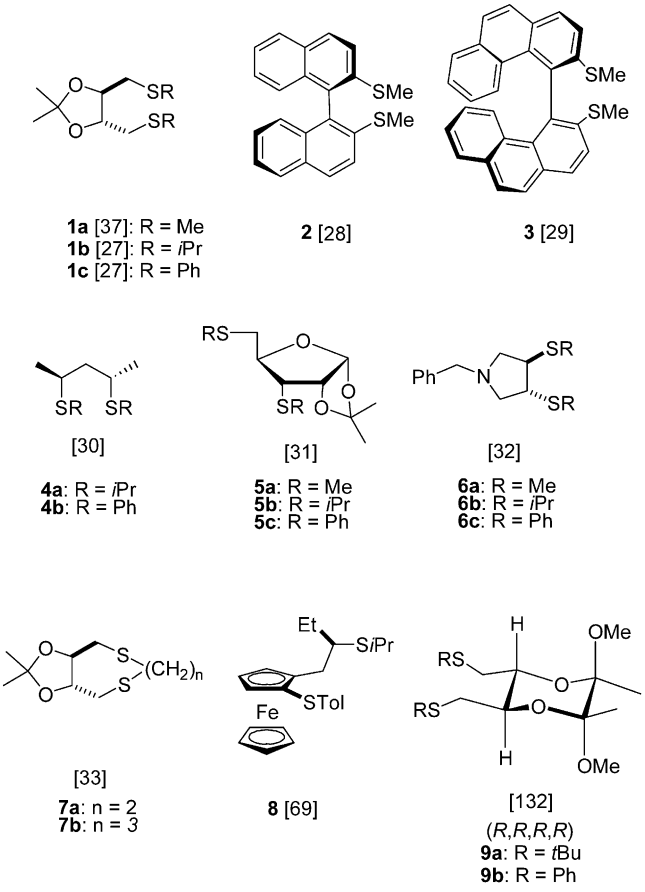

Fig. 1. Dithioether ligands **1**–**9**.

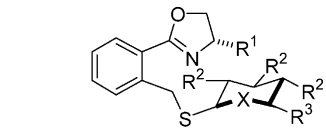

[13]

10a, X = O, R^1 = *i*Pr, R^2 = OC(O)Me, R^3 = $CH_2OC(O)Me$
10b, X = O, R^1 = *i*Pr, R^2 = OC(O)*t*Bu, R^3 = $CH_2OC(O)tBu$
10c, X = O, R^1 = Ph, R^2 = OC(O)Me, R^3 = $CH_2OC(O)Me$
10d, X = O, R^1 = Ph, R^2 = OC(O)*t*Bu, R^3 = $CH_2OC(O)tBu$
10e, X = CH_2, R^1 = *i*Pr, R^2 = R^3 = H

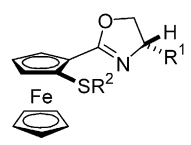

[14]

11a, R^1 = *i*Pr, R^2 = Ph
11b, R^1 = *t*Bu, R^2 = Ph
11c, R^1 = *i*Pr, R^2 = Me
11d, R^1 = *i*Pr, R^2 = Tol
11e, R^1 = Bn, R^2 = Ph

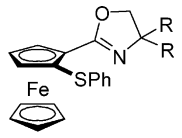

[14]

11f, R = H
11g, R = Me
11h, R = Bn

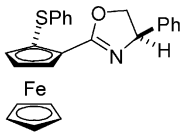

12 [14]

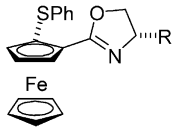

[14]

13a, R = *i*Pr
13b, R = *t*Bu

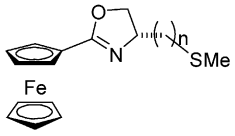

[113]

14a, n = 1
14b, n = 2

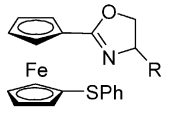

[115]

15a, R = *i*Pr
15b, R = *t*Bu
15c, R = Ph

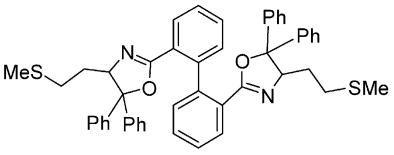

(*S,S*)-**16** [59]

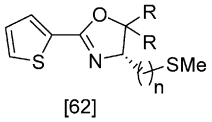

[62]

17a, n = 1, R = H
17b, n = 1, R = Ph
17c, n = 2, R = H
17d, n = 2, R = Ph

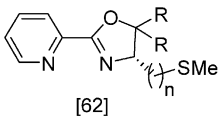

[62]

17e, n = 1, R = H
17f, n = 1, R = Ph
17g, n = 2, R = H
17h, n = 2, R = Ph

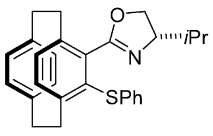

18 [100]

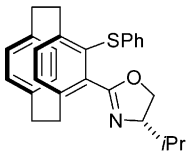

19 [100]

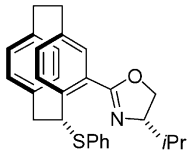

20 [100]

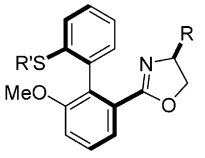

(*S,aS*)-**21** [116]

21a, R = *i*Pr, R' = Me
21b, R = *t*Bu, R' = Me
21c, R = R' = *i*Pr
21d, R = *t*Bu, R' = *i*Pr

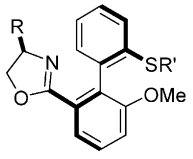

(*S,aR*)-**22** [116]

22a, R = *i*Pr, R' = Me
22b, R = *t*Bu, R' = Me
22c, R = R' = *i*Pr
22d, R = *t*Bu, R' = *i*Pr

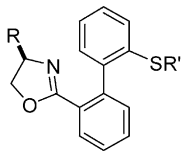

[116]

23a, R = *i*Pr, R' = Me
23b, R = *t*Bu, R' = Me
23c, R = R' = *i*Pr

Fig. 2. Thioether-oxazoline ligands **10**–**23**.

LOPHOS) [25] and 3,4-bis(diphenylphosphino)pyrrolidine (DEGUPHOS) [26] which have proven to be highly efficient in asymmetric catalysis.

Studying such a wide range of dithioether ligands allows us to span different structural possibilities involving the ligand backbone, the size of the metal chelate ring, the nature of substituent groups and symmetry, which can be decisive factors in the efficiency and stereoselectivity of the catalytic reactions. Symmetry has been shown to play an important role. A mixture of diastereomers may be a disadvantage for the selectivity of the catalytic process. Consequently, a C_2 symmetry may be more favourable than C_1 since it restricts the number of possible catalytic intermediate species when

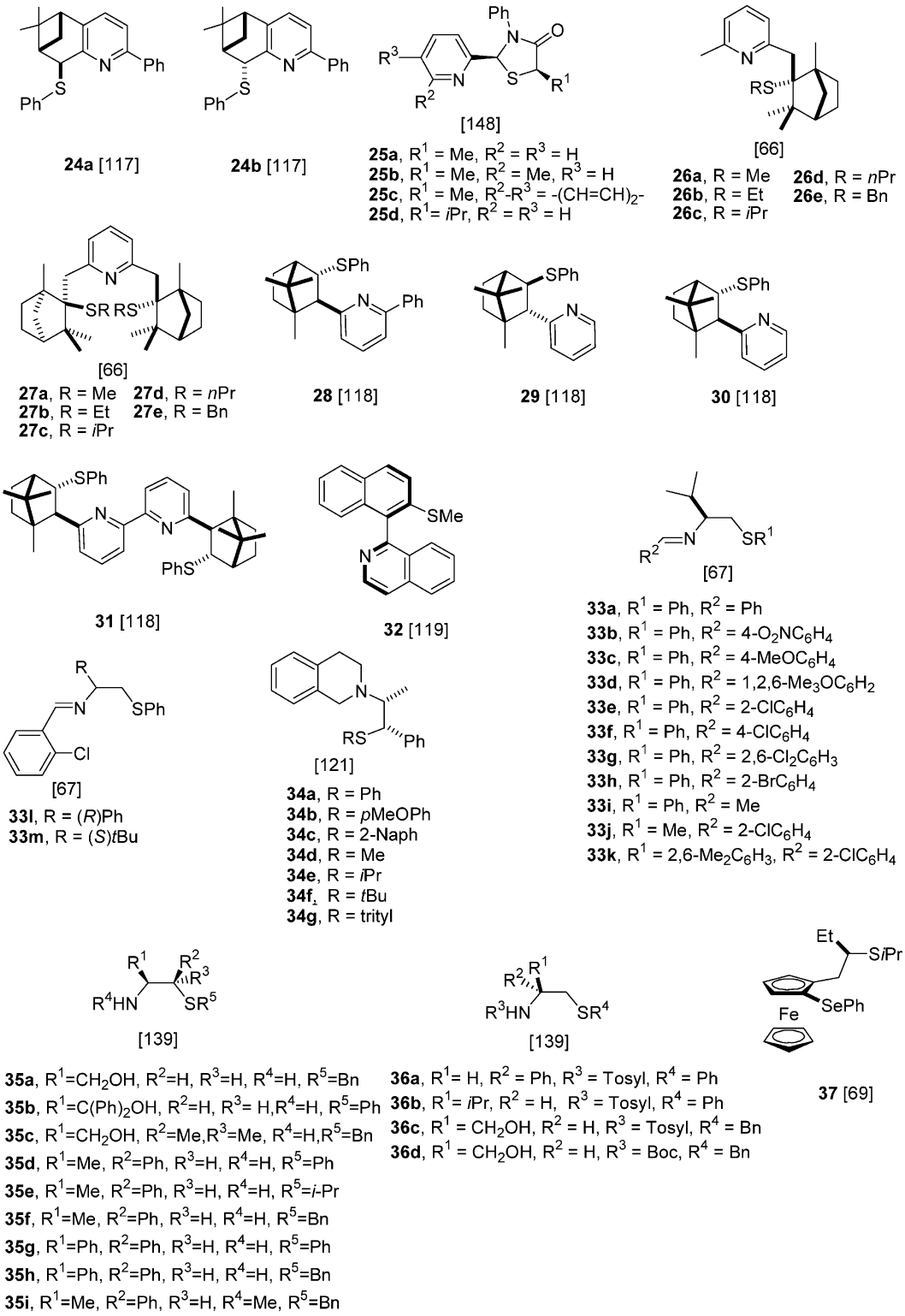

Fig. 3. Thioether-pyridine (**24**–**31**), -quinoline (**32**), -imine (**33**), -amine (**34**–**35**), -sulphonamide (**36a**–**c**), -urethane (**36d**) and -selenoether (**37**) ligands.

the ligand is coordinated to the metal. However, as discussed below, C_1 donor ligands can be advantageous in certain cases.

Initially, ligands with C_2 symmetry **1** [27], **2** [28], **3** [29] and **4** [30] that form seven- (**1**–**3**) and six-membered (**4**) chelate rings upon coordination to the metal were

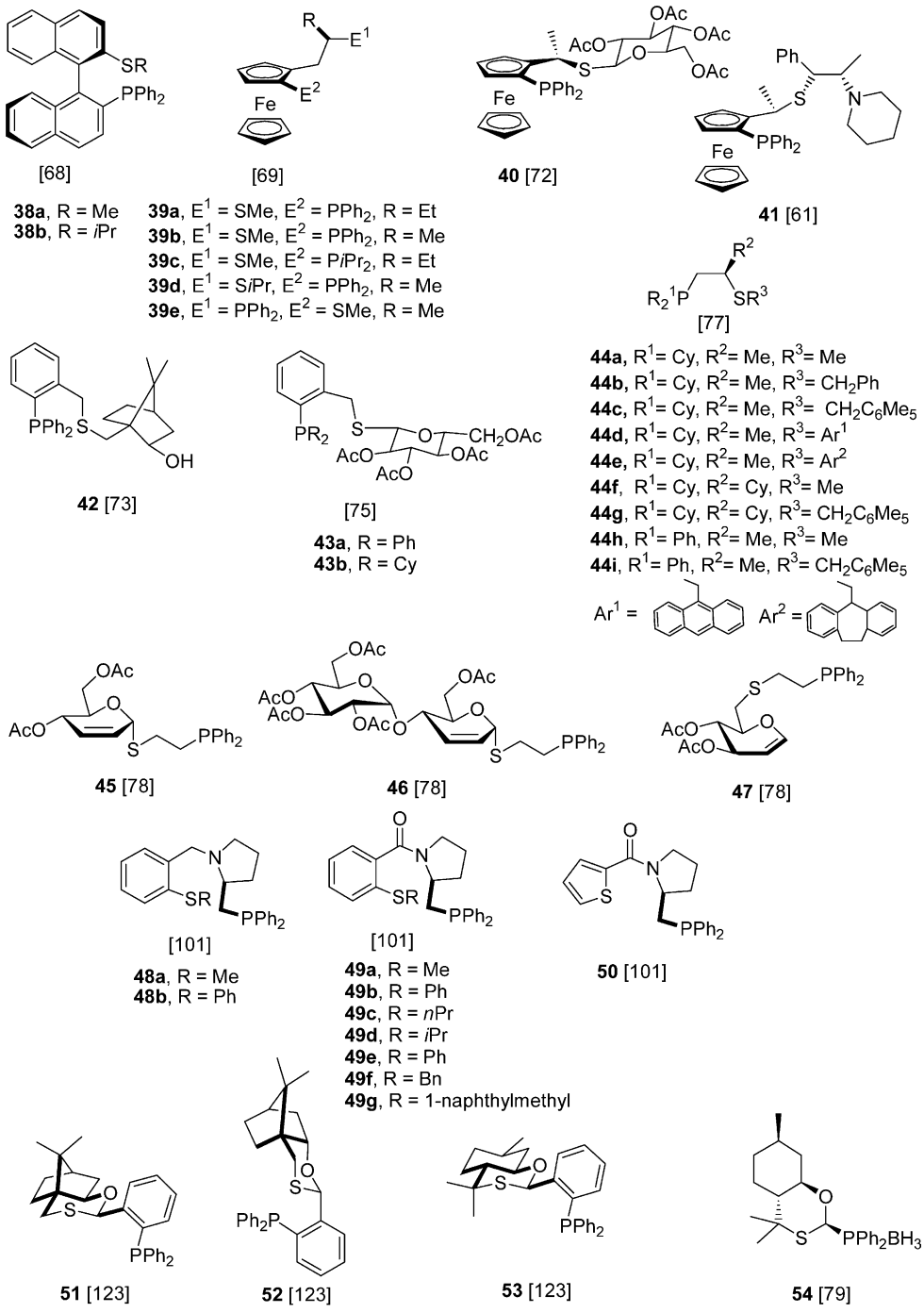

Fig. 4. Thioether-phosphine ligands **38**–**54**.

prepared. To decrease the flexibility of the metal chelate, the synthesis of two families of more rigid dithioether ligands with C_1 symmetry was described: ligands **5** [31], which form six-membered rings and ligands **6** [32], which form five-membered rings. Moreover, **6a**–**c** have the added advantage of a rigid backbone combined with the two stereocentres closer to the metal. Further attempts have been made to improve the ligand design by modulating the ligand rigidity and fixing the absolute sulphur configuration by constructing cyclic dithioethers **7** [33]. This should avoid sulphur inversion upon metal coordination, which is considered to erode the enantioselectivity in asymmetric catalytic processes.

Below we present the synthesis of complexes containing **1**–**7**, their characterization and their reactivity with hydrogen. The standard reactions for the synthesis of these complexes are summarized in the first part. In the following sections we describe the characterization and main structural features of the complexes in terms of the size of the chelate rings. This roughly agrees with the

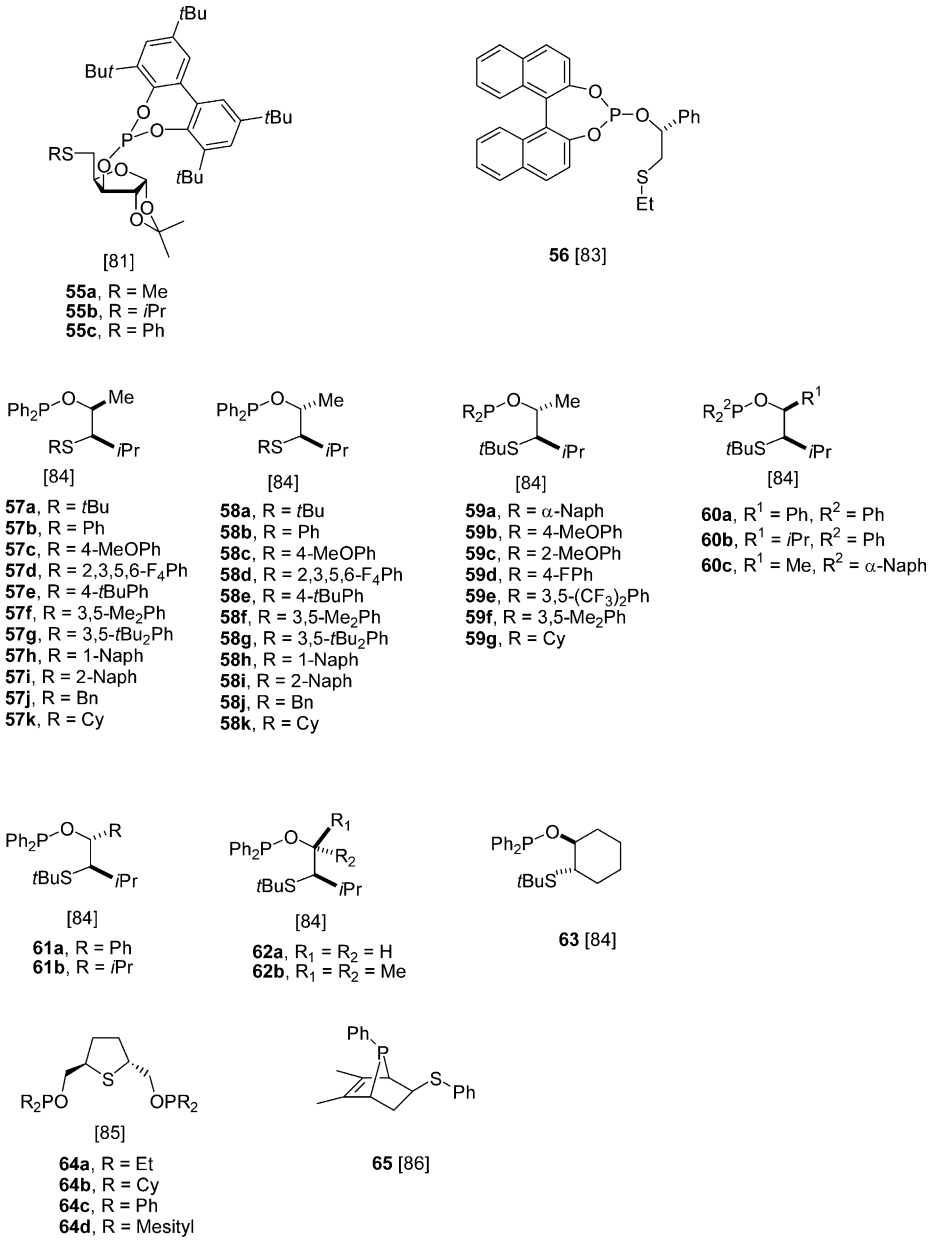

Fig. 5. Thioether-phosphite (**55**–**56**), -phosphinite (**57**–**64**) and -phosphacycle (**65**) ligands.

chronology in which they were presented in the literature.

2.1.2. Synthesis of complexes with dithioethers

In the literature there are descriptions of complexes of Rh, Ir, Pd and Pt with chiral dithioether ligands. The general synthetic procedures are summarized in Scheme 2.

2.1.2.1. Rh and Ir complexes. Cationic complexes [M(COD)(dithioether)]X (M = Rh, Ir; X = ClO_4, BF_4, PF_6; COD = 1,5-cyclooctadiene) have been prepared by reaction of the dithioether with $[M(COD)_2]X$ in dichloromethane, in which one COD is displaced (Scheme 2a) [27,29,31]. The cationic rhodium and iridium complexes are usually obtained in good yield by precipitation with diethyl ether. With less reactive dithioethers, the displacement of the COD ligand can be favoured by hydrogenation with dihydrogen bubbling [27].

2.1.2.2. Iridium dihydrido complexes. The general route to $[IrH_2(COD)(dithioether)]BF_4$ is the oxidative addition of dihydrogen to $[Ir(COD)(dithioether)]BF_4$ complexes in dichloromethane at low temperature (Scheme 2b) [27,31,32].

2.1.2.3. Palladium and platinum complexes. Palladium(II) and platinum(II) complexes $[MCl_2(dithioether)]$

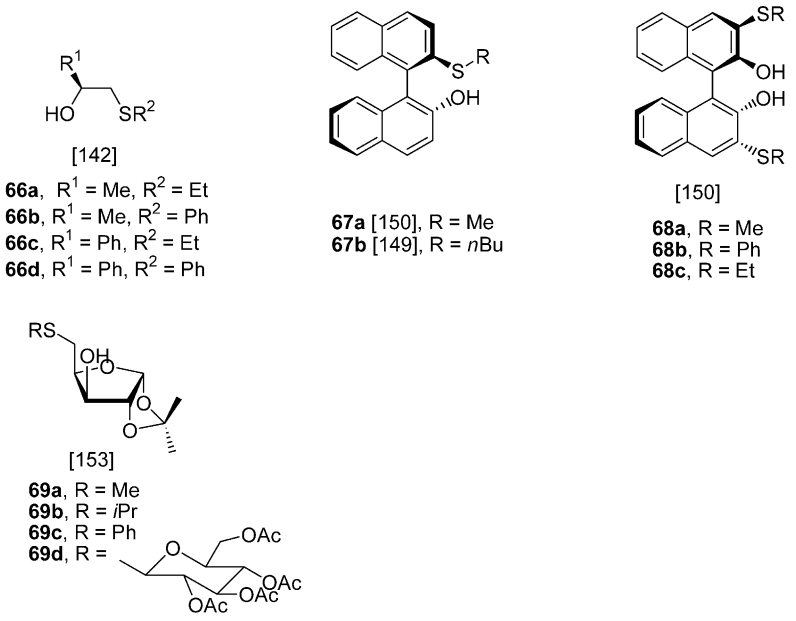

Fig. 6. Thioether-hydroxo ligands (**66**–**69**).

(M = Pd, Pt) are obtained by substitution of benzonitrile by the dithioether in $[MCl_2(PhCN_2)]$ (M = Pd, Pt) in dichloromethane as solvent (Scheme 2c) [34,35].

Diolefinic complexes $[Pt(COD)(dithioether)](BF_4)_2$ can be obtained by substituting the chloro ligands in $[PtCl_2(COD)]$ with the dithioether in the presence of $AgBF_4$ (Scheme 2d) [34].

Palladium allylic complexes $[Pd(\eta^3\text{-allyl})(dithioether)]PF_6$ (allyl = 1,3-PhC_3H_3Ph, *cyclo*-C_6H_9) are prepared by reaction of the dithioether with $[Pd(\eta^3\text{-allyl})Cl]_2$ in dichloromethane in the presence of NH_4PF_6 (Scheme 2e) [36].

2.1.3. Complexes with C_2 symmetrical ligands *1a–c*

James and McMillan [37] were the first to prepare **1a**, by taking the DIOP ligand as a model. Recently, the syntheses of **1b** and **1c** derivatives were also reported [27]. These ligands form seven-membered chelate rings when they coordinate in a bidentate way to metal centres such as iridium, rhodium, palladium and platinum. The complexes prepared are summarized in Fig. 8.

2.1.3.1. Iridium and rhodium complexes. Cationic complexes $[Ir(COD)(\mathbf{1a}–\mathbf{b})]BF_4$ (**81a**–**b**, Fig. 8) [27] and $[Rh(COD)(\mathbf{1a}–\mathbf{b})]BF_4$ (**82a**–**b**, Fig. 8) [38] were prepared according to Scheme 2a. Under the same conditions, the ligand **1c** did not react, which was attributed to the low donor ability of the sulphur atom bonded to the phenyl group. The complex **81c** was obtained by bubbling H_2 through the reaction mixture [27]. Attempts to prepare the corresponding rhodium complex in the same way were unsuccessful.

As mentioned previously, the coordination of the dithioether ligand to the metal generates a stereogenic centre in each sulphur atom. Therefore, the reaction could result in a mixture of stereomers with different spatial arrangements of the sulphur substituents and different conformations of the seven-membered chelate ring. Since ligands **1** have *R*,*R* absolute configuration of backbone carbon atoms [39], three possible diastereomers can be formed: $R_CR_CR_SR_S$ and $R_CR_CS_SS_S$ (both attributed to the *anti* isomers), and $R_CR_CR_SS_S$ or $R_CR_CS_SR_S$ (corresponding to *syn* isomers) (Fig. 9) [40]. However, for the five complexes prepared, variable temperature NMR (VT-NMR) measurements indicated that only one diastereomer was present in solution, which is one of the two possible *anti* isomers with an overall C_2 symmetry [27,38]. X-ray crystallography studies of **82b**, complex $[Rh(COD)(S,S\text{-}\mathbf{1b})]ClO_4$, confirmed an pseudo-equatorial location of the isopropyl groups in the *anti* $S_CS_CR_SR_S$ configuration (Fig. 10) [38].

2.1.3.2. Reactivity with H_2. The *cis*-dihydridoiridium(III) complexes $[IrH_2(COD)(\mathbf{1a}–\mathbf{c})]BF_4$ (**83a**–**c**, Fig. 8) were prepared in CD_2Cl_2 as indicated in Scheme 2b and were characterized in solution by NMR spectroscopy [27]. In these species both the metal and the sulphur atoms are stereogenic centres, increasing the number of possible diastereomers in solution. NMR characterization indicated only one diastereomer for complex **83a**, a mixture of two isomers in a 2:1 ratio for complex **83b** and several diastereomers for complex **83c**. At 25 °C, hydrogen was cleaved off and the parent complexes **81a**–**c** were recovered.

2.1.3.3. Palladium and platinum complexes. The palladium complexes $[PdCl_2(\mathbf{1a}–\mathbf{b})]$ (**84a**–**b**, Fig. 8), and

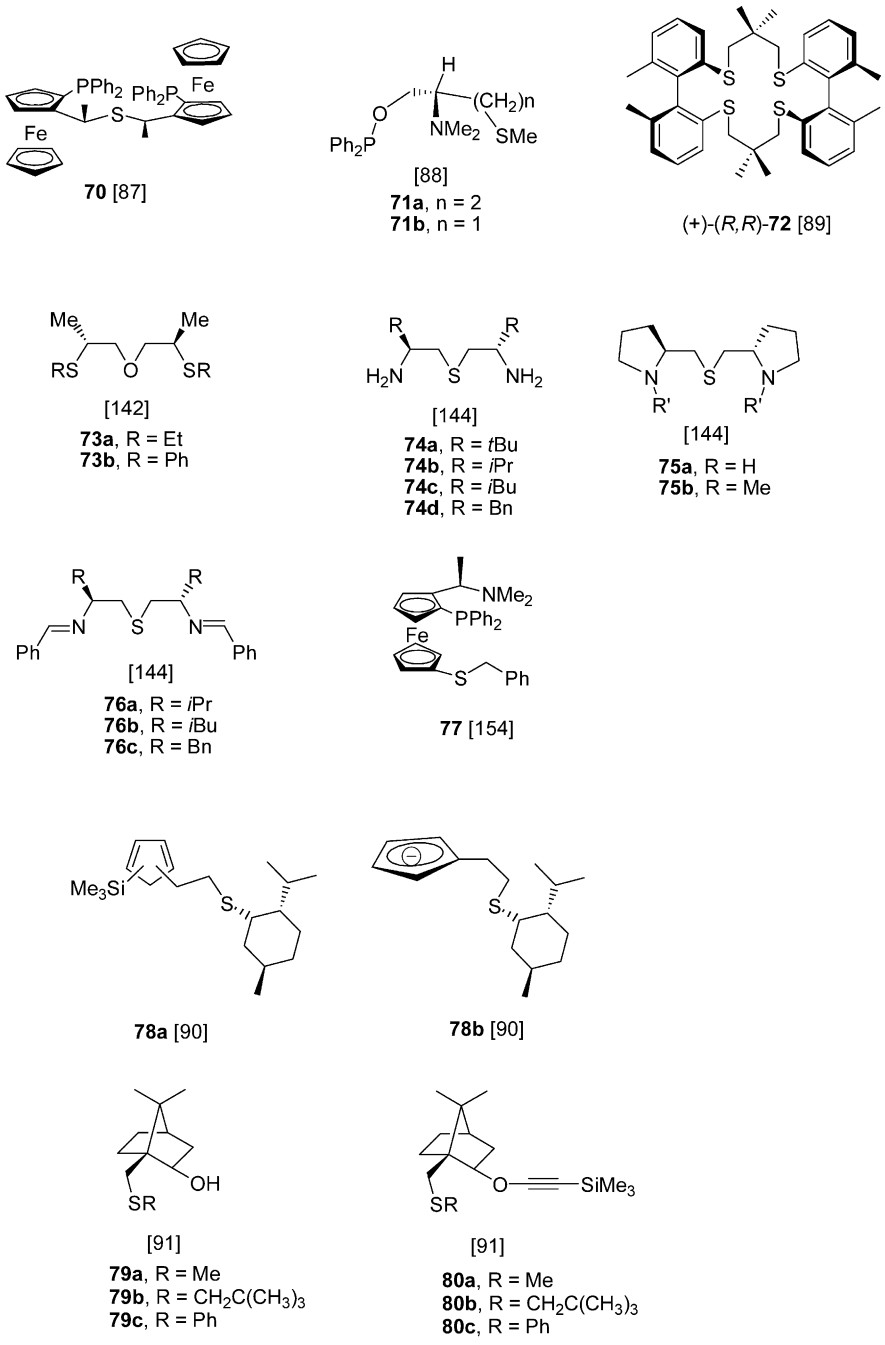

Fig. 7. Polydentate (**70**–**77**) and thioether π-donor (**78b**, **80a**–**c**) ligands.

[Pt(COD)(**1a**–**b**)]$(BF_4)_2$ (**85a**–**b**, Fig. 8) were prepared according to Scheme 2c and d, respectively [34]. However, no reaction with $[PtCl_2(PhCN)_2]$ was observed. Like iridium and rhodium, **1c** did not react with the palladium and platinum starting materials.

In contrast to the iridium and rhodium complexes, the NMR studies for the palladium and platinum complexes showed that the hindrance of the ligand influences the number of diastereomers in solution and their structure. VT-NMR and NOE experiments of **84b** and **85b**, which contain the most hindered ligand **1b**, showed only one diastereomer in solution with pseudo-equatorial disposition of the isopropyl groups in the *anti*-$R_CR_CR_SR_S$ configuration [41] and an overall C_2 symmetry (Fig. 11). For **84a**, two diastereomers were observed in solution at room temperature (r.t.) in a 3:2 ratio. For the major isomer, NMR studies in combination with models were consistent with a C_2 symmetry complex and a pseudo-equatorial location of the methyl groups in the *anti*-$R_CR_CR_SR_S$ configuration. The minor isomer was assigned to a C_1 symmetry species with a pseudo-axial and pseudo-equatorial arrangement of the methyl substitu-

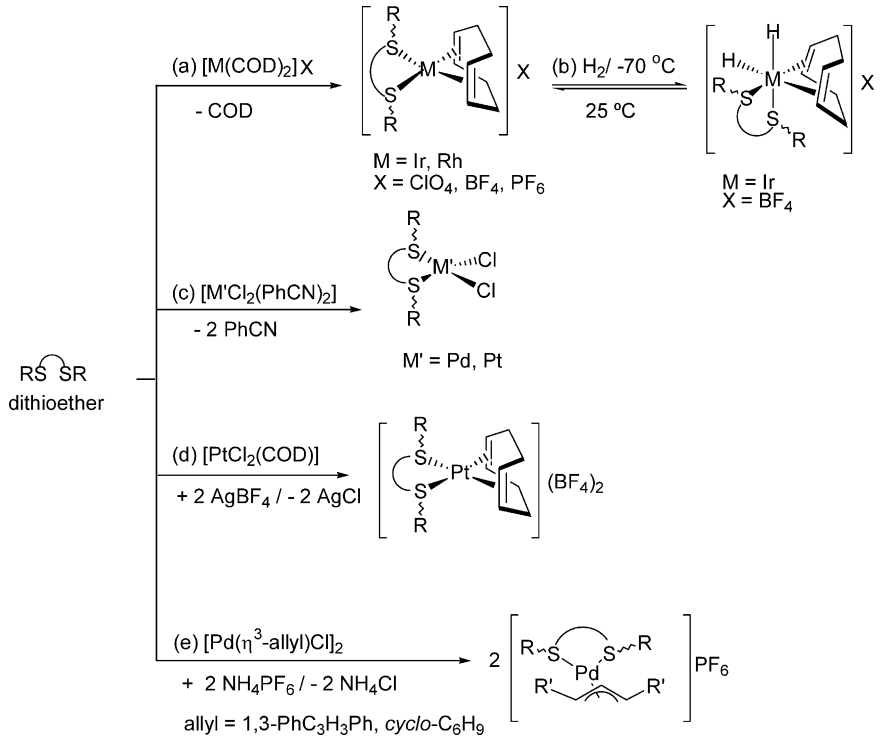

Scheme 2. General synthesis of complexes with chiral dithioether ligands.

ents. VT-NMR experiments indicated that no interconversion between the two diastereomers takes place at r.t. The VT-NMR studies of **85a** showed that it is extremely fluxional and its diastereomers did not show any isolated NMR resonance even at −90 °C.

2.1.4. Complexes with C_2 symmetrical ligands **2** and **3**

2.1.4.1. Rhodium, palladium and platinum complexes. The atropoisomeric binaphthyl **2** and biphenanthryl **3** derivatives [Rh(COD)(**2**)]X (X = BF_4 (**86a**), ClO_4 (**86b**)

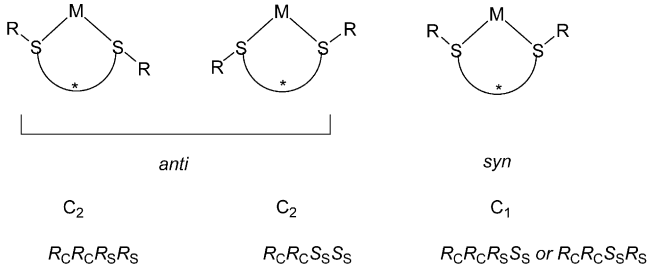

Fig. 9. Possible diastereomers for complexes containing ligands **1**.

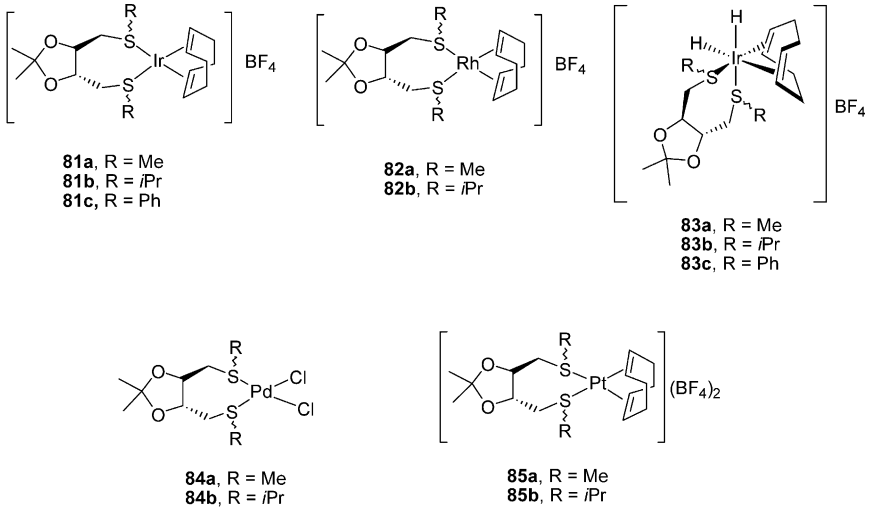

Fig. 8. Complexes with ligands **1a**–**c**: **81a**–**c**, **82a**–**b**, **83a**–**c**, **84a**–**b** and **85a**–**b**.

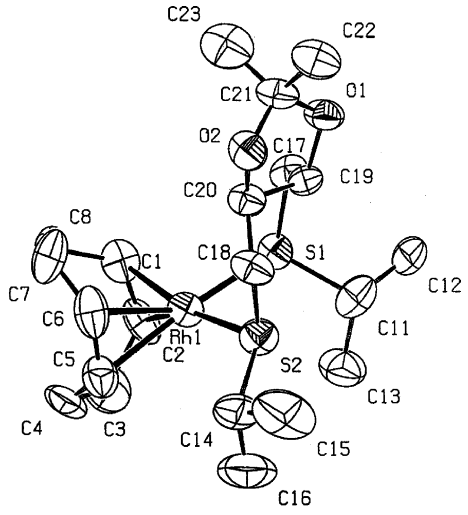

Fig. 10. ORTEP representation of the *anti* diastereomer for the cation $[Rh(COD)(S,S\text{-}\mathbf{1b})]^+$. Hydrogen atoms are omitted for clarity.

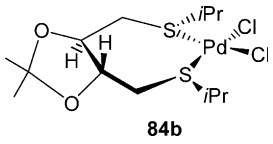

84b

Fig. 11. *anti* Diastereomer of **84b**.

[42], $[MCl_2(\mathbf{2})]$ (M = Pd (**88**), Pt (**89**)) [35] and $[Rh(COD)(\mathbf{3})]ClO_4$ (**87**) (Fig. 12) [29] were prepared according to the procedures described (Scheme 2a and c), except for the platinum complex **89**, which required UV irradiation at 254 nm to be formed. In these complexes, the ligands also form seven-membered metal chelates. Attempts to prepare complexes with a more sterically demanding group on the sulphurs, such as isopropyl, were unsuccessful.

All these complexes are fluxional in solution at r.t. [35]. They differ from the complexes of Rh (**82a**–**b**) and Pd (**84a**–**b**) containing **1a**–**b**, which did not show a fluxional process over the range of temperature scanned (from −90 to 50 °C). This dynamic behaviour is extremely pronounced for the rhodium complexes **86a**–**b** whose diastereomers did not show isolated NMR resonances even at −80 °C. For the palladium and platinum complexes, two diastereomers were observed in solution at −80 °C in ratios of 4:1 and 3:2, respectively. The NMR study (including NOE experiments) showed that the major isomer of the palladium complex has two pseudo-equatorial S-methyl substituents and an overall C_2 symmetry, where the seven-membered chelate ring adopts a distorted twisted chair conformation. The same metal chelate arrangement can be attributed to the minor isomer of the platinum complex. On the other hand, a pseudo-axial and pseudo-equatorial disposition of the methyl substituents was assigned for the minor isomer of the palladium complex and the major isomer of the platinum complex. NMR studies in combination with models indicate that the interconversion between diastereomers requires both changes in the chelate ring conformation and inversion of configuration at one stereogenic sulphur atom. The X-ray structure of **88** corresponds to the predominant isomer in solution. Though in general the structure with

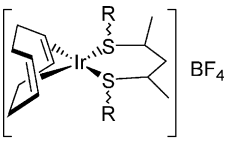

90a, R = *i*Pr
90b, R = Ph

Fig. 13. Complexes **90a** and **90b**.

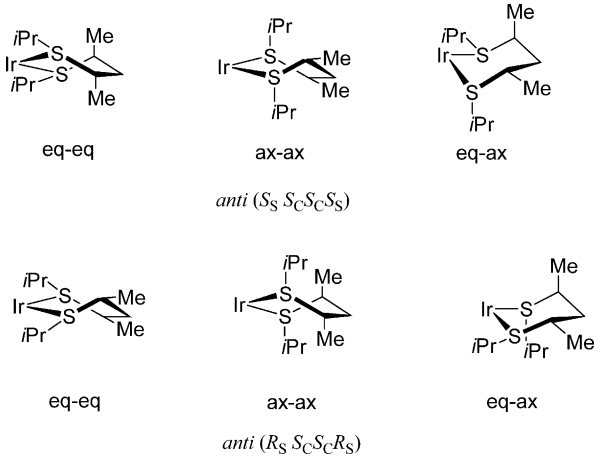

Fig. 14. Representation of the metal chelate conformations in the *anti* diastereomers with C_2 symmetry for complex **90a**.

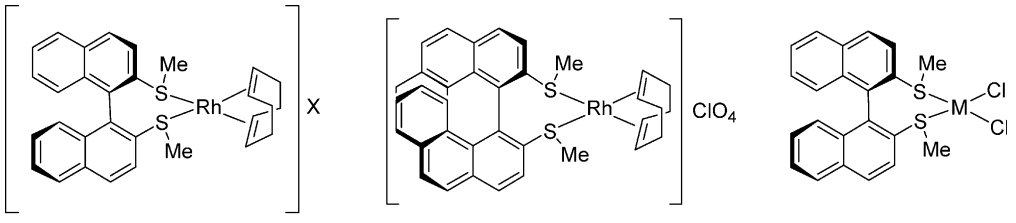

86a, X = BF_4
86b, X = ClO_4

87

88, M = Pd
89, M = Pt

Fig. 12. Complexes **86a**–**b**, **87**–**89**.

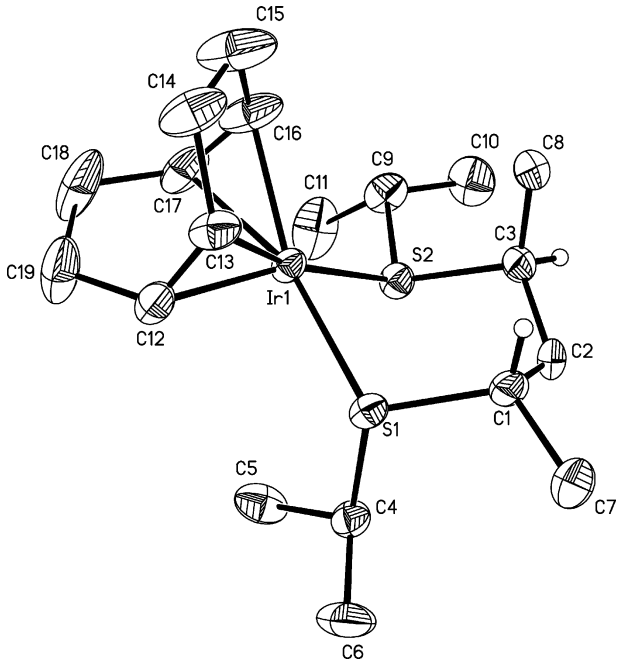

Fig. 15. ORTEP representation of the cation of **90a**. Hydrogen atoms are omitted for clarity.

the methyl groups in pseudo-equatorial disposition is expected to be the most stable (as observed for ligands **1**), interestingly this is not the case for **89**, for which the predominant isomer has one pseudo-axial methyl substituent. Though the explanation of this fact was based on the influence of short contact distance between the *ortho*-proton of the aryl group (adjacent to that bound to the sulphur) and the pseudo-equatorial methyl substituent in the X-ray structure of **88**, no comparative structural data were reported for **89** [35].

2.1.5. Complexes with C_2 symmetrical ligands *4a–b*

Ligands (*S*,*S*)-**4a** and (*S*,*S*)-**4b** were synthesized from (2*R*,4*R*)-pentanediol [30]. Iridium complexes [Ir(COD)-(**4a–b**)]BF_4 (**90a–b**, Fig. 13) were prepared in high yield by the standard procedure (Scheme 2a).

^{1}H-NMR spectra at r.t. for both complexes showed patterns that corresponded to the presence of only one species with C_2 symmetry, which may be attributed to one of the two possible *anti* diastereomers $S_SS_CS_CS_S$ or $R_SS_CS_CR_S$ with equatorial–equatorial or axial–axial conformations or to the chair equatorial–axial conformers interchanging fast in solution (Fig. 14). VT-NMR spectra of **90a** in CD_2Cl_2 were invariable in the temperature range studied (−40 to +25 °C). NOE experiments suggested that an equatorial–equatorial species was likely to be present in solution; nevertheless, rapid equilibration with other species could not be discarded. In fact, the structure in solid state of **90a** (Fig. 15), determined by X-ray diffraction, confirmed that the sulphur substituents are *anti*. The absolute configuration of the stereocentres is $S_SS_CS_CS_S$ and the sulphur substituents adopted an equatorial–axial disposition in a chair conformation of the six-membered ring.

2.1.6. Complexes with C_1 symmetrical sugar dithioethers ligands *5a–c*

Sugar derivatives are among the most easily accessible chiral ligands that have been used in homogeneous catalysis. They have provided high enantiomeric excesses for several asymmetric processes [43–50]. Their versatility and the presence of several stereogenic centres make possible the synthesis of series of ligands [43–54]. Therefore, a family of dithioether ligands with ribofuranoside backbone, (+)-**5a–c**, were prepared [31]. They form a six-membered chelate ring when coordinated to the metal centre.

Iridium complexes with 1,2-*O*-isopropylidene-3,5-bis(alkyl/arylthio)-α-D-(+)-ribofuranose **5a–c** [Ir(COD)-

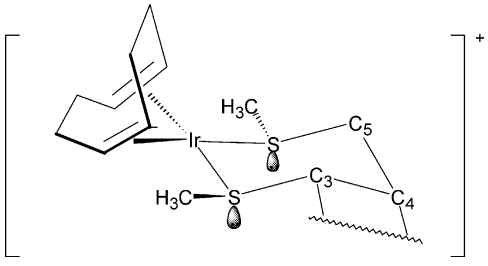

Fig. 17. Schematic molecular representation of **91a**.

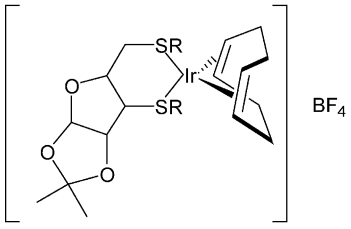

91a, R = Me
91b, R = *i*Pr
91c, R = Ph

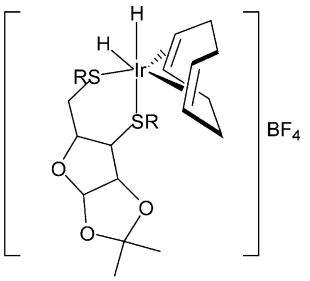

92a, R = Me
92b, R = *i*Pr
92c, R = Ph

Fig. 16. Complexes **91a–c** and **92a–c**.

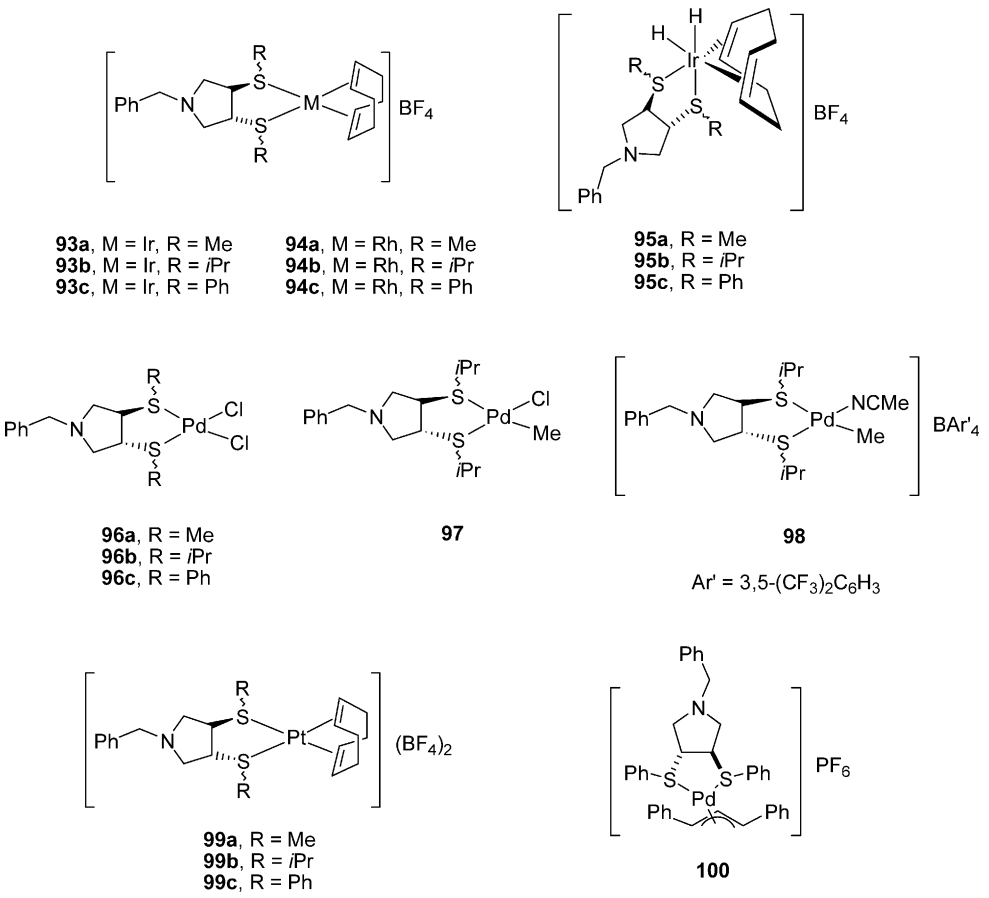

Fig. 18. Complexes **93a**–**c**, **94a**–**c**, **95a**–**c**, **96a**–**c**, **97**, **98**, **99a**–**c** and **100**.

(**5a**–**c**)]BF_4 (**91a**–**c**, Fig. 16) were also prepared by the standard method (Scheme 2a) [31]. In contrast to the C_2 symmetrical ligands, **5a**–**c** presents a C_1 symmetry. Therefore, four diastereomers can be formed: with *RR*, *SS*, *RS* and *SR* configuration at the sulphur atoms. Diastereomers *RR* and *SS* correspond to the *anti* and *RS* and *SR* to the *syn* invertomers. NMR measurements indicate that the reactions are highly diastereoselective and only one diastereomer was observed for all the complexes. For **91a**, NMR studies (including NOE experiments) in combination with molecular modelling showed that the dithiairidacyclohexane ring has a twist-chair conformation with a *S*,*R* absolute dithioether configuration and equatorial–equatorial disposition of the methyl substituents (Fig. 17).

2.1.6.1. Reactivity with H_2. The dihydrido complexes **92a**–**c** (Fig. 16) were formed as indicated in Scheme 2b at 0 °C and were characterized in solution by NMR spectroscopy [31]. For **92a** and **92c** three diastereomers were observed in a ratio 70:15:15. For **92b** two diastereomeric *cis*-dihydridoiridium complexes in a 50:50 ratio were observed. At 25 °C, hydrogen is cleaved off and the parent complexes **91a**–**c** were recovered.

*2.1.7. Complexes with C_1 symmetrical ligands **6a**–**c***

The family of ligands **6a**–**c** related to the 3,4-bis(diphenylphosphino)pyrrolidine type were synthesized and their iridium, rhodium, palladium and platinum complexes were prepared (Fig. 18).

2.1.7.1. Iridium and rhodium complexes. The iridium [32] and rhodium [55] diolefinic complexes [M(COD)(**6a**–**c**)]BF_4 (M = Ir (**93a**–**c**), M = Rh (**94a**–**c**)) were prepared by the standard procedures (Scheme 2a).

Complexes **93a** and **94a** were unstable in solution even under nitrogen atmosphere and could only be characterized in solid state (elemental analysis, FAB mass spectrometry and IR spectra). For the other complexes only one diastereomer, corresponding to the *anti* isomer with the (*SS*) dithioether absolute configuration could be distinguished from NMR data in combination with molecular modelling.

2.1.7.2. Reactivity with H_2. The iridium *cis*-[IrH_2-(COD)(**6a**–**c**)]BF_4 complexes (**95a**–**c**, Fig. 18), prepared as stated in Scheme 2b, form mixtures of two diastereomers in 2:1, 9:1 and 10:1 ratios for **95a**, **95b** and **95c**, respectively [32]. They can be attributed to the *anti* isomers with either (*SS*) or (*RR*) dithioether absolute

configurations. Molecular mechanics calculations showed that the most stable isomer for complexes *cis*-**95b** and *cis*-**95c** has the (*SS*) dithioether configuration. However, for *cis* **95a** no significant energy difference between the two isomers was observed, an observation that correlates well with the relative abundance of the two isomers observed by NMR. At −40 °C, hydrogen is cleaved off and the parent complexes **93a**–**c** are recovered.

2.1.7.3. Palladium and platinum complexes. Palladium and platinum complexes with ligands **6a**–**c** were also prepared (Fig. 18). The palladium complexes [$PdCl_2$-(**6a**–**c**)] (**96a**–**c**) were obtained by the standard method (Scheme 2c) [34]. Palladium complex [PdClMe(**6b**)] (**97**) was prepared from the corresponding diene complex [PdClMe (COD)] [56]. Reaction of **97** with $NaBAr'_4$ ($Ar' = 3,5\text{-}(CF_3)_2C_6H_3$) in acetonitrile led to the formation of the cationic complex [PdMe(MeCN)(**6b**)]BAr'_4 (**98**). The diolefinic platinum complexes [Pt(COD)(**6a**–**c**)]$(BF_4)_2$ (**99a**–**c**) were prepared by the synthetic method described in Scheme 2d [34]. These platinum complexes were unstable in solution, even under a nitrogen atmosphere and could be characterized only in solid state (elemental analysis, FAB mass spectrometry and IR spectra).

In contrast to the iridium and rhodium complexes, the NMR studies for the palladium complexes showed that hindrance of the ligand influences the number of diastereomers in solution and their structure [34]. VT-NMR and NOE experiments for **96b**, which contains the most hindered ligand **6b**, showed only one diastereomer in solution with a pseudo-axial and pseudo-equatorial disposition of the isopropyl groups. Only one diastereomer was detected for methyl complexes **97** and **98**. For palladium complexes **96a** and **96c**, two diastereomers were observed in dichloromethane at r.t. in a 2:1 ratio. For the major isomer of **96c**, NMR studies are consistent with a pseudo-axial location of the S-phenyl groups in the *anti* isomer with $R_CR_CR_SR_S$ absolute configuration or pseudo-equatorial disposition of the S-phenyl groups in the *anti* isomer with $R_CR_CS_SS_S$ absolute configuration (Fig. 19a). The minor isomer was assigned to have a pseudo-axial disposition of the phenyl substituents. Fig. 19b shows the two *syn* diastereomers with a $R_CR_CR_SS_S$ and $R_CR_CS_SR_S$ absolute configurations, the sulphur substituents located in pseudo-axial positions and the five-membered chelate ring adopting an envelope conformation. For **96a**, the two isomers adopt a pseudo-axial and pseudo-equatorial disposition of the methyl groups. In neither case did VT-NMR measurements indicate interconversion between the diastereomers at r.t.

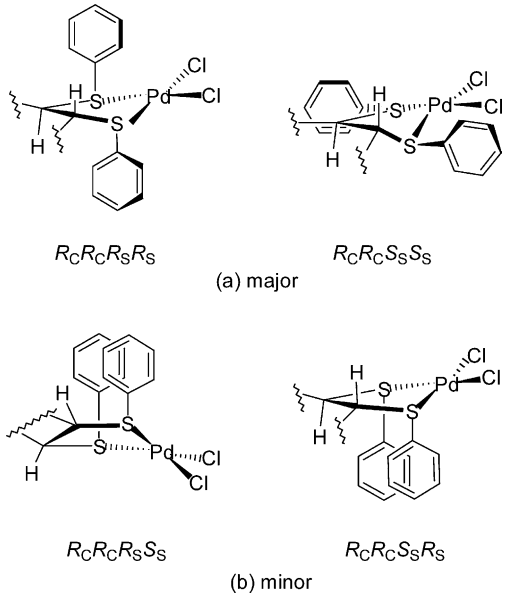

Fig. 19. Representation of the two possible (a) major *anti* and (b) minor *syn* diastereomers for complex **96c**.

The preferred disposition of the dithioether substituents in the complexes containing ligands **1a**–**c** is pseudo-equatorial. This is not the case for complexes containing **6a**–**c**, where the rigidity of the backbone permits other structures whose sulphur substituents are located in both pseudo-axial or pseudo-equatorial positions. Moreover, the unusual stabilization of the *syn* pseudo-axial disposition of **96c** may be explained by the π-stacking interaction between the two parallel phenyl groups.

With ligand **6c** the 1,3-diphenylallyl palladium complex [Pd(η^3-1,3-PhC_3H_3Ph)(**6c**)]PF_6 (**100**, Fig. 18) was prepared by the standard procedure (Scheme 2e). An NMR study showed the presence of four species in a ratio 50:22:17:11 attributed to isomers of different kinds (*syn*/*syn*, *syn*/*anti* and *exo*/*endo*): *exo*/*endo*, depending on the relative position of the allyl group and backbone ligand[1]; *syn*/*anti* depending on the relative position of allylic phenyl group (Fig. 20) [36].

*2.1.8. Complexes with C_1 symmetrical ligands **7a**–**b***

In an attempt to fix the absolute sulphur configuration, the bicyclic dithioethers **7a** and **7b** related to ligands **1** were synthesized [33].

2.1.8.1. Iridium complexes. The iridium complexes [Ir(COD)(**7a**–**b**)]BF_4 (**101a**–**b**, Fig. 21) were prepared

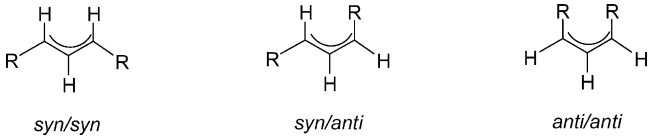

Fig. 20. Possible arrangements in 1,3-disubstituted allyl group.

[1] In each case, *exo* and *endo* must be defined since it depends on the reference that the authors take.

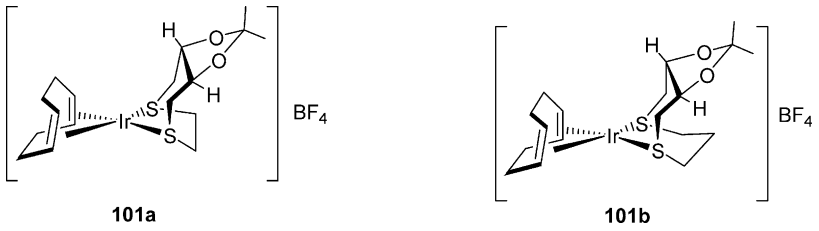

101a **101b**

Fig. 21. Complexes **101a** and **101b**.

by the general method (Scheme 2a) [30]. The NMR studies (including NOE experiments) indicate the presence of one conformer with an overall C_1 symmetry in an $R_C R_C R_S S_S$ configuration. The resulting complexes contain two rings. The seven-membered ring has a twisted chair conformation. The other ring is either a five-membered chelate ring with an envelope conformation (**101a**) or a six-membered ring with a chair conformation (**101b**) (Fig. 21).

2.1.8.2. Reactivity with H_2. Dihydrido complexes $[IrH_2(COD)(\mathbf{7a}–\mathbf{b})]BF_4$ (**102a**–**b**) were prepared as indicated in Scheme 2b [30]. In both cases, two diastereomers were obtained in a 2:1 ratio, although the reaction with H_2 can lead to four diastereomers (Fig. 22). The reason is that the oxidative addition of H_2 takes place in a *cis* fashion, either from the top (dioxolane ring face, Fig. 22a) or from the bottom (alkyl chain face, Fig. 22b) of the complex. For each direction of the attack, either the sulphur atom S or R migrates, so that two different isomers can be formed in each case. The NMR study (including NOESY experiments) indicated that the attack takes place from the dioxolane ring face, even though it is the most hindered, since the product obtained is less hindered than the one obtained if the H_2 addition took place from the alkyl chain face. Moreover, for **102a**, the NMR study showed that the major isomer originates from the migration of the sulphur atom with *S*-configuration and the minor isomer from the migration of sulphur atom with *R* configuration.

In contrast to the dihydrido complexes **83a**–**c** (obtained from **1**, Fig. 8), **92a**–**c** (Fig. 16) and **95a**–**c** (obtained from **6**, Fig. 18), complexes *cis*-**102a**–**b** are stable in solution at 25 °C. This could explain the low catalytic activities obtained with these iridium systems in asymmetric hydrogenation processes (see Section 3.2).

2.1.8.3. Palladium complexes. The 1,3-diphenylallyl palladium complex with **7b** $[Pd(\eta^3\text{-}1,3\text{-}PhC_3H_3Ph)(\mathbf{7b})]PF_6$ (**103**) was also prepared according to Scheme 2e [36]. An NMR study of **103** shows the existence of two diastereomers, *exo* and *endo* (depending on the relative position of the central allylic C–H bond and the dioxolane ring), the *exo* being the major isomer (see Section 3.1). The X-ray crystal structure of **103** (Fig. 23) showed the existence of two non-equivalent molecules (**103A** and **103B**) which correspond to the structure of the predominant isomer in solution (*exo*) with a *RS* dithioether absolute configuration. Both molecules differ in terms of the relative position of the phenyl allylic rings, which are nearly coplanar in **103A** and twisted in **103B**. Palladium coordination to the dithioether ligand leads to a boat conformation six-membered ring with the propylene moiety and a twisted chair conformation

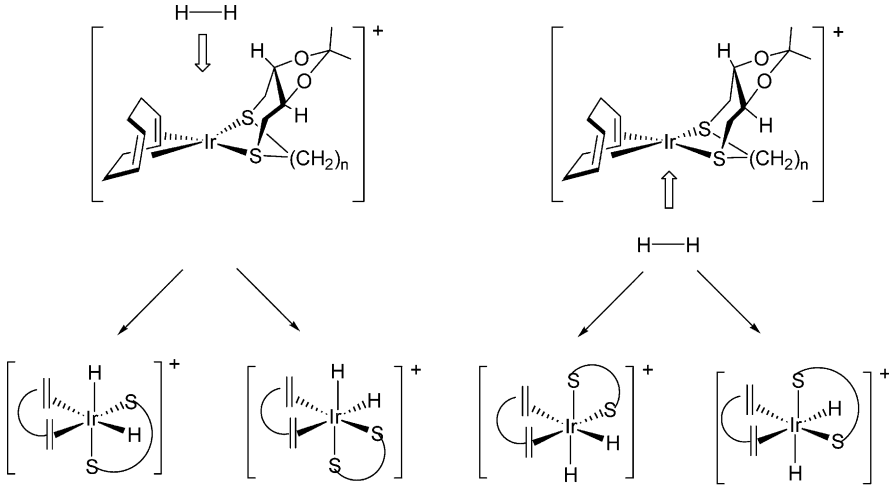

(a) (b)

Fig. 22. Four possible isomers of cations of **102a**–**b**. Attack of H_2 (a) from the dioxolane ring or (b) from the alkyl chain face (b).

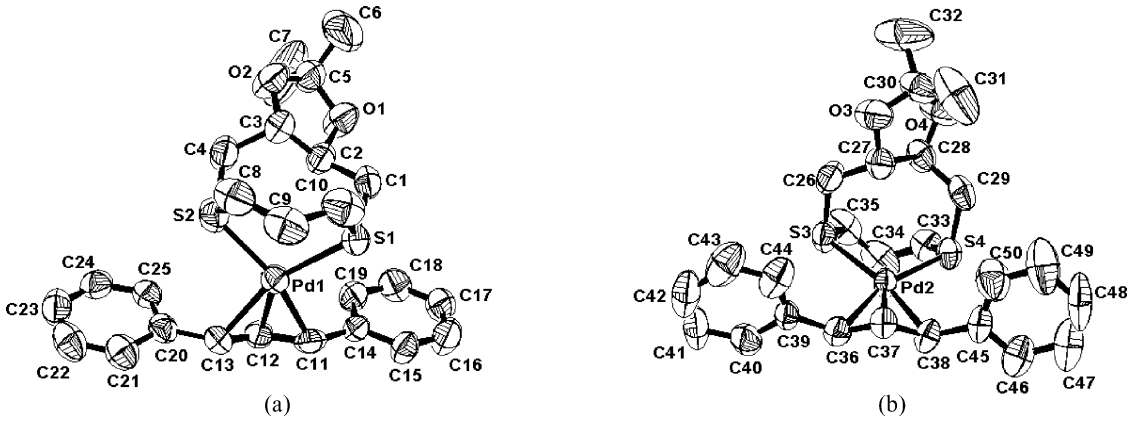

Fig. 23. ORTEP representation of the two cations of the isomers (a) **103A** and (b) **103B**. The hydrogen atoms have been omitted for clarity.

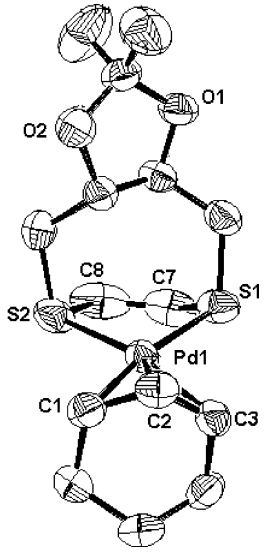

Fig. 24. ORTEP representation of the cation of **104**. The hydrogen atoms have been omitted for clarity.

seven-membered ring with the isopropylidene fragment. Since the two species are quite similar, an average for the *exo* structures is observed in solution.

The cyclohexenylallyl palladium complex with the ligand **7a** [Pd(η^3-cyclohexenyl)(**7a**)]PF_6 (**104**) has also been prepared [57]. An NMR study showed the existence of two diastereomers, *exo* and *endo* in a ratio 4:1, the *exo* being the major isomer (*exo* defined as the isomer in which the dioxolane ring points to the same direction as the central allylic C–H bond). The X-ray crystal structure of **104** shows the existence of only one isomer (Fig. 24) which corresponds with the structure of the predominant isomer in solution (*exo*) with a (*RS*) dithioether absolute configuration. Palladium coordination to the dithioether ligand leads to an envelope conformation of the five-membered ring and a twisted chair conformation for the seven-membered ring with the isopropylidene fragment.

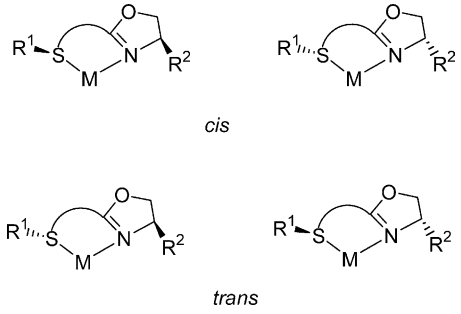

Fig. 25. Representation of the relative position of sulphur (R^1) and oxazoline (R^2) substituents in the metal chelate.

2.2. S,X-Donor bidentate ligands

Thioether have been combined with several donor atoms in heterodonor ligands. S,X-Donor ligands have several advantages over homodonors. They can provide different electronic environments due to the different *trans* influence of the sulphur and X atom. Depending on the nature of X, they can create strongly differentiated coordination positions, which can modify the chiral environment for substrate coordination or substrate reactivity. Moreover, depending on the lability of X, they can generate coordination vacancies in the complexes or extra stabilization with weak interactions.

In the following sections the coordination of S,N- and S,P-donor chiral ligands is described. In each section the ligands are ordered according to their chelate size and backbone.

2.2.1. S,N-Donor ligands

2.2.1.1. Thioether-oxazolines. Bis(oxazolines) are among the most successful N-donor ligands in homogeneous catalysis [58–60]. Therefore, a variety of mixed thioether-oxazolines (**10**–**23**, Fig. 2) have been prepared. Oxazoline substituents have been introduced in thioether ligands either as the sole chiral motif or together with other stereogenic units. For metal com-

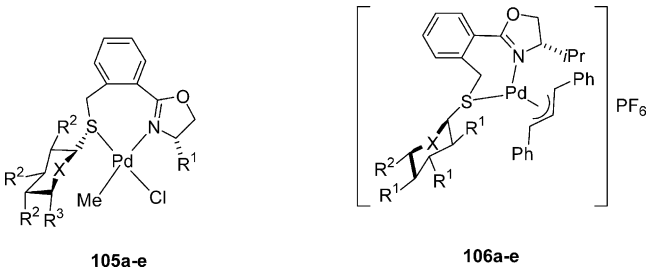

Fig. 26. Complexes **105a**–**e** and **106a**–**e**.

plexes of these mixed ligands, the relative position of the thioether and the oxazoline substituents (*cis*/*trans*) as well as the position of the sulphur substituent in the metal chelate (axial/equatorial) are relevant (Fig. 25). In a square-planar environment the preferred disposition minimising steric hindrance is, a priori, expected to be *trans*. The R^1 substituent would have less repulsion occupying an equatorial or pseudo-equatorial positions. Nevertheless, the disposition adopted finally may depend on factors such as: (i) the lack of substituents bonded directly to nitrogen, which generate less repulsion; (ii) the repulsive effect created by the lone electron pair; (iii) the influence of the other substituents of the chelate ring and (iv) the other ligands present in the complex. All these factors may determine the final more stable structure or may lead to mixtures of diastereomers.

Metal complexes of ligands **10** [13,61] with stereocentres in both oxazoline ring and sulphur substituent, ferrocene derivatives **11**–**13** [14] with a stereocentre in the oxazoline fragment and a stereogenic plane, the biphenyl bis(oxazoline) ligand **16** [59] and thiophene oxazoline thioethers **17** [62] have been synthesized.

Pregosin et al. combined the thiosugar substituent with the oxazoline moiety in a benzyl backbone to form chelating ligands **10a**–**e** which form seven-membered metal chelates [13]. Chloro methyl Pd(II) derivatives [PdClMe(**10a**–**e**)] (**105a**–**e**, Fig. 26) were prepared by the standard method from [PdClMe(COD)]. The structures of complexes **105a** and **105c** were determined by X-ray diffraction methods [61]. These complexes contained only one geometric isomer (N *trans* to Me). The sulphur substituent occupies a pseudo-axial position leaving the lone electrons pair in the pseudo-equatorial position. The sugar moiety and the oxazoline substituent are on the same side of the coordination plane (*cis*). Furthermore, in **105c** the phenyl substituent is somewhat closer in space than the isopropyl group for **105a** confirming that the *cis* position is stable.

Pd(II) complexes with allylic ligands [Pd(η^3-1,3-PhC_3H_3Ph)(**10a**–**e**)]PF_6 (**106a**–**e**, Fig. 26) were also prepared by the usual synthetic method (Scheme 2e) [13]. In this case, the number of possible diastereomers increases taking in account the position of the phenyl group relative to the central proton of the allyl ligand (Fig. 20). In fact, NMR NOESY experiments showed that these complexes formed mixtures of diastereomers in solution and the solid structure was not determined.

Chiral ligands with ferrocenyl backbone possessing a stereogenic plane have received a great deal attention due to their excellent catalytic behaviour [63–65]. Ferrocenyl derivatives **11a**–**e**, **12** and **13a**–**b** containing both, stereogenic plane and centre, form six-membered chelate rings with the metal. The Pd(II) allylic complexes [Pd(η^3-1,3-PhC_3H_3Ph)((S,S_P)-**11b**)]SbF_6 (**107a**, Fig. 27), [Pd(η^3-1,3-PhC_3H_3Ph)((S_P)-**11h**)]SbF_6 (**107b**, Fig. 27) and [Pd(η^3-1,3-PhC_3H_3Ph)((S,R_P)-**13b**)]SbF_6 (**108**) were prepared by the standard method in a dichloromethane/methanol mixture (Scheme 2e) [14]. Crystal structures were obtained for **107a** and **107b**. Both complexes adopted the *endo*/*syn*/*syn* conformation (the *endo* isomer is defined as the isomer in which the central allyl proton points to the ferrocene core). In the case of **107a**, the phenyl substituent of the sulphur and the ^{t}Bu group of the oxazoline are *trans* unlike the seven-membered complex **105a** (Fig. 27). The Pd–C_{allyl} distances *trans* to the N atom are smaller than the ones *trans* to S (2.15 and 2.18 Å for **107a** and **107b**, respectively vs. 2.21 and 2.26 for Å **107a** and **107b**, respectively). These data show that the S atom has a greater *trans* influence than the N oxazoline atom. In **107b** the two benzyl groups mount across the 1,3-diphenylallyl moiety. The plane of the phenyl in one of the benzyl groups is almost perpendicular to the allylic moiety. Therefore the two geminal benzyl groups have a significant effect on the conformation adopted by the allylic complex.

Bis(allyl) bimetallic palladium complexes containing ligand (S_C,S_C)-**16** were synthesized from standard allyl halide dimer starting materials (Scheme 2e) in the presence of ammonium hexafluorophosphate (**109a**

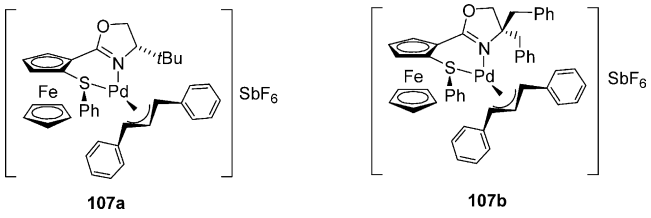

Fig. 27. Complexes **107a**–**b**.

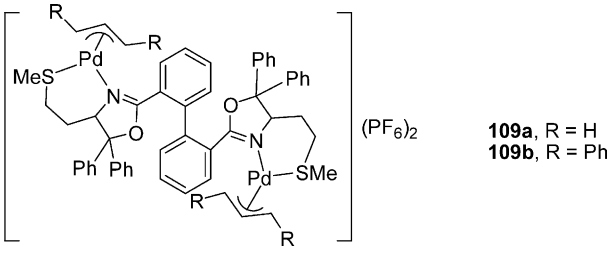

Fig. 28. Complexes **109a**–**b**.

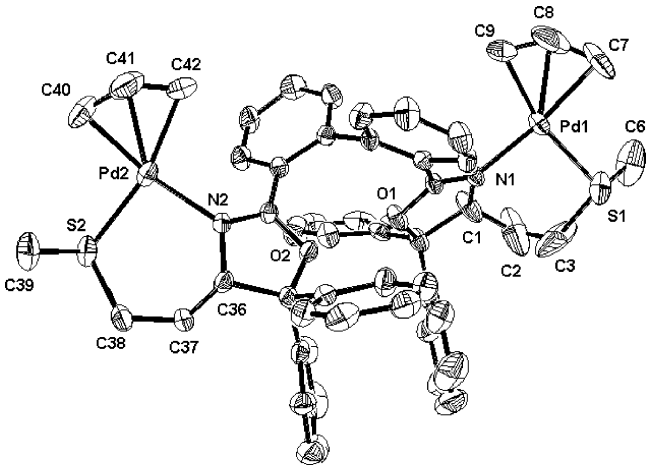

Fig. 29. ORTEP representation of the cation of **109a**. Hydrogen atoms are omitted for clarity.

and **109b**, Fig. 28) [59]. Due to the biphenyl backbone, **16** is obtained as an equimolecular mixture of diastereomers, (*ScRaSc*)- and (*ScSaSc*)-**16**. In spite of the existence of several donor atoms in the ligand structure, the ligand acts as a bridge between two metallic fragments, by S,N-coordination to palladium. In solution (chloroform and acetone as solvents), **109a** and **109b** showed broad signals in their NMR spectra (studied temperature range −50 to +25 °C), but two species could be differentiated in a ratio of ca. 70/30 for both complexes. In these compounds several species are expected due to the relative position between the allyl group and sulphur substituent, as well as the different stereogenic units (carbon and sulphur stereocentres, and the two axial configurations). However, the species observed in solution are probably due to the two different axial configurations, because the allyl rotation and the inversion of the sulphur atom, exhibit lower energies than the interconversion between the axial diastereomers. Complex **109a** was analysed by X-ray diffraction and only the S-axial isomer crystallized (Fig. 29). The sulphur atoms show *R* absolute configuration in each boat-six-membered metal chelate. In both palladium fragments, the allyl group exhibits *exo* arrangement relative to the position of the central allylic carbon and the sulphur methyl group.

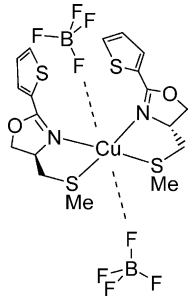

Fig. 30. Complex **110**.

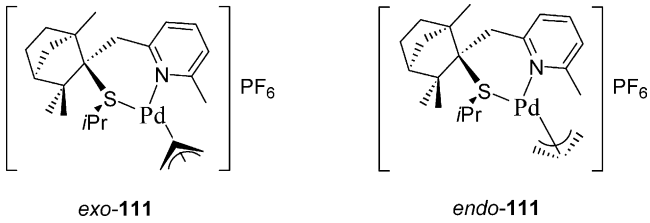

Fig. 31. *Exo*- and *endo*-isomers of **111**.

Thiophene-oxazolino-thioether ligands **17a–d** were prepared from L-cysteine and L-methionine [62]. Although they have three potential donor atoms, reaction of **17a** with $Cu(BF_4)_2$ led to the formation of $[Cu(\mathbf{17a})_2](BF_4)_2$ (**110**). X-ray structure **110** showed a square-planar coordination of Cu(II) in which **17a** was coordinated through the N-oxazoline and the S-thioether atoms (Fig. 30). The two ligands were arranged in a *cis* disposition probably to avoid the *trans* location of the better π-acceptors. The thiophene moieties were not coordinated, instead the BF_4^- anions were close to the fifth and sixth positions of a very distorted octahedron. Nevertheless it was not possible to determine the Cu–F distances due to the disorder of these anions

2.2.1.2. Thioether-pyridines. Heterobidentate thioether-pyridine and thioether-quinoline ligands with different stereogenic backbones have been described (**24–32**, Fig. 3). As far as we know, the only examples of isolated complexes have been the (*R*)-(−)-fenchone derivatives **26a–e** [66]. The hindered fenchone group was introduced at the sulphur atom as a strategy to prevent sulphur inversion. These ligands were prepared from the corresponding thiolpyridines. The reaction of **26c** with $[Pd(\eta^3\text{-}C_3H_5)(\mu\text{-}Cl)]_2$ in the presence of $AgPF_6$ in dichloromethane led to a mixture of the *exo* and *endo* isomers (3:4) of $[Pd(\eta^3\text{-}C_3H_5)(\mathbf{26c})]PF_6$ (**111**, Fig. 31) (*exo* indicates that the central allylic C–H bond and the sulphur substituent points to the same direction). From the mixture only the minor diastereomer *endo*-**111** crystallized. The thioether group also has a stronger *trans* influence pyridine since the $Pd–C_{allyl}$ distance *trans* to S is longer than the distance *trans* to pyridine

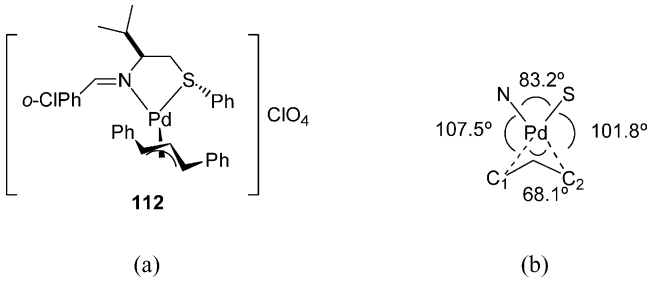

Fig. 32. (a) Complex **112**; (b) angles (°) of the coordination plane of **112**.

nitrogen atom. The fenchone methyl groups were effective in forcing a single absolute configuration on the sulphur atom (S). The conformation of the six-membered ring was a boat with the isopropyl substituent in axial position.

2.2.1.3. Thioether-imines. Imine ligands are better π-acceptors than other N-donors. It was interesting to study the *trans* influence in heterobidentate imino-thioether ligands. To do that, a series of imino-thioether ligands **33a**–**m** (Fig. 3) derived from (*S*)-valinol, (*R*)-phenylglycinol and (*S*)-*tert*-leucinol were synthesized [67]. These ligands generate five-membered chelate rings after complexation with the metal. The X-ray structure of the complex [Pd(η^3-PhC_3H_3Ph)(**33e**)]ClO_4 (**112**, Fig. 32) (prepared according to Scheme 2e) was determined. The phenyl group of the sulphur is in a pseudo-axial position and oriented *trans* to the isopropyl group to avoid unfavourable 1,3-interactions. Interestingly, although the N imine atom would be expected to exert a major *trans* influence, the Pd–C_{allyl} distances *trans* to N and to S are very similar (2.154 and 2.177 Å, respectively). In addition, the N–Pd–C_1 bond angle is larger than the S–Pd–C_2 bond angle, suggesting some interaction between the imine moiety and the C_1 allylic atom (Fig. 32b). This distortion may account for the further reactivity of this intermediate to be discussed below. This diastereomer was the only one detected in solution (>95%) from the COSY ^{13}C–^{1}H correlation and selected one-dimensional NOE experiments.

2.2.2. S,P-Donor ligands

Especially interesting is the combination of thioether with phosphorus donor ligands. In this case, the phosphorus atom has two substituents R^2 (Fig. 33) which can affect the position adopted for the R^1 sulphur substituent. Examples of thioether-phosphine (**38**–**54**, Fig. 4), thioether-phosphite (**55** and **56**, Fig. 5), thioether-phosphinite (**57**–**64**, Fig. 5) and a thioether-phosphabicycle (**65**, Fig. 5) are described in the following sections.

2.2.2.1. Thioether-phosphines.

2.2.2.1.1. Seven-membered chelate complexes. Seven-membered chelate complexes have been prepared with ligands containing binaphthyl (**38a**–**b**) [68] and ferrocenyl backbones (**39a**–**e**) [69–71].

Gladiali et al. [68] developed a convenient synthetic procedure for the isolation of the enantiomers (*R*)-**38a**–**b**. The complex [Rh(COD)((*R*)-**38a**)]OTf (**113**) was prepared by reaction of [Rh(μ-OMe)(COD)]$_2$ with the corresponding ligand in the presence of trimethylsilyl triflate (Scheme 3) [68]. Ligand **38a** was coordinated to the Rh(I) as a chelate through the P and the S atoms as was deduced by the ^{31}P-, ^{1}H- and ^{13}C-NMR spectra. The presence of only one set of signals, specially the sharp singlet in the ^{1}H-NMR for the S-methyl, suggested that only one diastereomer was formed in solution or that, if S-inversion took place, it was very slow on the NMR time scale. The authors proposed that the complex adopted a single conformation at r.t., probably the one with the methyl substituent in the pseudo-equatorial position.

Fig. 33. Relative position of the R^1 and R^2 substituents in S,P-donor ligands.

The ferrocenyl backbone has also been incorporated in thioether-phosphino ligands in the seven-member chelating ligands **39a**–**e** [69–71]. The structure of complex [Pd(η^3-1,3-PhC_3H_3Ph)(**39a**)]PF_6 (**114**) has an *exo*/*syn*/*syn* geometry as shown in Fig. 34 (*exo* indicates that the C–H vector is pointing away from the ferrocenyl core). This configuration is stabilized by three intramolecular C–H···π-interactions between one allylic phenyl group and one Ph of the PPh_2 moiety, the other interacts with an H from the Cp ligand and a third H···π-interaction take place between the CH_3 and the other aromatic ring of the allylic ligand. The 1,3-diphenylallyl ligand is slightly rotated clockwise along the Pd-allyl axis (seen from the allyl ligand towards the Pd atom) but the separation of the C_{allyl} atom *trans* to the P atom is only 0.447 Å above the P–Pd–S coordination plane. The SMe group is in the sterically favourable *exo* position (pointing away to the direction of the central allylic C–H bond).

2.2.2.1.2. Six-membered chelate complexes. Palladium complexes of ligands **40** [72] and **41** [61], featuring one less methylene unit between the donor atoms with respect to ligands **39**, showed a completely different arrangement of the sulphur and phosphorus substituents, thus giving rise to a totally different chiral environment.

The X-ray structure of complex [Pd(η^3-1,3-PhC_3H_3Ph)(**40**)]OTf (**115a**, Fig. 35), prepared by usual method depicted in Scheme 2e, reveals a markedly rotated 1,3-diphenylallyl ligand such that the terminal carbon trans to P-donor atom is ca. 0.85(3) Å below the coordination plane (Fig. 36a) [72]. This distortion is larger than in **114** (Fig. 36b). This rotation removes the allyl phenyl group from the sugar moiety, thus avoiding unfavourable steric effects. Nevertheless, the position of the sugar relative to the C_{allyl} central atom is *endo*, and so the two groups are pointing in the same direction. The sugar substituent is in the pseudo-equatorial position while the α-methyl is in an axial position. The position of the ferrocene moiety relative to the C–H central allylic bond is *exo* (both pointing towards opposite directions). In **115a**, unlike in the palladium

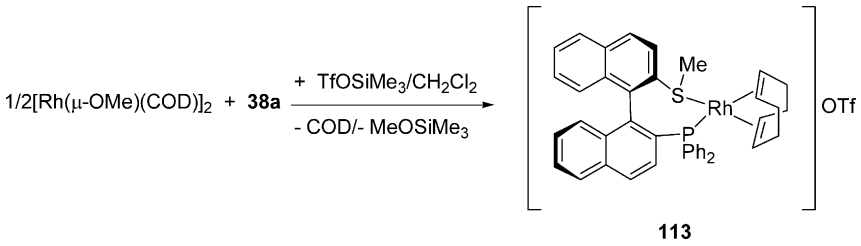

Scheme 3. Synthesis of **113**.

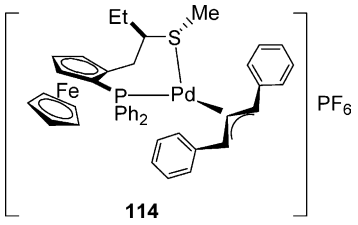

Fig. 34. Complex **114**.

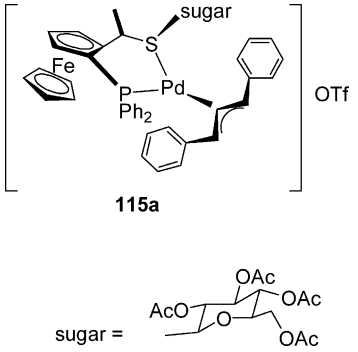

Fig. 35. Complex **115a**.

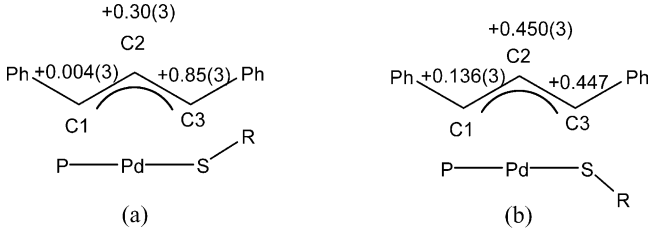

Fig. 36. Relative distances (Å) of the allylic carbons to the to the P–Pd–S plane in (a) **115a** and (b) **114**.

complex **114**, the SMe group is in the *endo* position. The main features of the structure with the ephedrine substituted ferrocene complex [Pd(η^3-C_3H_5)(**41**)]OTf (**115b**) are similar to **115a** except that the less hindered allylic η^3-C_3H_5 ligand is not distorted [61]. The nitrogen atom of the ephedrine does not participate in the coordination geometry.

Pregosin et al. prepared a series of Pd, Pt, Rh and Ir complexes with thioether-phosphino ligands **42** and **43**, characterized by the interposition of a benzyl unit between the donor atoms and by the introduction of stereogenic centres on the sulphur substituents [73–75].

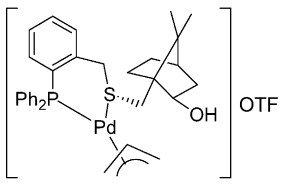

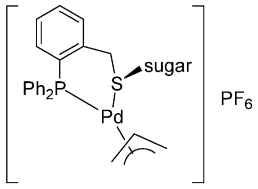

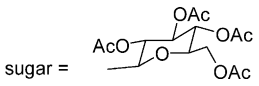

Fig. 37. Complexes (a) **116a** and (b) **117a**.

Allylic derivatives with **42** and **43** [Pd(η^3-C_3H_5)(**42**)]-OTf (**116a**), [Pd(η^3-1,3-PhC_3H_5Ph)(**42**)]BF_4 (**116b**) [73], [Pd(η^3-C_3H_5)(**43a**)]PF_6 (**117a**), [Pd(η^3-1,3-PhC_3H_5Ph)-(**43a**)]BF_4 (**117b**) and [Pd(η^3-1,3-PhC_3H_5Ph)(**43b**)]BF_4 (**117c**) [75] were prepared by the standard procedure (Scheme 2e). The X-ray structure of complexes **116a** [73] and **117a** [75] were determined (Fig. 37). Complex **117a** has two non-equivalent molecules (**A** and **B**) in the unit cell, which differ in the conformation at the ester functions in addition to some conformational changes at the phenyl rings. In both cases, **116a** and **117a**, the substituent of the sulphur occupies a pseudo-axial-position thus minimising the contact with the rest of the ligands and not interfering in coordination.

In the thioborneol Pd complex **116a** the isomer observed in the solid state corresponds to the one in which the central allyl carbon and the *exo*-borneol S–CH_2 are on opposite sides of the molecule (*exo* isomer) [73]. This structure corresponds to the major allyl rotational isomer in solution. In contrast, in complex **117a** the sulphur substituent is in the same side as the central allylic carbon (*endo* isomer). In both complexes **116a** and **117a** the Pd–C_{allyl} distance *trans* to P is longer (2.198(7) Å for **116a** and 2.25(1) Å for **117a**–**A**) than the Pd–C_{allyl} *trans* to S (2.145(8) Å for **116a** and 2.15(1) Å for **117a**–**A**) reflecting the higher *trans* influence of the phosphine. The three allylic carbons in **116a** are sitting below the S–Pd–P coordination plane (Fig. 38a) while in complex **117a**–**A** the allyl fragment is slightly rotated since one carbon is slightly below this plane and the other slightly above it (Fig. 38b).

An analogous Pt(II) complex [Pt(η^3-C_3H_5)(**42**)]PF_6 (**118**) was also prepared and the structure determined by

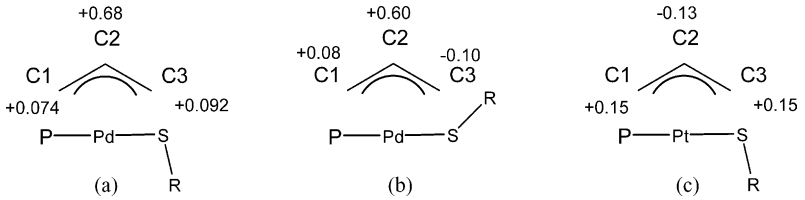

Fig. 38. Distances (Å) of the allylic carbons from the P–Pd–S-coordination plane for (a) **116a** and (b) **117a**–**A** and (c) *exo*-**118**.

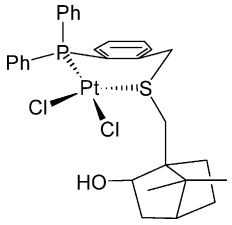

Fig. 39. Structure proposed for **119**.

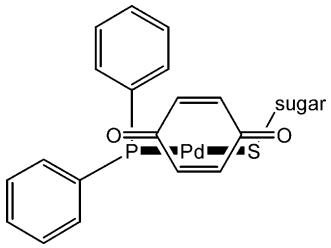

Fig. 40. Schematic representation of complex **120a**.

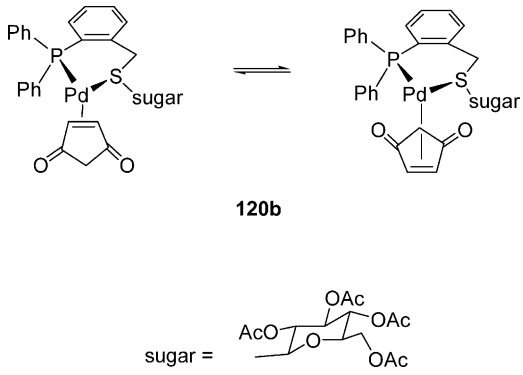

Scheme 5. Two isomers formed in solution for **120b**.

X-ray diffraction methods [74]. In this case, the *exo* isomer was the major but the *endo* isomer was also formed in the solid state in a ratio 3:1. As observed in most of these examples, the S-substituent also occupies a pseudo-axial position. Unlike its Pd analogue **116a**, the allyl ligand is almost symmetrically placed with respect to the S–Pt–P coordination plane in complex **118** (Fig. 38c). This can not be attributed to a decrease in repulsion with the sulphur and phosphorus substituents, since Pd–P and Pd–S distances (2.287(2) and 2.350(2) Å, respectively) are longer than the corresponding Pt–P and Pt–S distances (2.264(1) and 2.318(1) Å, respectively) and the M–C_{allyl} distances are quite similar (M–C(*trans* S) = 2.151(6) Å for **118** and 2.145(9) Å for **116a**; M–$C_{central}$ = 2.169(8) Å for **118** and 2.13(1) Å for **116a**; M–C(*trans* P) = 2.195(5) Å for **118** and 2.198(7) Å for **116a**).

The preparation of the corresponding Pt(II) dichloro complex [$PtCl_2$(**42**)] (**119**, Fig. 39) has also been reported [74]. NMR experiments indicated that complex **119** exists as a mixture (in ratio of 93:7) of two isomers. On the basis of NOESY correlations it was proposed that the major isomer adopts in solution a boat type chelate ring conformation with the norborneol substituent in axial position (Fig. 39).

Ligand **43a** was able to stabilize Pd(0) complexes. Reaction of $Pd_2(dba)_3$ with **43a** and diones formed the palladium(0) complexes [Pd(olefin)(**43a**)] (olefin = benzoquinone (**120a**), 4-cyclopentene-1,3-dione (**120b**))

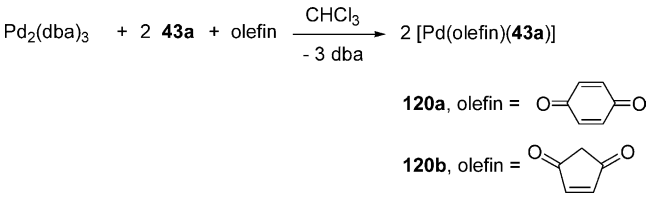

Scheme 4. Synthesis of **120a**–**b**.

(Scheme 4) [76]. The X-ray structure of **120a** showed that the Pd(0) was coordinated to the P and S atoms of **43a** together with one of the double bonds of the benzoquinone. The Pd–S distance (2.354(1) Å) was in the usual range for Pd(II)–S complexes suggesting that there was no special interaction between the S-donor atom and the zero-valent metal. In this structure the sugar moiety, the axial phenyl ring of the phosphorus atom and the non-coordinated atoms of the benzoquinone are all on the same side of the coordination plane (Fig. 40). As observed in the other structures, the sulphur substituents tend to adopt pseudo-axial positions, thus leaving the sulphur lone pair in a relatively open area of the structure.

The solution structure of **120b** shows the existence of two isomeric forms (3.2:1) corresponding to the two possible positions of the diene which rotates without dissociation (Scheme 5) [76]. The ^{31}P-NMR spectrum of **120a** in solution showed only one signal, nevertheless the presence of exchange cross peaks in the NOESY spectrum between the complex and traces of free benzoquinone indicates that a similar rotational process

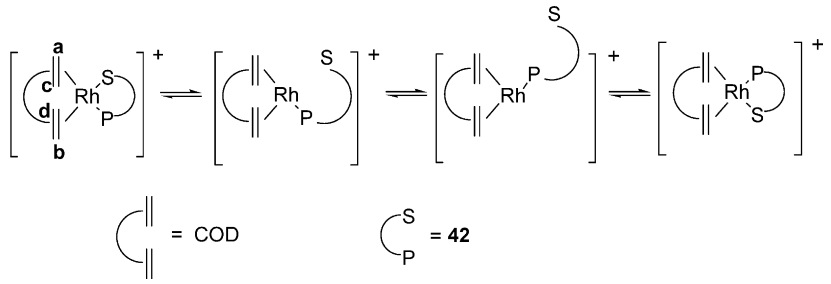

Scheme 6. Mechanism proposed for the isomerization of **121**.

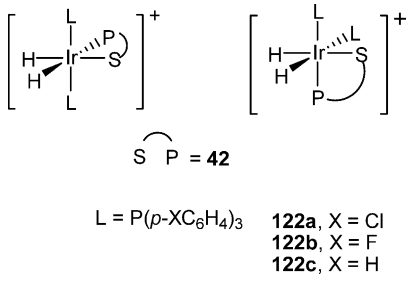

Fig. 41. Proposed isomers for cations **122a**–**c**.

occurs through a dissociation recombination process. These differences were attributed to the larger volume of the benzoquinone ligand.

The Rh(I) diolefin complex [Rh(COD)(**42**)]OTf (**121**) was also prepared. NMR data of this complex in solution are in agreement with the existence of two isomeric forms in fast exchange in the NMR time scale in a ratio of ca. 3:2 [74]. The observation by phase sensitive ^{1}H NOESY experiment of exchange between the olefinic protons **a** and **b** slowly with **c** and **d** led to the proposal of a mechanism for isomerization indicated in Scheme 6. This mechanism proceeds via dissociation of the sulphur atom, followed by rearrangement of the three-coordinated complex and reformation of the four-coordinated species. Olefin rotation was not excluded though it was considered unlikely since several bonds must be broken simultaneously.

Six-coordinated Ir(III) dihydride complexes $[IrH_2(\mathbf{42})(P(p\text{-}XC_6H_4)_3)_2]^+$ were prepared for X = Cl (**122a**), F (**122b**), H (**122c**) [74]. The ^{31}P-NMR spectra in solution of these complexes showed more than 16 well separated ^{31}P resonances, which were attributed to mixtures of the *cis* and *trans*-phosphino isomers (Fig. 41).

2.2.2.1.3. Five-membered chelate complexes. Thioether-phosphine ligands **44a**–**i** can form five-membered chelate rings upon coordination to the metal [77]. The substituent in the α-position to the thioether R^2 was introduced to force the substituent of the sulphur R^3 to adopt a *trans* position respect to R^2. Group 8 complexes $[NiCl_2(\mathbf{44c})]$ (**123**), $[PdCl_2(\mathbf{44c})]$ (**124**) and $[PtCl_2(\mathbf{44c})]$ (**125**) and [Rh(COD)(**44a**–**i**)]OTf (**126a**–**i**) were prepared from $[NiCl_2(DME)]$, (DME = dimethoxyethane) $[PdCl_2(COD)]$, $[PtCl_2(NBD)]$ (NBD = 2,5-norbornadiene) and $[Rh(COD)_2]OTf$, respectively (Scheme 7). The solid state structure of complexes **123** and **126c** was determined by X-ray diffraction methods. In both cases the distances M–L *trans* to the phosphorus atom were longer than the M–L distances *trans* to sulphur. The methyl substituent of the chelate ring occupied a pseudo-equatorial position and the sulphur substituent was forced to be *trans* to it adopting a pseudo-axial location. Ni, Pd and Rh complexes showed broad signals in solution due to sulphur inversion.

The thioether phosphino ligands **45**–**47** were obtained by introduction of a thioetherphosphino fragment either in the β-position of the anomeric carbon of a glucal (**45**) or a maltose derivative (**46**), or in the 6-position of a tri-*O*-acetyl-D-glucal (**47**) [78]. Cationic Rh(I) complexes [Rh(COD)(**45**–**47**)]BF_4 (**127**–**129**) with these ligands were prepared from [Rh(ACAC)(COD)] (ACAC = acetyl acetonate) in presence of tetrafluoroboric acid in

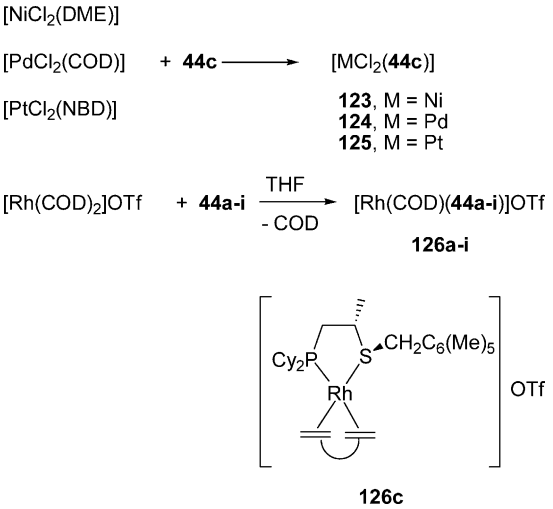

Scheme 7. Synthesis of **123**–**125** and **126a**–**i**.

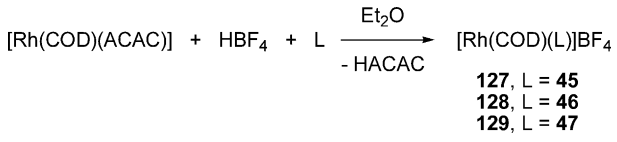

Scheme 8. Synthesis of **127**–**129**.

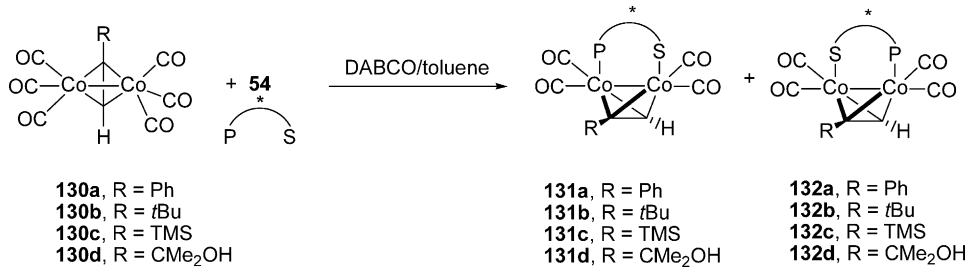

Scheme 9. Synthesis of **131a**–**d** and **132a**–**d**.

diethylether (Scheme 8). These ligands coordinate as chelates through the phosphorus and sulphur atoms as proven by ^{31}P-NMR and circular dichroism spectroscopies.

*2.2.2.1.4. Bridging ligand **54**.* Phosphinooxathiane ligand **54** was designed for use in the asymmetric intermolecular Pauson–Khand reaction [79]. Reaction of **54** with acetylene carbonyl dicobalt(0) complexes **130a**–**d** in presence of 1,4-diazabicyclo[2.2.2]octane (DABCO) in toluene afforded mixtures of two diastereomers (**131a**–**d**/**132a**–**d**, Scheme 9) that were separated by column chromatography or simple recrystallization. The X-ray structure of complex **131d** shows that sulphur and phosphorus atoms are coordinated to different metal atoms and occupy two eclipsed pseudo-equatorial positions. The five-membered metal chelate formed has an envelope conformation and the sulphur lone electron pair is in axial position. These complexes proved to be highly stereoselective reactants for the Pauson–Khand reaction with norbornadiene.

2.2.2.2. Thioether-phosphites. Phosphite ligands are much better π-acceptor than phosphines, are easier to prepare and have given excellent results in many homogenous catalysis processes [80]. Mixed thioether-phosphite ligands (**55**–**56**, Fig. 5) have been prepared.

2.2.2.2.1. Seven-membered chelate complexes. Chiral ligands **55a**–**c** featuring a 1,2-*O*-isopropylidene-α-D-xylofuranose unit and the corresponding rhodium (**133a**–**c**) and iridium complexes (**134a**–**c**) have been reported (Fig. 42) [81]. The r.t. ^{31}P-{^{1}H}-NMR spectra showed one signal for all complexes. When the temperature was lowered, the Rh and Ir complexes **133b**–**c** and **134b**–**c**, showed two set of signals attributed to two isomeric forms in fast exchange on the NMR time scale at r.t. Molecular mechanics calculations indicated that the most stable diastereomer would contain the thioether group in a pseudo-axial position with *R* configuration at sulphur atom in a twist-boat conformation of the seven-membered chelate ring. The less stable diastereomer had a boat conformation with the substituent of the sulphur atom in pseudo-equatorial position and with an *S*-configuration at sulphur centre. Reaction of iridium complexes **134a**–**c** with H_2 at 0 °C afforded the corresponding *cis*-dihydrido complexes **135a**–**c**. Based on the analysis of the coupling constants, the results of 2D-NOESY experiments and molecular mechanics calculations led to the proposal that unlike related dithioether complexes only one diastereomer was formed. The diastereomer has the thioether group located in pseudo-equatorial position with an *S* absolute configuration for the sulphur atom and with a chelate ring in a chair conformation. The proposed structure for the dihydrido complexes is shown in Fig. 42.

2.2.2.2.2. Six-membered chelate complexes. The rhodium diolefin complex [Rh(COD)(**56**)]BF_4 (**136**) was prepared by the standard reaction (Scheme 2a) with the aim of comparing the dynamic behaviour of the coordinated diolefin ligand [82]. NMR experiments showed selective exchange of the non-equivalent olefinic

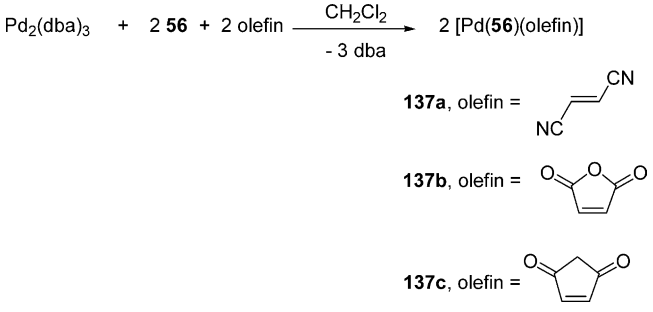

Scheme 10. Synthesis of **137a**–**c**.

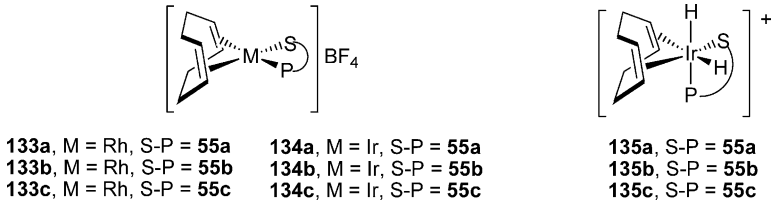

Fig. 42. Complexes **133a**–**c**, **134a**–**c** and **135a**–**c**.

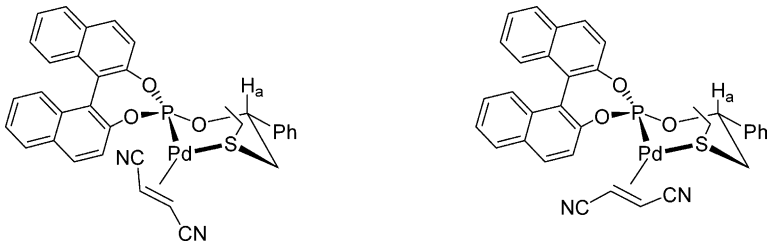

Fig. 43. Possible isomers in solution for **137a**.

protons of the COD as observed in the complex with the thioether-phosphine **121** (Scheme 6). The mechanism was proposed to proceed similarly via dissociation of the Rh–S bond, recombination of the T shaped species formed, rotation around the Rh–P and re-coordination of the S donor atom. Rotation of the diolefin was ruled out by observing that related diphosphine ligands with strong Rh–P bonds did not show proton exchange.

The thioether-phosphite **56** also stabilized Pd(0) complexes with electron withdrawing olefins [Pd(olefin)(**56**)] (olefin = fumaronitrile (**137a**), maleic anhydride (**137b**), 4-cyclopentene-1,3-dione (**137c**)) (Scheme 10) [83].The structure of **137b** shows the Pd(0) coordinated through the P, the S and the alkene. Those atoms P,S and the two carbon atoms of the double bond are nearly coplanar. In **137b** the ethyl substituent of the sulphur is below the plane and on the opposite face to the maleic anhydride. The chelating ring has a boat conformation in which the phenyl ring is in a pseudo-equatorial position and the ethyl substituent in a pseudo-axial one. The NMR exchange spectrum of this complex in solution showed, as in the case of **120b** (Scheme 5), that there were two isomers corresponding to the two possible coordination modes of the alkene. The fumaronitrile derivative **137a** in solution also shows the presence of two isomers arising from the two faces of the olefin (Fig. 43). NOE experiments allowed the assignment of both diastereomers. A strong NOE between the methyl group of the ethyl substituent on sulphur and the CHO methine protons (H_a, Fig. 43) suggested a chair chelate conformation of the ring in which the ethyl occupies a pseudo-axial and the phenyl a pseudo-equatorial position as observed in the crystal structure.

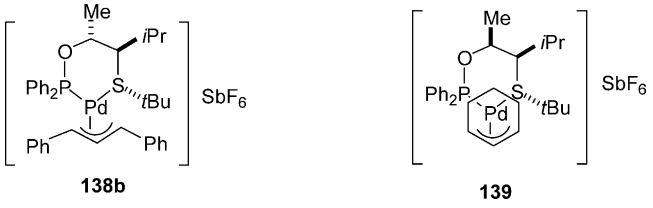

Fig. 44. Complexes **138b** and **139**.

2.2.2.3. Thioether-phosphinites. An extensive family of thioether-phosphinites (**57**–**63**) and a series of thioether-diphosphinites **64a**–**d** have been synthesized (Fig. 5).

Ligands **57**–**60** were designed with the aim of controlling the stereochemistry of the S atom upon coordination to metals [15,84]. To control sulphur inversion, substituents in the α and β positions with respect to S were introduced. Palladium dichloro [$PdCl_2$(**58a**)] (**138a**) and allylic [Pd(η^3-1,3-PhC_3H_3Ph)-(**58a**)]SbF_6 (**138b**) (Fig. 44)) complexes were prepared according to standard procedures (Scheme 2c and e). The X-ray structure and NMR analysis in solution of complex **138a** showed the formation of only one diastereomer, which, in solid state, adopted a twist-boat geometry with the backbone substituents in equatorial positions. The *tert*-butyl substituent and the adjacent isopropyl group were oriented *anti* to each other in the chelate. The conformation of the X-ray structure of complex **138b** was similar to the dichloro complex. The longer Pd–C_{allyl} *trans* to the P atom was attributed to the stronger *trans* influence of the phosphinite ligand. Unlike ferrocenyl **115a** (Fig. 35) and **114** (Fig. 34), the allyl substituent in **138b** was not significantly twisted out of the P–Pd–S plane. Although there was only one diastereomer in solid state, there were two species in solution as will be discussed (vide infra). The crystal structure of the palladium cyclohexenyl [Pd(η^3-cyclohexenyl)(**57a**)]SbF_6 (**139**) was also analysed (Fig. 44). Complex **139** exists in a half-chair chelate geometry which differs from the twist-boat geometry observed for ligand **58a**. The chelate conformation adopted depends strongly on the stereochemistry of the β-substituent.

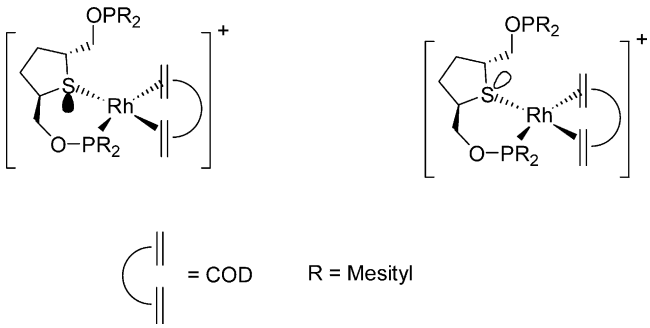

Fig. 45. Species proposed to form in solution for the cation of complex **140d**.

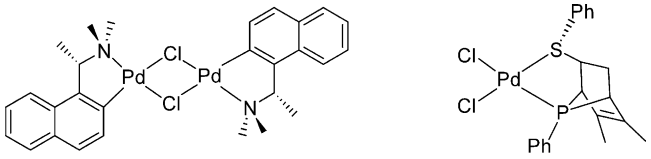

141 **142**

Fig. 46. Complexes **141** and **142**.

Thioether-diphosphinites **64a**–**d** derived from (*R*,*R*)-*trans*-2,5-tetrahydrothiophenedimethanol were prepared [85]. Reaction of the chiral non-racemic ligands **64a**–**d** with $[Rh(COD)_2]OTf$ led in all cases to mixtures of isomers (**140a**–**d**). In the case of complex **140d**, the formation of two isomers (25:75) in which the ligand acts as a S,P-bidentate ligand (Fig. 45) was deduced from the ^1H- and ^{31}P-NMR spectra. These complexes were not isolated.

2.2.2.4. Thioether-phosphabicycle. One example of a P,S-donor ligand containing a stereogenic P atom is the phosphabicycle **65** (Fig. 5). The (+)- and (−)-forms of **65** were prepared stereoselectively by a Diels–Alder reaction assisted with the palladium(II) complex **141** (Fig. 46) [86]. The ligand was synthesized in the coordination sphere of the metal and one of the intermediates, the dichloro complex $[PdCl_2(\mathbf{65})]$ (**142**, Fig. 46), was isolated. The X-ray structure of **142** shows that the geometry at the palladium centre is distorted square-planar. The absolute configurations of the stereocentres were $R_PS_SR_CR_CS_C$. The Pd–P and Pd–S distances were within normal values and the P–Cl distances differed significantly due to the greater *trans* influence of the P atom (Pd–Cl *trans* P 2.364(2) Å and Pd–Cl *trans* S 2.303(3) Å).

2.3. Polydentate ligands

Polydentate chiral ligands containing thioether functionality often include other donor atoms and macrocyclic backbones (ligands **27** (Fig. 3) and **70**–**77** (Fig. 7)).

The bisfenchone derived ligands **27a**–**e** were prepared [66] and one of them reacted with $[Pd(\eta^3\text{-}C_3H_5)(\mu\text{-}Cl)]_2$ in presence of $AgBF_4$ to afford the tetracoordinated complex $[PdCl(\mathbf{27e})]BF_4$ (**143**, Fig. 47). There was no

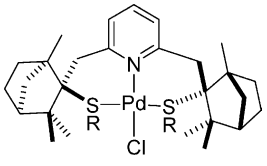

R = Benzyl

143

Fig. 47. Complex **143**.

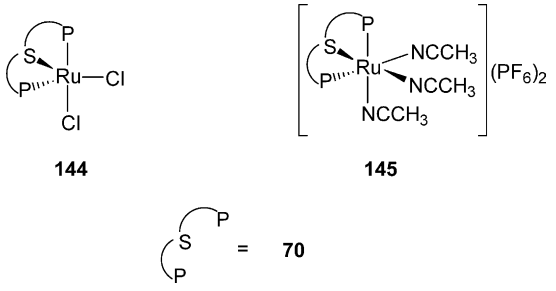

144 **145**

Fig. 48. Complexes **144** and **145**.

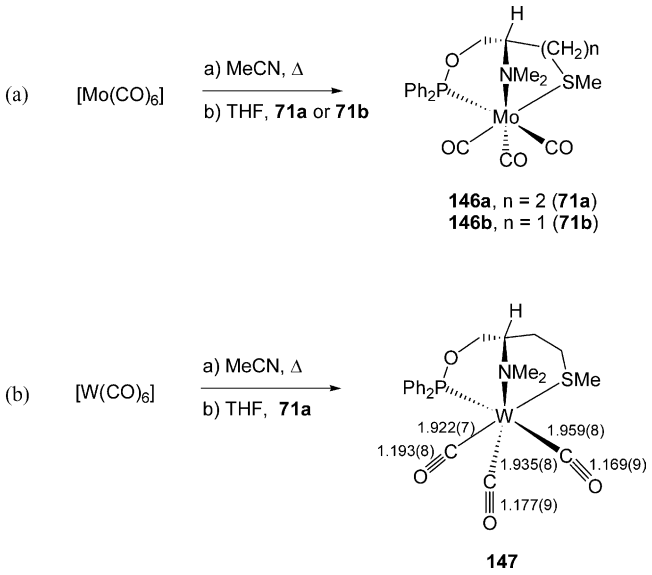

Scheme 11. Synthesis of complexes (a) **146a**–**b** and (b) **147** showing selected distances (Å).

coordination of the allyl ligand as confirmed by the X-ray structure determination.

A thioether-diphosphine with a ferrocenyl backbone **70** has been prepared [87]. The dichloro derivative of Ru(II) $[RuCl_2(\mathbf{70})]$ (**144**) was synthesized from $[RuCl_2(PPh_3)_3]$. This ligand adopts a *fac* arrangement in the coordination with the metal. The ^{31}P-NMR spectra consisted of two doublets separated by ca. 13 ppm with a coupling constant (36.8 Hz) characteristic of bis(phosphino) ligands coordinated in a *cis* fashion. This led the authors to propose the formation of a *fac* trigonal-bipyramidal structure (Fig. 48). Reaction of this dichloro complex in acetonitrile in the presence of the halide scavenger $TlPF_6$ gave *fac*-$[Ru(CH_3CN)_3(\mathbf{70})](PF_6)_2$ (**145**) (Fig. 48). The coordination of the acetonitrile was confirmed by ^1H- and ^{13}C-NMR spectroscopy.

L-Methionine and L-cysteine derivatives **71a**–**b** containing phosphinito-amino-thioether groups were prepared in order to study their stereocontrolling ability in six- and seven-coordinated complexes [88]. The W and Mo carbonylic complexes $[Mo(\mathbf{71a}\text{–}\mathbf{b})(CO)_3]$ (**146a**–**b**) and $[W(\mathbf{71a})(CO)_3]$ (**147**) were prepared from the

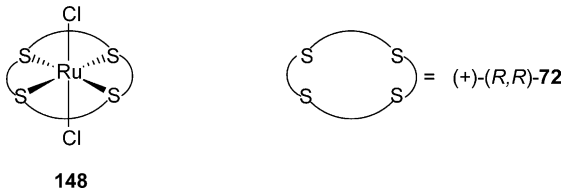

148

Fig. 49. Complex **148**.

corresponding hexacarbonyl complex through the acetonitrile intermediate (Scheme 11). The X-ray structure of **147** confirmed the coordination of **71a** as a tridentate P,N,S-donor ligand. The W–X (X = P, N, S) and W–CO distances (Scheme 11b) reflect the different *trans* influences of the donor atoms (P > N > S). The configuration at the sulphur in the crystal structure is (S_S) but in solution it was reported that rapid interconversion (S_S)⇔(R_S) and ring conformation rearrangement were taking place and consequently the signals observed were averaged between all the possible diastereomers. The reaction of **71a** with [Pd(η^3-allyl)(μ-Cl)]$_2$ dimer led to the formation of complexes where this ligand acts as a P,N donor.

Chiral macrocyclic thioether ligands have also been reported. The (+)-(*R*,*R*)- and (+)-(*S*,*S*)-enantiomers of the 18-membered tetradentate crown thioether **72** were prepared [89]. The (+)-(*R*,*R*)-**72** enantiomer reacted with $K_2[RuCl_5(H_2O)]$ to afford the complex *trans*-[$RuCl_2$((+)-(*R*,*R*)-**72**)] (**148**). The X-ray structure of this complex shows the hexacoordination of the Ru(II) with the S-atoms occupying the equatorial plane (Fig. 49). The electron pairs of the four sulphur atoms alternately occupy the axial positions of the macrocycle, thus providing an up-down-up-down conformation. This disposition generates a helical cavity at the axial sites of the complex **148**.

2.4. Thioether π-donor ligands

Combination of thioether with π-donor moieties such as cyclopentadiene (**78b**, Fig. 7) and acetylene (**80a**–**c**, Fig. 7) have also been reported.

In the synthesis of transition metal complexes with Lewis acid properties, the half-sandwich 16-electron complexes of Fe or Ru are an important class of compounds. To prepare chiral Lewis acid the Cp-ring was connected to a stereogenic unit with a functional group capable of intramolecular coordination. The Cp-thioether trimethylsilyl derivative with a neomenthyl substituent **78a** was prepared [90]. Reaction of the latter with [$RuCl_2(PPh_3)_3$] afforded complex [RuCl(**78b**)-(PPh_3)$_2$] (**149**) in which the sulphur was not coordinated (Scheme 12a). Coordination of the sulphur moiety took place by reaction of **149** with AgOTf to produce the cationic complex [Ru{η^5:η^1-**78b**}(PPh_3)$_2$]OTf (**150**, Scheme 12b). Coordination of the sulphur was deduced by NMR experiments. Complex **150** was not stable and decomposed after few hours at r.t., possibly due to S–C bond scission.

Chiral isoborneol thioether derivatives **79a**–**c** were used to prepare acetylenic ethers **80a**–**c** [91]. These trimethylsilyl derivatives reacted with octacarbonyldicobalt(0) to produce thioether acetylene dimeric complexes **151a**–**c** which after treatment with *N*-methylmorpholine-N-oxide (NMO) afforded the bidentate species **152a**–**c** (Scheme 13a). NMR experiments in solution showed the presence of only one species. Based on density functional theory (DFT) calculations of the four

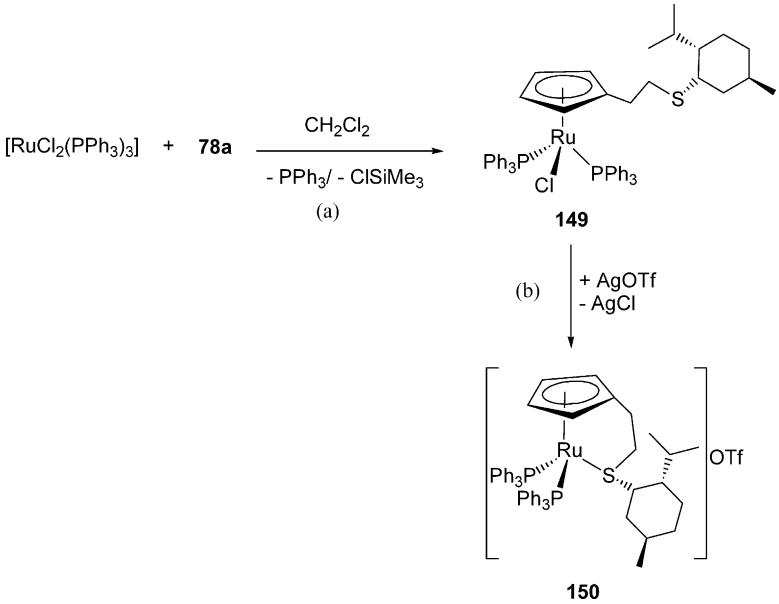

Scheme 12. Synthesis of (a) **149** and (b) **150**.

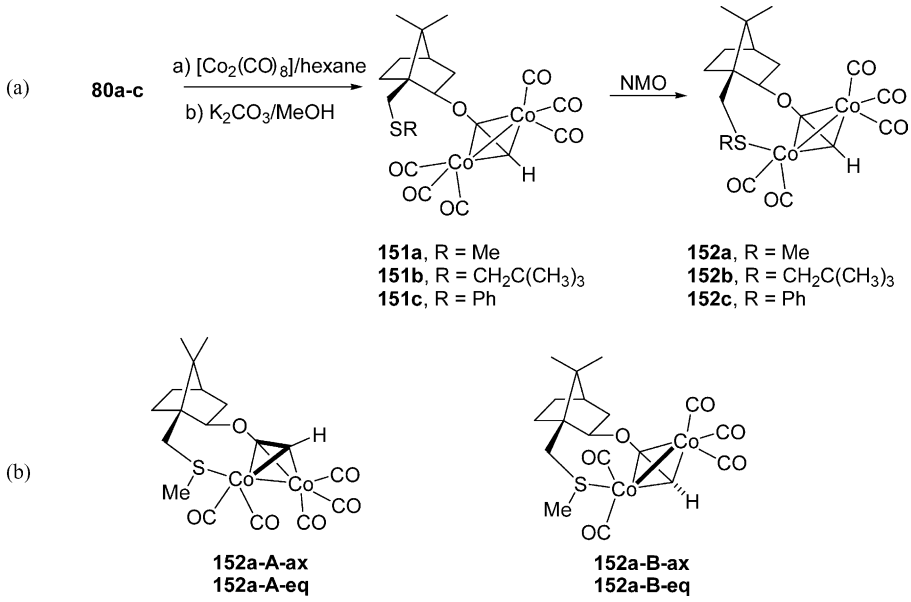

Scheme 13. (a) Synthesis of **151a**–**c** and **152a**–**c**. (b) Possible species for **152a**.

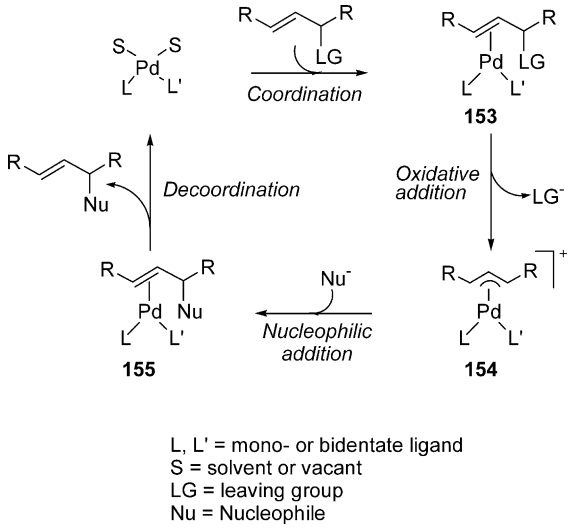

Scheme 14. Mechanism accepted for Pd-catalysed allylic substitutions with soft nucleophiles.

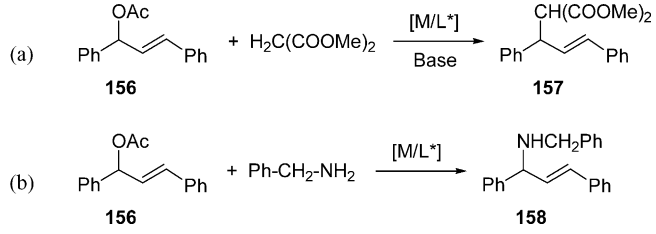

Scheme 15. Model allylic substitution reactions of **156** with soft nucleophiles: (a) dimethyl malonate (alkylation) and (b) benzylamine (amination).

possible diastereomers that can be formed it was proposed that the species **152a**–**A**–**ax** with the thioether methyl substituent in the more stable axial position would form in solution (Scheme 13b). These complexes were used in the internal Pauson–Khand reaction with strained olefins giving high yields and diastereoselectivities.

3. Catalytic processes with chiral thioether ligands

3.1. Allylic substitution

The Pd-catalyzed allylic substitution is one of the catalytic homogenous processes that has attracted most attention in recent decades and for which the catalytic cycle is well established [92] (Scheme 14). This is due in part to the relative ease of isolating catalytic intermediates, especially the palladium allylic species **154** (Scheme 14) although some related Pd(0) species (**155**, Scheme 14) have also been characterized in solution [93].

Consequently the enantioselectivity of the process with *soft* nucleophiles (those derived from conjugate acids with $pK_a < 25$) is controlled by the external nucleophilic attack on the more electrophilic terminal allylic carbon of **154**. Two model Pd-catalyzed allylic substitutions are pictured in Scheme 15. *rac*-3-Acetoxy-1,3-diphenyl-1-propene **(156)** is widely used as a substrate for alkylation reactions with dimethyl malonate (Scheme 15a) or for amination reactions with benzylamine (Scheme 15b) as nucleophile.

Since the first enantioselective catalytic process described by Trost in 1977 [94], many catalytic systems have been tested and have provided excellent enantiomeric excesses. Among the chiral ligands, bidentate nitrogen and phosphorus donors (either homo as heterodonors) are widely used [95–97]. However, other

Table 1
Pd-catalyzed allylic alkylations of *rac*-3-acetoxy-1,3-diphenyl-1-propene (**156**) with dithioether chiral ligands[a]

Entry	Ligand	%Conv. (days) [b]	%e.e. [c]	References
1	**1b**	74(7)	27 (R)	[36]
2	**6b**	100(2.5)	30 (S)	[36]
3	**6c**	100(7)	81 (S)	[36]
4	**7a**	100(1)	13 (S)	[36]
5	**7b**	100(1)	42 (S)	[36]
6	**8**	84(4.2) [d]	20 [e] (S)	[71]

[a] $[Pd(\eta^3\text{-}C_3H_5)Cl]_2$/L with dimethylmalonate under basic Trost conditions [158], CH_2Cl_2, r.t.
[b] Determined by ^{1}H-NMR based on substrate.
[c] %Enantiomeric excess determined by HPLC.
[d] Isolated yield.
[e] %Enantiomeric excess determined by ^{1}H-NMR with $[Eu(tfc)_3]$.

donor atoms such as sulphur or selenium [98–101], and monodentate ligands [102–107], have also exhibited very good catalytic behaviour. These processes are commonly catalyzed by palladium systems, but other metals, like molybdenum, rhodium or iridium, are also efficient, specially in regio and stereoselectivity control [92,108–110]. As far as thioether ligands are concerned, structural data (both in solution and solid state) of the allylic palladium intermediates have been reported for several types of ligands, mainly for heterodonors but for sulphur homodonors as well. The fact that a mixture of diastereomers can be obtained upon coordination of the thioether ligand to a metal (vide supra) can cause a decrease of stereoselection if the relative rates of the intermediates are similar. However, in spite of this feature, excellent enantiomeric excesses have been achieved.

Here we describe the catalytic data reported since the last review [12], followed by a comparison of structural information of the palladium intermediates involved in allylic substitution reactions and the selectivity observed in these catalytic processes.

3.1.1. S,S-Donor ligands

Up to now, chiral dithioether ligands have been shown to provide low to good enantioselectivities in the Pd-catalyzed allylic alkylation (Table 1). Among ligand backbones based on tartaric acid (**1**, **6** and **7**, Fig. 1), the five-membered heterocycle pyrrolidine **6c** afforded the best enantioselectivity (entry 3, Table 1) [36]. In contrast, the ferrocenyl-dithioether **8** (Fig. 1) gave low asymmetric induction (entry 6, Table 1) [71].

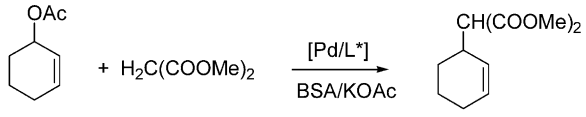

Scheme 16. Allylic alkylation of *rac*-3-acetoxy-1-cyclohexene with dimethyl malonate.

Table 2
Pd-catalyzed allylic alkylations of *rac*-3-acetoxy-1,3-diphenyl-1-propene (**156**) with thioether-oxazoline chiral ligands[a]

Entry	Ligand	%Conv. (hours) [b]	%e.e. [c]	References
1 [d]	**10b**	40(96)	97 (*S*)	[13]
2 [d]	**10d**	62(6)	96 (*S*)	[13]
3	**14b**	98(36)	93 [e] (*R*)	[113]
4	**11a**	98(3)	89 (*S*)	[14,114]
5	**11b**	98(10)	98 (*S*)	[14,114]
6	**12**	98(1)	89 (*R*)	[14]
7	**13a**	98(3)	90 (*S*)	[14,114]
8	**13b**	98(1)	90 (*S*)	[14]
9	**15a**	25(144)	20 (*S*)	[115]
10	**15b**	28(144)	60 (*S*)	[115]
11	**15c**	28(144)	75 (*S*)	[115]
12 [f]	**18**	98(32)	54 (*R*)	[100]
13 [f]	**19**	98(21.5)	63 (*S*)	[100]
14 [f]	**20**	98(1.5)	94 (*S*)	[100]
15 [g]	**23a**	93(48)	82 [h] (*S*)	[116]
16	**16**	100(72) [i]	45 (*R*)	[59]

[a] $[Pd(\eta^3\text{-}C_3H_5)Cl]_2$/L under basic Trost conditions [158], CH_2Cl_2, r.t.
[b] Catalyst precursor: $[Pd(\eta^3\text{-}1,3\text{-}PhC_3H_3Ph)(ligand)]PF_6$.
[c] S = MeCN.
[d] S = tetrahydrofuran.
[e] Isolated yields.
[f] Determined by ^{1}H-NMR based on substrate.
[g] %Enantiomeric excess determined by HPLC.
[h] %Enantiomeric excess determined by ^{1}H-NMR with $[Pr(hfc)_3]$.
[i] %Enantiomeric excess determined by ^{1}H-NMR with $[Eu(tfc)_3]$.

When ligands **7a**–**b** were applied in the Pd-catalyzed allylic alkylation of rac-3-acetoxy-1-cyclohexene with dimethyl malonate (Scheme 16) lower e.e.'s were observed (up to 34%) [57].

3.1.2. S,X-Donor ligands

Several types of heterodonor chiral ligands containing a thioether group have been developed for their application in asymmetric catalysis but in particular, S,N-, S,P- and S,Se-donors ligands have been tested in asymmetric allylic substitutions.

3.1.2.1. S,N-Donor ligands. In enantioselective allylic substitutions the most widely studied thioether bearing ligands have been the S,N-donor type [16–18]. Although chiral thioether-oxazolines (Fig. 2) have afforded excellent results, other combinations such as thioether-pyridine, thioether-imine and thioether-amine (Fig. 3) have also been investigated.

3.1.2.1.1. Thioether-oxazolines. Thioglucose-derived ligands containing a chiral oxazoline moiety (**10a**–**d**, Fig. 2) have been prepared and used as chiral ligands in palladium-catalyzed allylic alkylation of **156** (Scheme 15a) providing one of the best results achieved in this reaction with mixed S,N-donor ligands (selected data in Table 2, entries 1 and 2). Mild size effects of the thiosugar substituents on enantioselectivity were ob-

served however, if the thiosugar is replaced by a thiocyclohexyl group (**10e**, Fig. 2), the enantiomeric excess falls to 75% [13].

The success of systems of this kind seems to lie in the combination of thiosugar function with the proximity of all stereogenic units to the palladium allylic fragment because the Pd–N bond distance is shorter than the Pd–P distance in related phosphino-thiosugar palladium complexes [73,75].

Chiral ferrocenyl ligands have been developed by several groups for application in asymmetric catalysis [63–65,111,112]. In particular, three different kinds of thioether derivatives of ferrocenyloxazolines have been tested in asymmetric allylic alkylations. When the thioether group is tethered to oxazoline moiety (**14a–b**, Fig. 2) moderate to good levels of both yields and enantioselectivities were reached; the best asymmetric induction was obtained with **14b** (Table 2, entry 3) [113]. This is probably due to the increased in tether length between the donor atoms, which coordinate to palladium and bring the asymmetric environment closer to the allylic ligand in the catalytic species.

In a different approach, the thioether group is introduced into the cyclopentadienyl rings to produce 1,2- or 1,1′-disubstituted ferrocene derivatives. Chiral thioether ferrocenyl-oxazolines (**11a–e**, **12**, **13a–b**, Fig. 2) containing one stereocentre on the oxazoline ring have been prepared and successfully applied in palladium-catalyzed allylic alkylation (Table 2, entries 4–8). However, with ligands **11f–h** (Fig. 2) bearing achiral oxazoline substituents, lower enantioselectivities were observed (8–72%e.e.) [14,114].

Moreover, thioether ferrocenyl oxazolines without a stereogenic plane (**15a–c**, Fig. 2) afforded low enantioselectivities and poor yields (Table 2, entries 9 and 10 vs. entries 4, 7 and 5, 8) [115]. These results indicate that the matching effect between stereocentre and stereogenic plane in ferrocene-based S,N-donor ligands may provide high levels of enantioselectivity in palladium-catalyzed allylic substitutions.

This strategy was also used to design S,N-donor ligands based on the [2,2]paracyclophane backbone containing both stereogenic centre and plane (**18–20**, Fig. 2). These ligands were tested in allylic alkylation reactions and the highest catalytic activity was observed with the Pd/**20** catalytic system (Table 2, entry 14). The enantioselectivity obtained by using benzylic substituted cyclophane **20** was also better than the benzene ring substituted ligands **18** and **19** (Table 2, entries 14, 12 and 13, respectively). In addition, **18** with (S_P)-configuration afforded the alkylated product (*R*)-**157** whereas **19** with (R_P)-configuration provided (*S*)-**157** (Scheme 15a), even though both show the same stereocentre at the oxazoline group [100].

Chiral oxazoline thioether ligands with an axis-fixed (**21–22**) and -unfixed (**23**) biphenyl backbone (Fig. 2) have been prepared and applied in palladium-catalyzed allylic alkylation of **156** (Scheme 15a). In general, the activity of the catalytic systems with **21–22** was low; however with *R*-axial ligands activity improved. Good enantiomeric excesses (ca. 70%) were achieved with methylthio derivatives. Ligand **23a**, which has a free rotation biphenyl axis, afforded only one of two possible diastereomeric complexes with palladium and provided the highest activity and enantioselectivity (Table 2, entry 15) for this kind of chiral thio-oxazoline ligands [116]. This is probably due to the preferential formation of one of the axial palladium isomers containing the 1,3-diphenylallyl group, as observed for analogous palladium bis(oxazolines) systems [59].

Dithioether-bis(oxazoline) ligand **16** with an unfixed biphenyl backbone has also been used in allylic alkylation reaction [59]. In contrast to other analogous biphenyl derivatives, such as type-**23** ligands, the selectivity was lower (Table 2, entry 16 vs. entry 15) because of the different kind of coordination in the palladium intermediates (see Section 2.2.1.1).

3.1.2.1.2. Thioether-pyridines. There are only a few examples of chiral pyridine-derived bearing thioether functionalities and their application in enantioselective catalytic processes. The use of epimeric phenylthiotetrahydroquinolines **24a** and **24b** (Fig. 3) as chiral ligands in allylic alkylation model reactions (Scheme 15a) afforded enantioselectivities up to 83%e.e. [117].

Chiral thioalkyl-pyridine ligands containing a (*R*)-(−)-fenchone-derived moiety (**26a–e**, Fig. 3) have proven to be effective in the same catalytic reaction (Scheme 15a). Moderate to excellent levels of enantioselectivity (53–92%) have been attained in quantitative yields. The asymmetric induction of the catalytic reaction using (−)- or (+)-benzyl derivatives was further optimized to reach 96 and 98% of enantiomeric excess respectively [66].

In contrast, the activity and selectivity of palladium catalytic system with thiophenyl-pyridine ligands bearing a (+)-camphor-derived moiety (**28–30**, Fig. 3) were low but an enhancement of enantioselectivity up to 77%e.e. was observed if the pyridine ring contains a phenyl group on the 6-position [118].

The chiral ligand 1-(2-thiomethyl-1-naphthyl)isoquinoline **32** (Fig. 3) was synthesized and tested in the allylic alkylation of **156** (Scheme 15a). However, the palladium catalyst so formed, required 2 weeks for total conversion with e.e. only 2% [119].

3.1.2.1.3. Thioether-imines. A series of (*S*)-valinol-, (*R*)-phenylglycinol- and (*S*)-*tert*-leucinol-derived imine ligands containing a thioether group (**33a–m**, Fig. 3) have been developed and successfully applied in the palladium catalyzed asymmetric allylic alkylation affording up to 96% of e.e. in a good yield (Scheme 15a) [67]. The results showed that enantioselectivity is not sensitive to electronic effects caused by substituents on

Table 3
Pd-catalyzed allylic alkylations [a] and aminations [b] of *rac*-3-acetoxy-1,3-diphenyl-1-propene (**156**) with thioether-phosphine chiral ligands

Entry	Ligand	Nu [c]	T (°C)	%Conv. (hours) [d]	%e.e. [e]	References
1 [f]	**40**	DMM	r.t.	n.d.	88 (n.d.)	[72]
2 [f]	**43a**	DMM	r.t.	n.d.	64 (*R*)	[75]
3 [f]	**43b**	DMM	r.t.	73(72)	53 (*R*)	[75]
4	**39a**	DMM	20	99(0.16)	90 (*R*) [g]	[71]
5	**39a**	DMM	−20	99(24)	97 (*R*) [g]	[71]
6	**39a**	$BnNH_2$	20	93(24)	84 (*S*) [h]	[71]
7	**39a**	$BnNH_2$	−20	50(24)	94 (*S*) [h]	[71]
8	**51**	DMM	−30	80(24)	94 (*R*)	[123]
9	**52**	DMM	−30	82(24)	78 (*S*)	[123]
10	**51**	$BnNH_2$	−30	15(24)	86 (*S*)	[123]
11	**52**	$BnNH_2$	−30	27(24)	60 (*R*)	[123]

[a] $[Pd(\eta^3\text{-}C_3H_5)Cl]_2$/L under basic Trost conditions [158], CH_2Cl_2.
[b] $[Pd(\eta^3\text{-}C_3H_5)Cl]_2$/L, $BnNH_2$, CH_2Cl_2.
[c] Nu: dimethylmalonate (DMM) or benzylamine ($BnNH_2$).
[d] Isolated yields.
[e] %Enantiomeric excess determined by HPLC.
[f] Catalytic runs as Ref. [159].
[g] %Enantiomeric excess determined by ^{1}H-NMR with $[Eu(tfc)_3]$.
[h] Enantiomeric excess determined by ^{1}H-NMR with Pirkle alcohol.

the imine group whereas the steric bulk in *ortho*-position of aryl group attached to imine has a subtle effect. The bulkiness of the aryl substituent at sulphur (**33k**) provided the highest enantioselectivity of all the ligands investigated (96%e.e.); however, the replacement by a methyl group (**33j**) only reduced the enantiomeric excess to 90%. The increase of steric hindrance of the backbone (**33m**) caused both the e.e. and yield to fall [67,120].

3.1.2.1.4. Thioether-amines. Chiral 1,2-aminothioethers derived from (*S*)-valinol were tested in allylic alkylation reaction but they were not active [120]. In contrast, the activity with norephedrine-based 1,2-aminothioethers ligands (**34a**–**g**, Fig. 3) improved notably even though the levels of enantioselectivities were low (9–15%e.e.). Only with the *tert*-butyl derivative was a good asymmetric induction (72%e.e.) achieved [121].

3.1.2.2. S,P-Donor ligands. Different combinations of S,P-donor ligands such as thioether-phosphine (Fig. 4), thioether-phosphite and thioether-phosphinite (Fig. 5) have been studied. In many cases they have proven to be effective in enantioselective Pd-catalyzed allylic substitutions.

3.1.2.2.1. Thioether-phosphines. The ferrocenylphosphine thiosugar ligand **40** (Fig. 4) with multiple stereogenic units afforded an e.e. of 88% in the palladium allylic alkylation (Table 3, entry 1) [72]. However, when the thiosugar moiety was the sole stereogenic unit on S,P-ligand (**43a**–**b**, Fig. 4) only moderate enantioselectivities were achieved (Table 3, entries 2 and 3). Good activities but low enantiomeric excesses were obtained with a similar thioether-phosphine ligand using a stereogenic norboneol fragment (**42**, Fig. 4), but the authors attributed their performance to the effects of size chain between sulphur donor and the kind of stereogenic unit [73,75].

By changing the stereogenic centre to the β-position of the side chain of ferrocenylthiophosphine (**39a**, Fig. 4) the enantioselectivity was improved significantly (Table 3, entries 4 and 5 vs. entry 1). Higher selectivities were also obtained in allylic amination (Scheme 15b) using ligand **39a** (Table 3, entries 6 and 7) [71].

A series of (*S*)-proline-derived phosphine ligands bearing thioether functionalities (**48**–**50**, Fig. 4) were prepared and applied in palladium catalyzed asymmetric allylic alkylation (Scheme 15a) affording enantioselectivities from 31 to 88% of (*S*)-**157** depending on the steric bulkiness of sulphur atom substituents [101,122].

Recently, chiral phosphinooxathiane ligands **51**–**53** (Fig. 4) have been successfully used in alkylation and amination reactions of substituted allyl acetates [123]. The chiral norbornane-phosphinoxathianes provided moderate to excellent levels of enantioselectivity in allylic alkylation of **156** (Table 3, entries 8 and 9) and enantioselectivities of 13–85% with low regioselectivities to the branched product in the allylic alkylation of cinnamyl acetate. The allylic amination reaction (Scheme 15b) was also explored with these chiral phosphinooxathianes (Table 3, entries 10 and 11).

3.1.2.2.2. Thioether-phosphites. Thioether-phosphite ligands with a furanoside backbone (**55a**–**c**, Fig. 5) have proven to be effective in the model enantioselective palladium-catalyzed allylic alkylation and amination substitutions (Scheme 15) providing up to 58 and 67%e.e., respectively. In this case, both functionalities have similar donor properties, but the catalytic results indicate that the thioether moiety hardly affects the enantioselectivity. It is then assumed that the nucleo-

Table 4
Pd-catalyzed allylic alkylations [a] and aminations [b] of *rac*-3-acetoxy-1,3-diphenyl-1-propene (**156**) with thioether-phosphinite chiral ligands [15,84]

Entry	Ligand	Nu [c]	T (°C)	%e.e. [d]
1	**57a**	DMM	−20	91 (*S*)
2	**57b**	DMM	0	42 (*S*)
3	**57j**	DMM	0	91 (*S*)
4	**58a**	DMM	−20	98 (*S*)
5	**58b**	DMM	0	70 (*S*)
6	**58j**	DMM	0	81 (*S*)
7	**59a**	DMM	−20	30 (*S*)
8	**59d**	DMM	−20	93 (*S*)
9	**60b**	DMM	−20	75 (*S*)
10	**61b**	DMM	−20	69 (*S*)
11	**57a**	$BnNH_2$	−20	99 (*S*)
12	**58a**	$BnNH_2$	−20	95 (*S*)

[a] $[Pd(\eta^3\text{-}C_3H_5)Cl]_2$/L under basic Trost conditions [158], CH_2Cl_2. Quantitative yields in 3 h.
[b] $[Pd(\eta^3\text{-}C_3H_5)Cl]_2$/L, $BnNH_2$, CH_2Cl_2.
[c] Nu: dimethylmalonate (DMM) or benzylamine ($BnNH_2$).
[d] %Enantiomeric excess determined by HPLC.

philic attack takes place *trans* to the thioether group [52].

The allylic alkylation reactions of unsymmetrical substrates catalyzed by palladium, rhodium and iridium complexes containing a chiral binaphthylphosphite-thioether ligand **56** (Fig. 5) was investigated [83]. Yields of up to 70% were achieved but, in all cases, the palladium catalysts were more active than the rhodium and iridium systems. Both, the regio and enantioselectivities, were moderate and, in general, high enantioselectivities were accompanied by low regioselectivities.

3.1.2.2.3. Thioether-phosphinites. A family of mixed S,P-donor ligands **57**–**63** (Fig. 5) has been synthesized and successfully applied in the enantioselective palladium catalyzed allylic substitutions [84]. Electronic and steric effects of the ligands on the enantioselectivity of the allylic alkylation reaction were studied varying sulphur, backbone and phosphorus substituents (selected data in Table 4, entries 1–10). The best results were reached with **57a** and **58a** containing bulky alkyl substituents in both backbone and thioether group to control the sulphur inversion. As is shown in Table 4 (entries 11 and 12), higher enantioselectivities were also achieved in allylic amination using **57a** and **58a**. Varieties of other heteroatom nucleophiles in allylic substitution of *rac*-3-acetoxy-1,3-diphenyl-1-propene were investigated but low yields and enantioselectivities were attained [84].

The alkylation and amination of 1,3-dialkylpropenyl substrates employing **58a** were sensitive to the size of the alkyl substituents of the allyl, obtaining better enantioselectivities in the order $^i\text{Pr} > \text{Pr} \gg \text{Me}$. When the even bulkier 1,3-dicyclohexylpropenyl was used as substrate no product was observed [84].

The regioselective allylic alkylation of trisubstituted propenyl acetates was also explored with **57a** and **58a** affording high yields and asymmetric inductions up to 94%e.e. [84]

In addition, this family of mixed phosphorus/sulphur ligands were tested in the palladium catalyzed allylic substitution of cyclic substrates. The dependence of enantioselectivity on the size of sulphur and phosphorus substituents, and on the relative stereochemistry and the size of the groups attached to ligand backbone was investigated. The allylic alkylation of rac-3-acetoxy-1-cyclohexene with dimethyl malonate (Scheme 16) using **57a** gave the alkylated product in 90%e.e. with yields higher than 90%. Moreover, the replacement of the phenyl substituents of phosphinite moiety by a bulkier α-naphthyl group (**60c**) improved the enantioselectivity up to 94%. Excellent results (91%e.e., 97% yield) were also obtained in the allylic amination of the same substrate with benzylamine. The allylic alkylation and amination of others cycloalkenylacetates were accomplished with **60c** affording enantiomeric excesses of 91–97% in quantitative yields [15,84].

3.1.2.3. S,Se-Donor ligands. To our knowledge, there is only one example of the application of mixed chalcogen atoms to the asymmetric allylic alkylation of **156** (Scheme 15a) [71]. The chiral ferrocenyl thioselenoether **37** (Fig. 3) displayed low reactivity and selectivity (44%e.e.) though the selectivity was better than that of the analogous ferrocenyl dithioether **8** (20%e.e.). The authors attribute the low reactivity of these systems to the weak π-acceptor abilities of the sulphur and the selenium groups [71].

3.1.3. S,X-Polydentate ligands

The catalytic performance of a series of tridentate chiral pyridine dithioether **27a**–**e** (Fig. 3) in the model allylic alkylation reaction (Scheme 15a) has been investigated. The alkylated product was obtained in high yields and good enantiomeric excesses (78–85%e.e.); however, except for the dithiomethyl derivative, the activity and the enantioselectivity were slightly lower than those obtained with analogous bidentate thioether-pyridine [66].

Chiral dithioether-bipyridine **31** (Fig. 3) was also evaluated in the same catalytic reaction. Its activity was comparable to that of the related ligand **26** (Fig. 3) but the enantiomeric excess was poorer (48%e.e.) [118].

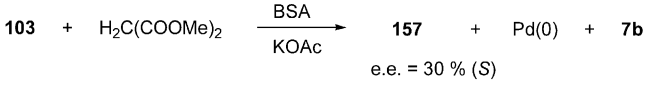

Scheme 17. Stoichiometric allylic alkylation for **103**.

3.1.4. Mechanistic aspects

In this part we have selected the most relevant structural information of the palladium intermediates, mainly in solution, in order to relate the catalytic data to the selectivity of the catalyzed allylic substitution.

3.1.4.1. S,S-Donor ligands. Two research groups have studied chiral homodonor dithioether ligands in allylic substitution reactions. Enders et al. tested a S,S-bidentate ligand with a ferrocenyl backbone (**8**, Fig. 1), obtaining low asymmetric induction for the model allylic alkylation reaction of Scheme 15a (20%e.e., see above), in contrast to their analogous S,P-derivatives (**39a**–**e**, Fig. 4) [71]. However S,S-homodonor ligands containing rigid five-member heterocycle backbones (*O*-isopropylidene and pyrrolidine, ligands **1a**–**c**, **6a**–**c**, **7a**–**b**, Fig. 1) induced up to 81% of e.e. [36]. In order to understand their catalytic behaviour, the structure of 1,3-diphenylallyl palladium intermediates, **103** (Fig. 23) and **100** (Fig. 18) were studied (see 2.1.2.3).

As previously mentioned (Section 2.1) **103** shows, in solution, the existence of two allylic species (ratio ca. 7:3, d.e. = 40%), due to the relative position of the central allylic carbon and the isopropylidene ring, *exo* and *endo*. Stoichiometric alkylation with **103** and dimethyl malonate, under basic conditions (Scheme 17), gives **157** (Scheme 15a) with comparable enantiomeric excess that obtained under catalytic conditions (ca. 30% vs. 42%, respectively). The good matching between diastereomeric excess of **103** (d.e. = 40%) and enantiomeric excesses for both catalytic and stoichiometric alkylation, as well as the absolute configuration obtained for the alkylated product ((*S*)-**157**), have led to the suggestion that the *exo* isomer is the major species, assuming that the nucleophilic attack rate on the allyl moiety is similar for both diastereomers. However, the existence of several intermediates for **100**, containing **6c** (see above) does not prevent high e.e. for the catalytic reaction (81% (*S*)). This was probably due to a kinetic control of the external nucleophilic attack.

3.1.4.2. S,N-Donor ligands.

3.1.4.2.1. Thioether-oxazolines. Structural data related to allylic intermediates containing thioether-oxazolines are reported for thioglucose-oxazolines [13] and thioether derivatives of ferrocenyl-oxazolines [14,114].

^{1}H-NMR spectra of 1,3-diphenylallyl palladium complexes **106e** and **106a**–**b** containing ligands **10e** and **10a**–**b**, respectively (Fig. 26), show the existence in solution of a mixture of diastereomers, in the ratios 1:0.8 (**106e**), 1:0.9:0.04 (**106a**) and 1:0.6:0.02 (**106b**). The two major isomers are assigned (by NOE contacts and anisotropic effects induced by the allyl group) to *syn*/*syn*/*exo* and *syn*/*syn*/*endo* arrangements, respectively [13].

Regarding the S-configuration, and in contrast to the known low inversion barrier at the sulphur centre, Pregosin et al. indicate that the oxazoline substituent (isopropyl) and the sugar moiety are on the same side of the S–Pd–N coordination plane. This was attributed to the substantial space required for the sulphur lone pair [124]. ^{13}C-NMR terminal allyl chemical shifts for the three complexes show that the allyl carbon *trans* to sulphur atom exhibits a higher frequency than for the allyl carbon *trans* to the nitrogen, the difference between the two is higher for the *endo* isomer. Then, assuming that the higher frequency signal corresponds to the more electrophilic terminus, the nucleophile mainly attacks the *endo* isomer, *trans* to the S atom. Taking into account that the enantioselectivity of the catalytic process is governed by the external nucleophilic attack on these allylic complexes (e.e. up to ca. 97%), which are in equilibrium (d.e. up to ca. 25%), one of the diastereomers must react faster than the others, in this case the *endo* one.

For palladium complexes containing thioether derivatives of ferrocenyl oxazolines **107a** (Fig. 27) and **108** (with ligands **11b** and **13b**, respectively), the structural characterization in solution (COSY, ^{13}C–^{1}H correlation and 2D NOE NMR experiments) shows that the complexes also exist as a mixture of two isomers. These are the *syn*/*syn* isomers with respect to the relative position of the phenyl allyl groups (as indicated by the coupling constants between the allyl protons), but with different relative positions of the central allyl C–H bond to the ferrocene core (*endo*, pointing to; *exo*, pointing away) [14,114]. These studies have led to the proposal that the major structure is of the M-type (Scheme 18), which is the same conformation as the X-ray solid-state structure for **107a** (Scheme 18).

^{13}C-NMR chemical shifts, as indicated above, are very useful for identifying the more electrophilic allyl terminus, which is *trans* to sulphur atom for each isomer. As shown in Scheme 18, the largest difference corresponds to the M-conformation for **107a** ($\Delta(\delta) =$ 17.7 ppm) and W-conformation for **108** (($\Delta(\delta) = 16.9$

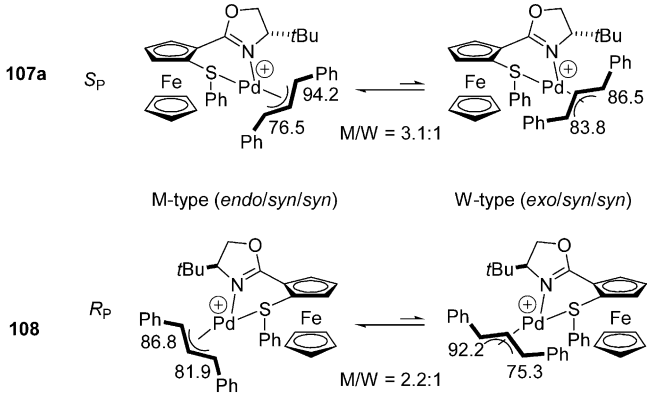

Scheme 18. 1,3-diphenylallyl palladium isomers for cations **107a** and **108**. Figures indicate ^{13}C NMR chemical shifts (ppm) of the terminal allyl carbon atoms.

ppm). Together with the X-ray data (bond distances Pd–C_{allyl} terminus *trans* S > Pd–C_{allyl} terminus *trans* N (see Section 2.2.1.1)), sulphur induces a higher *trans* influence than the iminic nitrogen atom. These structural data are in agreement with the absolute configuration observed for the substitution product obtained in the model catalytic reaction, (*S*)-**157** (Scheme 15a). Comparing diastereomeric excesses of the Pd intermediates and enantiomeric excesses of **157**, we observe that e.e.'s are higher than d.e.'s, indicating that M-**107a** must react faster than W-**107a** and W-**108** faster than M-**108**.

3.1.4.2.2. Thioether-pyridines. Kellogg et al. [66] studied the catalytic behaviour of thiol- and thioether-pyridine derivatives. They obtained very high enantioselectivities (up to 98%e.e.) in the model allylic alkylation process using thioethers **26a**–**e** and **27a**–**e** (Fig. 3). However, the analogous thiol- and bis(thiol)-pyridine ligands showed very low activity, probably due to the deprotonation of thiol groups under basic medium. To explain the chiral recognition of the above mentioned thioether-pyridine systems, the authors tried to prepare allyl palladium complexes with thioether- and bis(thioether)-pyridine ligands. Nevertheless, for the latter systems, the allyl complex seemed to be too labile and degraded to give the chloro complex **143** containing ligand **27e**, whose X-ray structure shows the S,N,S-tridentate coordination to the metal (Fig. 47). In the case of mono-thioether ligands, for which the best enantioselectivities were obtained, precursor complex **111** (Fig. 31) containing ligand **26c** (Fig. 3) was isolated, showing, in solution, a mixture of two isomers, *endo* and *exo* (in a ratio 3:4) depending on the relative position of the allyl and thioether substituents. No stereochemical conclusions can be deduced, because the intermediate species are unknown.

3.1.4.2.3. Thioether-imines. Anderson et al. [67] used Pd containing chiral thioether-imine ligands as effective catalytic precursors (e.e. up to 96%). In contrast to other chiral S,N-donor ligands (see above), the authors proved that, for these systems, nucleophilic attack on the allyl group is not *trans* to the sulphur atom, but *trans* to the imine donor, and so the enantioselectivity is controlled by the steric environment of the chelate ligand, more than by electronic effects. The X-ray structure of complex **112** (Fig. 32) containing ligand **33e** (Fig. 3) shows that the allyl group adopted a W conformation and the sulphur phenyl substituent is *trans* to the isopropyl group, avoiding an unfavourable interaction. In addition one structure is mainly present in solution, which shows a *syn*/*syn* allyl arrangement with a W conformation (Fig. 32). The two bond distances Pd–C allyl terminus are very similar and the difference of ^{13}C-NMR chemical shifts for terminal allyl carbon atoms is small ($(\Delta(\delta) = 3$ ppm). Both pieces of data indicate the relatively higher *trans* influence of the sulphur atom compared to the iminic nitrogen. Keeping in mind the absolute configuration of the organic product, (*R*)-**157** (Scheme 15a), if **112** is the only species present in solution, the nucleophile must mainly attack the allyl terminus *trans* to nitrogen atom. In addition, the proposed late Pd(0) intermediate species leads to stabilization of the less steric demanding complex, which forms when the nucleophile attacks on the allyl terminus *trans* to nitrogen atom.

3.1.4.3. S,P-Donor ligands.

3.1.4.3.1. Thioether-phosphine. Pregosin et al. have used several thioether-phosphino ligands (**42** and **43a**–**b**, Fig. 4) in the allylic substitution process with the model substrate, obtaining moderate enantioselectivities [73,75]. The 1,3-diphenylallyl palladium complexes [Pd(η^3-1,3-PhC_3H_3Ph)(**42**)]BF_4 (**116b**), [Pd(η^3-1,3-PhC_3H_3Ph)(**43a**)]BF_4 (**117b**) and [Pd(η^3-1,3-PhC_3H_3Ph)(**43b**)]BF_4 (**117c**) (Fig. 50) were obtained as a mixture of isomers. These can be the *exo* and *endo* isomers (depending on the relative position of the allyl moiety and the sulphur substituent, the *exo*-norborneol or the sugar group) and the *syn*/*syn* and *syn*/*anti* isomers (depending on the allyl configurations). For complexes **116b** and **117c**, two of the different possible isomers are observed with ratios of 4:1 and 4:3, respectively, while for **117b** up to four isomers are detected (46:45:6:3).

^{13}C-NMR data for **116b**, **117b** and **117c** show that the terminal allyl chemical shifts for the carbon *trans* to sulphur are at lower frequency than those for the allyl terminus *trans* to the P-donor (ca. 76–89 vs. 95–104 ppm). However, the chemical shifts corresponding to the terminal carbon *trans* to sulphur are not very different from those reported for (1,3-diphenylallyl)palladium complexes containing bidentate bisphosphines, like (*S*,*S*)-CHIRAPHOS (**159**, Fig. 51) (88.1 and 90.1 ppm) [125] or JOSIPHOS (**160**, Fig. 51) (65.6–78.2 ppm) [126]. Dynamic studies for **116b**, **117b** and **117c** indicate that the η^3-η^1-η^3 isomerization occurs by dissociation of the carbon *trans* to sulphur and *cis* to phosphorus, in contrast to the non-substituted allyl complex, **116a**, due to the steric hindrance between the PPh_2 group and the phenyl allyl substituent [73]. From these results the authors suggest that this isomerization process is controlled sterically, not electronically.

Better results were obtained with chiral ferrocenyl S,P-donor ligands containing a stereogenic plane as well as stereogenic centres in the sulphur group, achieving 97%e.e. As discussed above, the solid state structure of the 1,3-diphenylallyl complex **115a** (Fig. 35), shows a significantly rotated allyl group, where the terminal allyl carbon *trans* to phosphorus atom is clearly below the coordination plane (Fig. 36) [72]. This type of structure, which is also the main species in solution (in which two species are present), 'prepares' the olefin Pd(0) late-

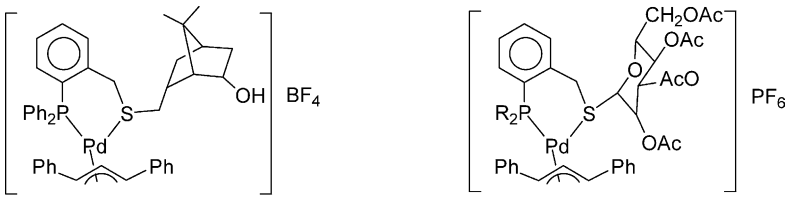

Fig. 50. Complexes **116b**, **117b** and **117c**.

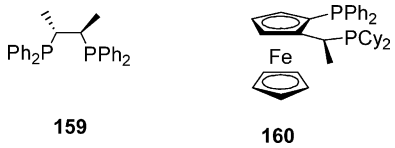

Fig. 51. Phosphines **159** and **160**.

intermediate (**155**, Scheme 14), leading to the nucleophilic attack *trans* to the phosphine moiety.

The ferrocenyl ligands **39a–e** (Fig. 4) with a stereogenic in β-position of the side chain provided excellent asymmetric inductions (up to 97%) [71]. Small substituents on thioether groups favour the nucleophilic attack in *cis* position to the S-donor moiety in the palladium intermediates, as is shown by the structural studies for **114** (Fig. 34) containing ligand **39a**. In solution, this complex shows in solution four isomers (ratio ca. 86:9:3:2), the major species being assigned unambiguously, by NMR experiments, to the *exo*/*syn*/*syn* isomer. For this species, the ^{13}C chemical shift for the allyl terminus *trans* to the phosphorus atom (102.5 ppm) indicates a much more electrophilic behaviour than those *trans* to sulphur atom (78.2 ppm). The X-ray structure also presents this arrangement. Like **115a** (Fig. 36a), the 1,3-diphenylallyl group is also rotated (0.447 Å) below the coordination plane P–Pd–S and the higher enantiomeric excess (97% vs. 88%) is explained by the intramolecular C–H···π-arene interactions between one allylic phenyl group with the *exo*-phenyl group of the PPh_2 moiety and the other allylic phenyl group with an SCH_3 proton. These structural features mean that the nucleophilic attack is mainly on the allyl terminus *trans* to the phosphorus atom.

3.1.4.3.2. Thioether-phosphinite. As stated above, Evans et al. designed chiral thioether-phosphinite ligands (**57–63**, Fig. 5) which achieve excellent yields and selectivities in allylic alkylations and aminations, with open and cyclic allylic esters [15,84]. Related to these ligands, two allylic palladium intermediates **138b** and **139** have been characterized, in solution and solid state (Fig. 44). The X-ray diffraction data indicate that Pd–C allyl terminus bonds are longer for those carbon atoms *trans* to phosphinite moiety than *trans* to sulphur group, in agreement with a stronger *trans* influence of the phosphinite group [2,127]. In solution, **138b** exists as a mixture of two diastereomers, in a 2.3:1 ratio, due to the relative position of the central allylic carbon and the *tert*-butyl substituent on the sulphur moiety. The major isomer is assigned to *exo* arrangement (both groups pointing in the same direction) by NOE data; which is consistent with the structure observed in solid state. The difference between the diastereomeric ratio and the enantioselectivity observed in the model allylic alkylation (d.e. = 39% vs. e.e. = 98%) indicates that the nucleophile reacts faster with the *exo*-isomer than the *endo* one, because of the strain between the S-substituent and the allylic phenyl group for the *exo* isomer. Upon addition of the nucleophile, the late Pd(0) species formed is favoured because of the loss of steric hindrance between olefin (**155**, Scheme 14) and the chiral S,P-donor ligand.

The Pd-catalyzed allylic substitutions of acyclic substrates were tested with a large variety of ligands giving excellent enantioselectivities [92]. However, often ligands that lead to almost optically pure substitution products, afford low asymmetric inductions when cycloalkenyl acetates are used, with the important exception of ligands developed by Trost, which generate a stereogenic pocket around the metallic centre and are effective for both acyclic and cyclic substrates [94,128]. Evans et al. also tested these thioether-phosphinite ligands in the allylic substitution of cycloalkenyl acetates, obtaining very high enantiomeric excesses (see above). In contrast to **138b**, NMR data of complex **139** reveal the presence of only one allyl palladium isomer (ratio >98:2), consistent with the X-ray structure. However, the e.e obtained in the allylic substitution of the rac-3-acetoxy-1-cyclohexene using dimethyl malonate as nucleophile (Scheme 16) was 90%e.e., which is lower than expected for a diastereomeric pure complex.

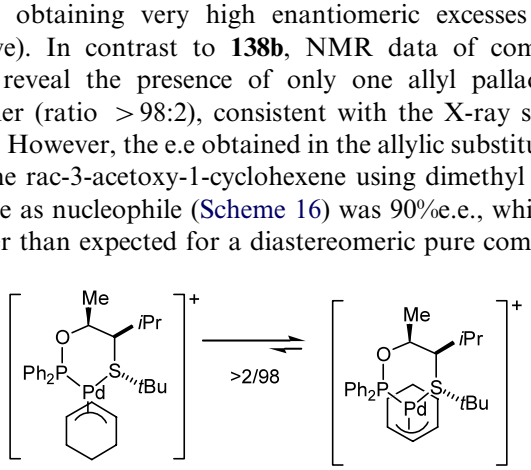

139

Scheme 19. Isomers of cation complex **139**.

The absolute configuration of the product indicates that the nucleophilic attack is in *trans* to the phosphorus group. The reason for this low stereoselectivity can be found in the existence of the minor more reactive isomer, as is evidenced by the NMR spectra of **139** (Scheme 19). This feature is also supported by the complex containing the isomer of **57a** [Pd(η3-cyclohexenyl) (**58a**)]$^+$, for which the enantioselectivity (38% e.e.) and the diastereomeric ratio (72% d.e.) indicates higher reactivity towards the nucleophile of the minor species [84]. This observation is clearly in contrast to the trend observed for acyclic substrates.

3.2. Hydrogenation

The asymmetric hydrogenation of prochiral compounds catalyzed by chiral transition metal complexes has been in widespread use in stereoselective organic synthesis and some processes have found industrial applications [129–131]. Over the years, the scope of this reaction has been gradually extended in terms of both reactant structure and catalyst efficiency. Phosphorus ligands are among the most widely used chiral ligands in this process [129]. However, reports of catalytic asymmetric hydrogenation reaction using thioether ligands are scarce. In this section we first describe the application of dithioether ligands and finally the mixed thioether-phosphorus ligands.

3.2.1. S,S-Dithioether ligands

The use of chiral dithioethers in asymmetric hydrogenation has been reported in a number of studies [11,12,132]. In particular **1a**–**c**, **5a**–**c**, **6a**–**c** and **7** (Fig. 1) have shown low to moderate enantioselectivities (from 6 to 68%) in the enantioselective iridium catalyzed hydrogenation of itaconic acid (**161**, Scheme 20) under mild conditions (Table 5). The results indicate that the structure of the ligand backbone, the size of the metal chelate ring and the R substituents influence the activity and enantioselectivity of the process. The enantiomeric excess is higher for **5** [31] and **6** [32] with a more rigid backbone, than for the derivatives **1** [27] which form a more flexible seven-membered chelate ring. However, the results in Table 5 do not show obvious trends based on the R substituents. Thus, for precursors containing ligands **1** and **5** enantiomeric excesses are the highest when bulky and electron rich isopropyl substituents are present in the thioether groups; for ligands **6** the best enantioselectivity is obtained with phenyl groups bonded to the sulphur atoms. Unexpectedly, the bicyclic dithioethers **7**, in which the sulphur inversion is fixed, showed lower activity and enantiomeric excess than the related more flexible ligands **1** [30]. These results suggest that further modification of the steric and electronic properties in the alkyl chain of ligands **7** would give higher e.e.'s and activities.

On the other hand, in contrast to phosphine systems [133], dithioether catalytic systems had higher rates and optical inductions with acid substrate, as itaconic acid, than with substrates with an amido group such as (*Z*)-α-(acetamido)cinnamic acid and methyl α-(acetamido)acrylate dithioether systems (data not shown).

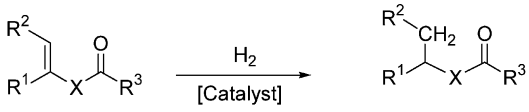

161, R^1 = COOH, R^2 = H, X = CH_2, R^3 = OH
162, R^1 = Ph, R^2 = CH_3, X = NH, R^3 = CH_3

Scheme 20. Hydrogenation of **161** and **162**.

Table 5
Asymmetric hydrogenation of itaconic acid (**161**) and *N*-acetyl-1-phenylethenamine (**162**) with $[Ir(COD)_2]BF_4$/**1**, **5**–**7** [a] and $[Rh(NBD)_2]SbF_6$/**9** [b]

Entry	Ligand	Substrate	P_{H_2} (bar)	%Conv. (hours) [c]	%e.e. [d]	References
1	**1a**	**161**	1	100 (24)	22 (*S*)	[27]
2	**1b**	**161**	1	91 (6)	47 (*S*)	[27]
3	**1c**	**161**	1	100 (4)	6 (*S*)	[27]
4	**5a**	**161**	1	35 (12)	14 (*R*)	[31]
5	**5b**	**161**	1	100 (12)	62 (*R*)	[31]
6	**5c**	**161**	1	100 (12)	17 (*R*)	[31]
7	**6b**	**161**	1	100 (2)	35 (*R*)	[32]
8	**6c**	**161**	1	100 (2.5)	68 (*R*)	[32]
9	**7a**	**161**	1	33 (19)	14 (*R*)	[30]
10	**7b**	**161**	1	13 (19)	9 (*R*)	[30]
11	**9a**	**162**	4	37 (24)	18 (*S*)	[132]
12	**9b**	**162**	4	95 (24)	21 (*S*)	[132]

[a] Substrate/Ir = 40, CH_2Cl_2 = 6 ml, T = 25 °C.
[b] The catalyst was prepared in situ in methanol {substrate (0.5 mmol/[Rh]/ligand = 1:0.01:0.011}.
[c] % Conversion measured by GC.
[d] %Enantiomeric excess measured by polarimetry.

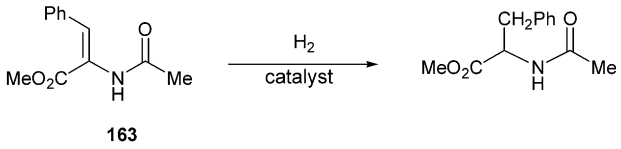

163

Scheme 21. Hydrogenation of **163**.

Dithioethers **9a** and **9b** (Fig. 1) related to **1** have recently been described [132]. These ligands have been reported to be more rigid than **1** derivatives, due to the presence of the 1,4-dioxane six-membered conformationally rigid ring compared with the flexible 1,3-dioxolane five-membered ring in **1**. These ligands showed moderate to low enantioselectivities (Table 5, entries 11 and 12) in the asymmetric hydrogenation of N-acetyl-1-phenylethenamine (**162**, Scheme 20) using rhodium based catalysts.

3.2.2. S,P-Donor ligands

Although asymmetric induction by heterodonor ligands (such as P,O-, P,N- and P,S-) has been an efficient strategy to improve enantioselectivity, only the mixed thioether-phosphorus ligands have been used with limited success in asymmetric hydrogenation.

Systems $[Rh(COD_2)]^+$/**64a**–**d** (Fig. 5) were the first examples of transition metal catalysts containing a P,S-donor ligands (thioether-phosphinites) used to hydrogenate prochiral olefins [85]. Moderate enantioselectivities were achieved in the hydrogenation of methyl α-acetamidocinnamate (Scheme 21). The enantiomeric excess is the highest for the bulky and electron-rich ligand **64b** (55%).

Lately, a series of mixed thioether-phosphine ligands based on the chiral episulphides (**44**, Fig. 4) [77] and thioether-phosphite ligands with a xylofuranose backbone (**55**, Fig. 5) [81] have been used in the asymmetric hydrogenation of α-enamide methyl esters and itaconic acid, providing enantioselectivities up to 51%.

3.3. Transfer hydrogenation

Reduction of prochiral ketones is one of the most attractive methods for preparing secondary chiral alcohols (Scheme 22). Transfer hydrogenation reactions using primary and secondary alcohols (e.g. 2-propanol, benzyl alcohol, 1-phenylethanol) or formic acid/triethyl amine as hydrogen sources, are practical procedures for avoiding the use of molecular hydrogen and mild conditions can be applied [134]. Two general reaction paths are accepted for hydrogen transfer reactions: the hydridic route (Scheme 23a) and the direct route (Scheme 23b) [135–137].

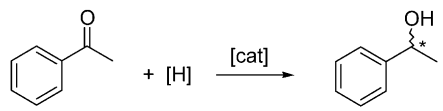

164

Scheme 22. Transfer hydrogenation of acetophenone **164**.

Rh systems with the atropoisomeric binaphthyl derivatives thioether-phosphine (*R*)-**38a**–**b** (Fig. 4) [68,138] provided low conversions (15–25% after 1 h reaction time) and low e.e. (20% (*R*) with **38b**) in the reduction of acetophenone using $[Rh(\mu\text{-OMe})(COD)]_2$ as catalyst precursor in 2-propanol/KOH basic mixture. Although the analytical data for [Rh(**38a**)(COD)]OTf (**113**, Scheme 3) provided only one diastereomer in solution the chiral induction was not very effective. Nevertheless, the bulkier substituent isopropyl provided somewhat higher e.e. (20% with **38b** vs. 14% with **38a**). With longer reaction times the racemization of the 1-phenylethanol occurred due to the base. When the Ir(I) system, prepared in situ from $[Ir(\mu\text{-Cl})(COD)]_2$/**38b** was used, the conversion (6%) and e.e. (11%) were very low.

The C_2 sulphur bridged bis(ferrocenyl) ligand **70** (Fig. 7) was prepared [87]. The conversion and enantioselectivity obtained with ruthenium complex **145** (Fig. 48) using ^{i}PrOH/^{i}PrOK at reflux was 24.2% (3 h) and 20.1% (*R*) e.e., respectively. For related systems with bis(ferrocenyl)phosphino ligands it was observed that increasing the temperature the e.e. decreased, probably due to racemization. Therefore, the low e.e. obtained with the diphosphinothioether system **70** may be due to the fact that it is only active at reflux temperature. Compared to the related diphosphinothioether systems the thioether derivative is less active but the e.e. is similar.

Racemization of the alcohol can be avoided by the use of the formic acid/triethylamine system, which forms CO_2. This hydrogen source was used in the asymmetric hydrogenation transfer of acetophenone using iridium complexes with ligands **35** (Fig. 3) derived from L-cysteine and the e.e. were invariant during the reaction time. Achiral model Ir-amino thioether systems showed higher activities than the corresponding analogous diamines [139]. The S,N-coordination of the aminothioether ligands was assumed since analogous alcohol amines were not active at the same conditions. The chelate ring size had influence in the activity of the system since the conversion achieved with the 6-membered chelate ligand L-methionine was lower. Thus a series of chiral ligands based on L-cysteine with variation of R^1–R^5 substituents (**35a**–**i**, Fig. 3) was prepared and their catalytic activity in the reduction of acetophenone studied. System Ir/**35a** provided high activity (98% after 1 h) and low e.e. 12% (*S*).

The influences of the R^1–R^5 substituents can be summarized as follows: (i) sterically demanding substituents R^1–R^3 did not affect the e.e. (12%e.e. with **35a** vs. 5%e.e. with **35b** or vs. 7%e.e. with **35c**). This was attributed to their relatively remote position respect to the substrate. (ii) Introduction of substituents in the N

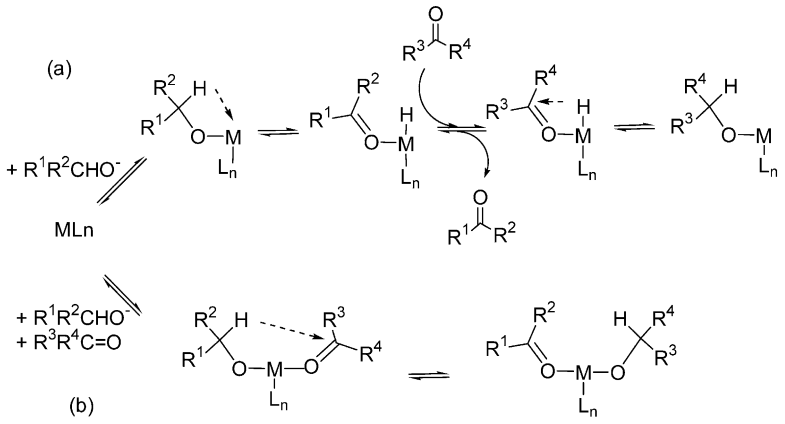

Scheme 23. Proposed mechanism for the hydrogen transfer reaction (a) hydridic route and (b) direct route.

atom (**36a**–**d**, Fig. 3), drastically reduced catalytic activity (20% conversion in 40 h with **36c** and practically no conversion in 40 h with **36d**). (iii) Replacement of the benzyl group of the S atom by a trityl group resulted in a dramatic decrease in activity, while the selectivity was identical in both cases.

Aminothioether ligands derived from (1*R*,2*S*)-norephedrine (**35d**–**f**), (1*R*,2*S*)-ephedrine (**35i**) and (1*R*,2*S*)-2-aminodiphenylethanol (**35g**–**h**) were also tested in Ir(I)-catalyzed asymmetric transfer hydrogenation reactions [139]. Increased activities and enantioselectivities were observed with respect to those obtained with **35a**–**c** in the reduction of acetophenone with formic acid/triethylamine. In the case of norephedrine derivatives, the e.e. increased from 23% (*S*) to 41% (*S*) and to 65% (*S*) on changing the sulphur substituent from phenyl (**35d**) to *iso*-propyl (**35e**) and to benzyl (**35f**), respectively. Using 2-propanol as a hydrogen donor, the e.e. obtained in the presence of ligands **35d**–**i** generally increased. In particular, e.e of 80% (*R*) and 82% (*S*) were obtained with ligands **35h** and **35i**, respectively. The nature of the hydrogen-donor also influenced the product configuration, as exemplified by the case of ligand **35h**, which gave the *S* enantiomer as the major product in the reaction carried out with formic acid/triethylamine. Reduction of ketones other than acetophenone was investigated. Enantioselectivities up to 97% were obtained with ligand **35h** in the reduction of naphtylmethylketone.

In a mechanism proceeding by a hydridic route (Scheme 23a) the enantioselectivities are independent of the H-donor. The fact that in the amino sulphides systems the enantioselectivity was affected by the H-donor suggested that a mechanistic route with direct hydrogen transfer to the substrate could not be excluded.

3.4. Hydrosilylation

The asymmetric catalytic hydrosilylation of ketones or alkenes with organosilanes is a versatile method providing optically active alcohols [140]. Acetophenone (**164**) is a model substrate for this reaction affording 1-phenylethanol after hydrolysis (Scheme 24a). Hydrosilylation of styrene has been also studied, to obtain the same product after oxidation (Scheme 24b).

The chiral crown thioether (+)-(*R*,*R*)-**72** (Fig. 7) was applied in the hydrosilylation of acetophenone to obtain 1-phenylethanol after hydrolysis [89]. The catalyst precursor was prepared in situ from [Rh(μ-Cl)(COD)]$_2$ and (+)-(*R*,*R*)-**72** and provided 35% chemical yield and 57% (*S*) optical yield. In the ruthenium complex **148** (Fig. 49) the chiral macrocyclic ligand generated a helical cavity able to determine the coordination of the substrate. The geometry of this cavity was assumed to be the responsible for the optical discrimination observed in the hydrosilylation. No details concerning the coordination of this ligand in Rh complexes were given.

The hydrosilylation of styrene with the system [Pd(η^3-allyl)(μ-Cl)]$_2$/**38b** (1:4) at 25 °C gave 72% conversion (40

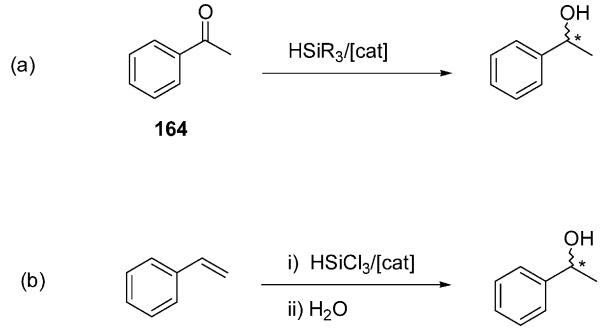

Scheme 24. Hydrosilylation of (a) acetophenone and (b) styrene.

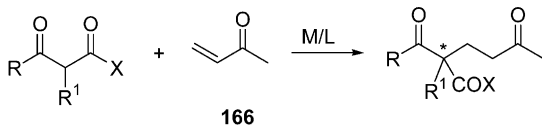

Scheme 25. Michael addition of β-dicarbonyl compounds with **166**.

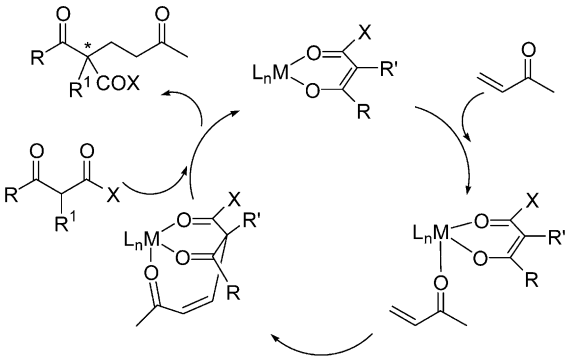

Scheme 26. Proposed mechanism for Michael addition.

h) with high regioselectivity in the branched isomer 1-phenylethanol (91%) and good e.e. (51% (*R*)) [68]. In this case the differences with the methyl derivative (**38a**) were high since this late gave only 41% conversion, 82% regioselectivity in the branched alcohol and negligible e.e. 4% (*S*).

3.5. Michael addition

The Michael reaction of β-dicarbonyl compounds and α,β-unsaturated ketones can be catalyzed by a number of transition metal compounds and lanthanides (Scheme 25) [141]. The selectivity is increased compared to the classic base-catalyzed method due to their neutral reaction conditions avoiding undesired side reactions. Asymmetric version of this reaction has been performed using chiral diol, diamine and diphosphine ligands. In the last years bidentate and polydentate thioethers have started to be considered as chiral ligands for this reaction.

The general mechanism proposed for catalyst precursors containing Ni(II), Cu(II), Co(II), Fe(III) and lanthanides (Scheme 26) begins with the formation of the diketonate, coordination of the enone in a *s-cis* conformation, alkylation of the coordinated 1,3-diketonato and dissociation of the product [141].

Thioether-oxazolines with thiophene or pyridine groups **17a**–**h** (Fig. 2) have been applied in the model metal-catalyzed Michael reaction of ethyl cyclopentanone-2-carboxylate (**165**) with methylvinylketone (**166**) (Scheme 27) [62] with several metal salts MX_n ($CrCl_3 \cdot 6H_2O$, $Mn(OAc)_2 \cdot 4H_2O$, $FeCl_3 \cdot 6H_2O$, $Ni(OAc)_2 \cdot 4H_2O$, $NiCl_2 \cdot 6H_2O$, $Co(OAc)_2 \cdot 4H_2O$, $CoCl_2 \cdot 6H_2O$, $RhCl_3 \cdot 3H_2O$, $Cu(OAc)_2 \cdot H_2O$, AgOAc, $ZnCl_2$). After 16 h of reaction time the Fe(III) and Ni(II) systems

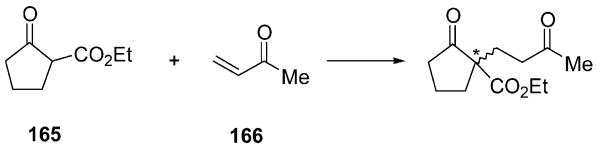

Scheme 27. Michael reaction of **165** with **166**.

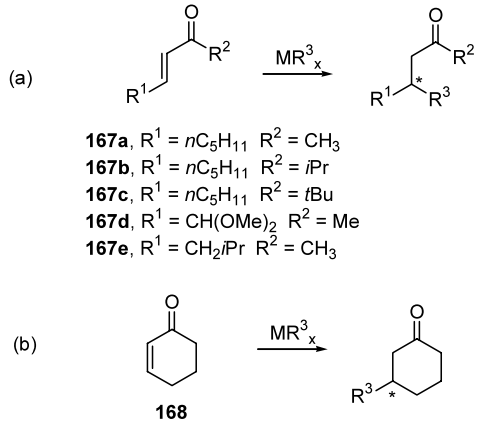

Scheme 28. 1,4-conjugate additions of (a) linear and (b) cyclic alkenes.

turned out to be the most active showing >95% conversion. As for enantioselectivity, e.e.'s different from zero were obtained only with the pyridine ligands; thiophenes did not show any selectivity at all. Best e.e. result (19%) was obtained with **17d** in combination with $Ni(OAc)_2 \cdot 4H_2O$.

Bidentate thioether-hydroxo ligands **66a**–**d** (Fig. 6) and tridentate ether-dithioethers **73a**–**b** (Fig. 7) [142,143] were applied in the Michael addition depicted in Scheme 27. Although several metal salts MX_n (see above) were tested, e.e.'s never exceeded 10%. Slightly better results were obtained using the C_2 symmetric diamino-thioether and diimino-thioether tridentate ligands **74**–**76** (Fig. 7) which were prepared from α-aminoacids [144]. At r.t., conversions after 12 h were > 95% with Fe(III), Ni(II) and Co(II) and the highest e.e. (17%) was obtained using the combination $NiCl_2 \cdot 6H_2O$/**74c**.

3.6. 1,4-Conjugate additions

Enantioselective Cu-catalyzed 1,4-conjugate addition of organometallic reagents to linear or cyclic enones is an interesting procedure for making C–C bonds (Scheme 28) [145]. Organozinc and organoaluminium reagents are frequently used. The accepted mechanism for this reaction involves activation of the enone with the MR_x reagent through the carbonyl (Scheme 29) [146]. Since conformational exchange can take place between the *syn*/*anti s-cis* and *s-trans* forms of the activated enone (Scheme 29), linear enones usually provide lower e.e. than cyclic ones.

The further transition state is formed by interaction of the cuprate $[CuR_2^3]^-$ with the alkene and the organometallic reagent with the ketone (Fig. 52). For this reason heterodonor *hard* (N- or O-)-*soft* (S-) ligands can be efficient systems for this reaction since sulphur can bind the cuprates $[CuR_2]^-$ and the *hard* atom can stabilize interaction with the organometallic reagent [147].

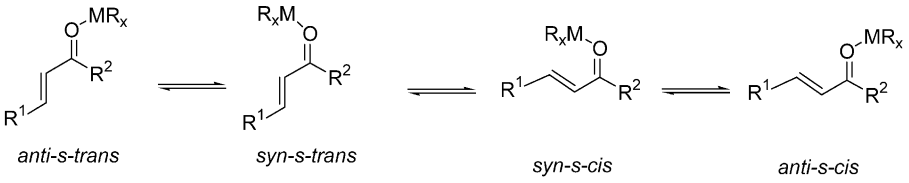

Scheme 29. *syn*/*anti s-cis* and *s-trans* forms of the activated enone.

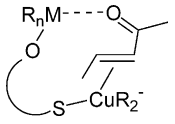

Fig. 52. Transition state for Cu-catalysed conjugate additions.

S,N-donor pyridine-thiazolidinones **25a**–**d** (Fig. 3) were prepared for use in the Cu(I) catalyzed 1,4-conjugate addition of diethylzinc to the model reaction with cyclohexenone (**168**, Scheme 28b) [148]. The catalyst precursor was prepared in situ from CuOTf/**25**. These systems were highly selective in the 1,4-product (>95%) with isolated yields >70% (2–6 h). The e.e. did not depend strongly on the substitution of the pyridine ring (47% (*R*) e.e. with **25a** compared with 39% (*R*) e.e. with **25b**) but were affected for the thiazolidine substituent affording a 62% (*R*) e.e. with the isopropyl substituent **25d**.

Hydroxy thioether ligands **67a**–**b** (Fig. 6) with a binaphthyl chiral structure have been prepared and used in the copper catalyzed conjugate addition to *trans*-3-nonen-2-one (**167a**, Scheme 28a) [149,150]. The catalyst precursor formed by the complex $[Cu(MeCN)_4]BF_4$/(Ra)-**67b** (1/2 ratio) gave good results for conversion and selectivity (88% conversion, 79% selectivity in the 1,4-product and e.e. of 71% (*R*)) using $AlMe_3$. These results improve the enantioselectivity obtained with the analogous hydroxy-thiocarbamate binaphthyl ligand.

Introduction of thioether in the 3,3′-position of the binaphthol structure **68a** (Fig. 6) resulted in a decrease of the enantioselectivity (33% (*R*) e.e.) under the same conditions [149]. The enantioselectivity was further optimized by using $ZnEt_2$. This system afforded the highest value of e.e. obtained with these ligands (77%e.e. (*R*)). Substitution of the methyl substituent by phenyl or ethyl groups provided lower e.e.'s.

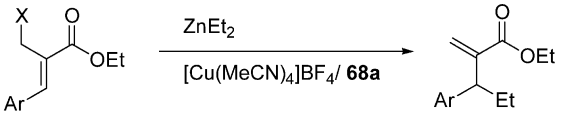

Ar = Ph, 4-$C_6H_4NO_2$, 4-C_6H_4Cl, 4-C_6H_4Me, 1-$C_{10}H_7$
X = Br, Cl, OMs, OCHO

Scheme 30. Conjugate addition of **169**.

The system $[Cu(MeCN)_4]BF_4$/(*Sa*)-**68a** was used to study the 1,4-addition of $ZnEt_2$ in a series of substituted enones **167a**–**d** (Scheme 28a) with the aim of elucidate which of the possible activated enones interacted with the Cu/**68a** catalyst [151]. Increasing the bulkiness of R^1 substituent the enantioselectivity and conversion of the reaction decreased (**167a**:Conv. 85%, e.e. 72%; **167b**:Conv. 61%, e.e. 39%; **167c**:Conv. 0%). Introducing an additional donor atom in the R^1 position of the substrate (**167d**) also decreased activity and enantioselectivity. These results suggested that an *anti-s-cis* species was interacting with catalyst (Scheme 29). The best result of enantioselectivity was obtained with substrate **167e** (79%e.e.)

The $[Cu(MeCN)_4]BF_4$/(*Sa*)-**68a** system was also applied in the addition of $ZnEt_2$ to allylic electrophiles **169** (Scheme 30) [152]. At −20 °C this catalyst system afforded **170** in high chemo and regioselectivity. The highest e.e.'s were obtained with chloride as leaving group with substrate **169** for Ar = 4-$C_6H_4NO_2$ at −40 °C (e.e. 64% (−)).

Hydroxy thioether derivatives **69a**–**d** (Fig. 6) [153] were prepared from xylose. They were used in the catalyzed 1,4-conjugate addition of $ZnEt_2$ to cyclohexenone **168** using CuOTf. The sulphur substituent influenced in the results, since conversions were higher (98%) with the isopropyl derivative and the best enantioselectivity (62% (*S*)) was obtained with the phenyl substituent, while with the bulkiest substituent (**69d**) conversion and enantioselectivity decreased. When these ligands were applied in the 1,4-addition of $AlMe_3$ to **167a** using $[Cu(MeCN)_4]BF_4$, the conversions (up to 73%) and enantioselectivities (up to 34% (*R*) with **69c**) were low. In all the cases the regioselectivity in the 1,4-product ranged from good (70%) to high (>90%).

Asymmetric conjugate additions of dialkylzinc and triethylaluminium reagents onto aryl and alkylidene malonates (Scheme 31) were performed using the ferrocenyl P,N,S-donor ligand **77** (Fig. 7) [154]. The

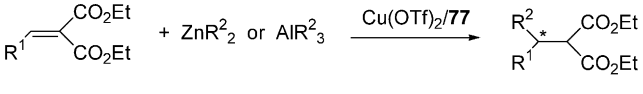

171a, R^1= Me
171b, R^1 = *n*Bu
171c, R^1 = Ph

Scheme 31. Conjugate addition of organozinc and organoaluminium to **171a**–**c**.

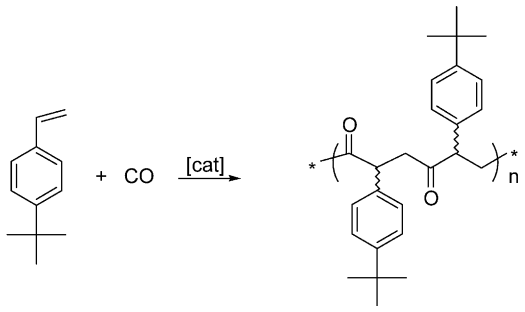

Scheme 32. Copolymerization of CO/*tert*-butylstyrene.

catalyst was prepared in situ by addition of the ligand to a solution of CuOTf. Cu/**77** catalyst was used in the conjugate addition of $ZnEt_2$ to substrate **171b** at 0 °C to afford a total conversion in 3 h (isolate yield 85%) with an e.e. of 57% (*S*). The analogous ferrocenyl ligand without the thioether group gave similar conversion and slightly but significantly lower e.e. (45% (*S*)). No details on the coordination of the ligand were reported.

The five-membered chelating thioether-sulphonamides **36a**–**c** (Fig. 3) were prepared and studied in the 1,4-conjugate addition of diethylzinc to cyclohexenone [155]. The catalyst prepared from CuCN and **36a** gave the highest chemical yield (66%) but did not give any enantioselectivity. Since the analogous sulphonamide without the thioether group is one of the best ligands for this reaction, the participation of sulphur may be the reason for the absence of enantioselectivity.

3.7. Copolymerization

Sulphur-containing ligands have rarely been used in the copolymerization of olefins with carbon monoxide to obtain polyketones (Scheme 32) [156,157].

Dithioether palladium(II) complex [PdMe(MeCN)-(**6b**)]BAr'_4 (**98**, Fig. 18) was used in the alternating CO/*tert*-butylstyrene copolymerization [56]. A productivity of 3.4 g gPd^{-1} h^{-1} ($M_n = 7950$ g mol^{-1}) was obtained which is similar to other chiral ligands for this reaction. The interesting feature of this system is that unlike other bis(thioether) ligands the copolymer has a prevailing isotactic structure probably due to the high rigidity of the catalytic species [156,157].

4. Final remarks and perspectives

Chiral thioethers have been increasingly applied in transition metal-catalyzed homogeneous processes. In recent years, extensive series of chiral thioether containing ligands, both homo (S,S-) and heterodonors (S,X-) have been developed. In many cases, these ligands have been systematically modified in the sulphur substituents, in the backbone and X-donor moiety. Studies on their coordination chemistry have allowed a better understanding of how the stereochemical information is transferred in the enantioselective processes. Remarkable examples of this are the extensive studies in palladium complexes applied in the allylic substitution reaction. Nevertheless, many of the catalyst precursors still lack information about the coordination of these kinds of ligands in the metallic intermediates.

In their application in asymmetric catalysis, thioethers have the disadvantage that they can generate mixtures of diastereomers. Nevertheless, it has been demonstrated that if a suitable sulphur substituent, chelate ring size and adjacent substituents in the backbone are chosen, sulphur inversion and, therefore, the number of diastereomers can be controlled.

For instance, with respect to the homodonor dithioethers, chelate ring size combined with the appropriate substituent at sulphur allows one to obtain good results. The optimum results for hydrogenation and allylic alkylation reactions were with five- or six-membered rings with rather bulky substituents. The enantioselectivities with these ligands have been as high as 68%e.e. in hydrogenation and up to 81% in the model allylic alkylation, even though mixtures of diastereomers were formed in the latter cases.

S,X-heterodonor ligands can provide a variety of electronic and steric properties that are specially suited for allylic substitution reactions in which the enantioselectivity depends on the nucleophilic discrimination of the two terminal allylic carbons. For S,N-donor ligands, the combination of thioether-oxazolines with stereogenic sugar unit at sulphur or with added stereogenic plane have provided excellent levels of chiral induction. Thioether-phosphines or thioether-phosphinites have also been excellent stereo-controllers in this reaction. Binaphthyl or sugar derived backbones in S,O-donor allow one to obtain e.e. of up to 75% in the 1,4-conjugate addition reaction. Lower enantioselectivities (up to 50%) are obtained with thioether-phosphines in hydrosilylation. In the case of the Michael additions the enantioselectivities reported have also been low (ca. 20%).

Some of the possible S,P-donor combinations have not been fully developed. For instance, there are few examples of thioether-phosphites and the modification of the substituents on the phosphorus atom, including stereogenic P-centres, has not been explored.

In summary, chiral thioethers represent a valuable class of ligands to be applied in asymmetric catalysis, also in view of some peculiar properties, which differentiate them from more popular ligands such as those of phosphorus. In particular, the stereoelectronic assistance of organosulphur functionalities and the possibility of stereocontrol through stereogenic sulphur atoms can provide interesting results in many applications.

Acknowledgements

We thank the Generalitat de Catalunya (Departament de Universitats, Recerca i Societat de la Informació, AIRE2000-12) and CONACYT (Ref. 34982) for financial support. Authors thank the referee's for helpful comments

References

[1] S.E. Livingstone, Q. Rev. Chem. Soc. 19 (1965) 386.
[2] S.G. Murray, F.R. Hartley, Chem. Rev. 81 (1981) 365.
[3] H.-B. Kraatz, H. Jacobsen, T. Ziegler, P.M. Boorman, Organometallics 12 (1993) 76.
[4] A.T. Hutton, in: G. Wilkinson (Ed.), Comprehensive Coordination Chemistry, vol. 5, Pergamon Press, New York, 1987, p. 1131 (Chapter 51.8).
[5] A. Müller, E. Diemann, in: G. Wilkinson (Ed.), Comprehensive Coordination Chemistry, vol. 2, Pergamon Press, New York, 1987, p. 551 (Chapter 16.2).
[6] E.W. Abel, S.K. Bhargava, K.G. Orrell, in: S.J. Lippard (Ed.), Progress in Inorganic Chemistry, vol. 32, Wiley, 1984, p. 1.
[7] K.G. Orrell, Coord. Chem. Rev. 96 (1989) 1.
[8] L.H. Pignolet (Ed.), Homogeneous Catalysis with Metal Phosphine Complexes, Plenum Press, New York, 1983.
[9] M.C. Simpson, D.J. Cole-Hamilton, Coord. Chem. Rev. 155 (1996) 163.
[10] B. Cornils, W.A. Herrmann (Eds.), Applied Homogenous Catalysis with Organometallic Compounds, VCH, Weinheim, 1996.
[11] M. Rakowski Dubois, Chem. Rev. 89 (1989) 1.
[12] J.C. Bayón, C. Claver, A.M. Masdeu-Bultó, Coord. Chem. Rev. 193–195 (1999) 73.
[13] K. Boog-Wick, P.S. Pregosin, G. Trabesinger, Organometallics 17 (1998) 3254.
[14] S.-L. You, X.-L. Hou, L.-X. Dai, Y.-H. Yu, W. Xia, J. Org. Chem. 67 (2002) 4684.
[15] D.A. Evans, K.R. Campos, J.R. Tedrow, F.E. Michael, M.R. Gagné, J. Org. Chem. 64 (1999) 2994.
[16] G.J. Dawson, C.G. Frost, C.J. Martin, J.M.J. Williams, S.J. Coote, Tetrahedron Lett. 34 (1993) 7793.
[17] C.G. Frost, J.M.J. Williams, Tetrahedron: Asymmetry 4 (1993) 1785.
[18] C.G. Frost, G. Christopher, J.M.J. Williams, Tetrahedron: Lett. 34 (1993) 2015.
[19] H.B. Kagan, T.P. Dang, J. Am. Chem. Soc. 94 (1972) 6429.
[20] R. Noyori, H. Takaya, Acc. Chem. Res. 23 (1990) 345.
[21] S. Akutagawa, in: A.N. Collins, G.N. Sheldrake, J. Crosby (Eds.), Asymmetric Hydrogenation with Ru-Binap: Chirality in Industry, Wiley, Chichester, 1992, p. 325.
[22] S. Akutagawa, in: M. Scaros, M.L. Prunier (Eds.), Asymmetric Hydrogenation with Ru-BINAP: Catalysis of Organic Reactions, Marcel Dekker, New York, 1994, p. 135.
[23] S. Akutagawa, Appl. Catal. A Gen. 128 (1995) 171.
[24] J. Bakos, I. Tóth, B. Heil, L. Markó, J. Organomet. Chem. 279 (1985) 23.
[25] O. Pàmies, G. Net, A. Ruiz, C. Claver, Eur. J. Inorg. Chem. 6 (2000) 1287.
[26] U. Nagel, E. Kinzel, J. Andrade, G. Prescher, Chem. Ber. 119 (1986) 3326.
[27] M. Diéguez, A. Orejón, A.M. Masdeu-Bultó, R. Echarri, S. Castillón, C. Claver, A. Ruiz, J. Chem. Soc. Dalton Trans. (1997) 4611.
[28] D. Fabbri, G. Delogu, O. De Lucchi, J. Org. Chem. 58 (1993) 1748.
[29] N. Ruiz, A. Aaliti, J. Forniés-Cámer, A. Ruiz, C. Claver, C.J. Cardin, D. Fabbri, S. Gladiali, J. Organomet. Chem. 545 (1997) 79.
[30] L. Flores-Santos, E. Martin, A. Aghmiz, M. Diéguez, C. Claver, A.M. Masdeu-Bultó, M.A. Muñoz-Hernández, to be published.
[31] O. Pàmies, M. Diéguez, G. Net, A. Ruiz, C. Claver, J. Chem. Soc. Dalton Trans. (1999) 3439.
[32] M. Diéguez, A. Ruiz, C. Claver, M.M. Pereira, A.M.d'A. Rocha Gonsalves, J. Chem. Soc. Dalton Trans. (1998) 3517.
[33] L. Flores-Santos, E. Martin, M. Diéguez, A.M. Masdeu-Bultó, C. Claver, Tetrahedron: Asymmetry 12 (2001) 3029.
[34] M. Diéguez, A. Ruiz, A.M. Masdeu-Bultó, C. Claver, J. Chem. Soc. Dalton Trans. (2000) 4154.
[35] S. Gladiali, D. Fabbri, L. Kollàr, C. Claver, N. Ruiz, A. Alvarez-Larena, J.F. Piniella, Eur. J. Inorg. Chem. (1998) 113.
[36] S. Jansat, M. Gómez, G. Muller, M. Diéguez, A. Aghmiz, C. Claver, A.M. Masdeu-Bultó, L. Flores-Santos, E. Martin, M.A. Maestro, J. Mahía, Tetrahedron: Asymmetry 12 (2001) 1469.
[37] B.R. James, R.S. McMillan, Can. J. Chem. 55 (1977) 3927.
[38] A. Orejón, A.M. Masdeu-Bultó, R. Echarri, M. Diéguez, J. Forniés-Cámer, C. Claver, C.J. Cardin, J. Organomet. Chem. 559 (1998) 23.
[39] Notice, that by error, they were labelled as *S,S* in Ref. [38].
[40] E. Martin, B. Toledo, H. Torrens, F.J. Lahoz, P. Terreros, Polyhedron 17 (1998) 4091.
[41] Notice, that by error in the assignation of the configuration of the asymmetric carbon atoms, it was labeled as *anti*-$S_CS_CR_SR_S$ in Ref. [34].
[42] C. Claver, S. Castillón, N. Ruiz, G. Delogu, D. Fabbri, S. Gladiali, J. Chem. Soc. Chem. Commun. (1993) 1833.
[43] A.S.C. Chan, W. Hu, C.C. Pai, C.P. Lau, J. Am. Chem. Soc. 119 (1997) 9570.
[44] T.A. Ayers, T.V. RajanBabu, Process Chem. Pharm. Ind. (1999) 327.
[45] M.T. Reetz, T. Neugebauer, Angew. Chem. Int. Ed. 38 (1999) 179.
[46] M. Diéguez, O. Pàmies, A. Ruiz, S. Castillón, C. Claver, Chem. Eur. J. 7 (2001) 3086.
[47] K. Yonehara, T. Hashizuma, K. Mori, K. Ohe, S. Uemura, Chem. Commun. (1999) 415.
[48] D.S. Clyne, Y.C. Mermet-Bouvier, N. Nomura, T.V. RajanBabu, J. Org. Chem. 64 (1999) 7601.
[49] K. Yonehara, K. Ohe, S. Uemura, J. Org. Chem. 64 (1999) 937.
[50] H. Park, T.V. RajanBabu, J. Am. Chem. Soc. 124 (2002) 734.
[51] O. Pàmies, M. Diéguez, G. Net, A. Ruiz, C. Claver, J. Org. Chem. 66 (2001) 8364.
[52] O. Pàmies, G.P.F. van Strijdonck, M. Diéguez, S. Deerenberg, G. Net, A. Ruiz, C. Claver, P.C.J. Kamer, P.W.N.M. van Leeuwen, J. Org. Chem. 66 (2001) 8867.
[53] M. Diéguez, A. Ruiz, C. Claver, Chem. Commun. (2001) 2702.
[54] M. Diéguez, O. Pàmies, A. Ruiz, C. Claver, New. J. Chem. 26 (2002) 827.
[55] M. Diéguez, A. Ruiz, C. Claver, M.M. Pereira, M.T. Flor, J.C. Bayón, M.E.S. Serra, A.M.d'A. Rocha Gonsalves, Inorg. Chim. Acta 295 (1999) 64.
[56] A. Bastero, C. Claver, A. Ruiz, Catal. Let. 82 (2002) 85.
[57] S. Jansat, M. Gómez, G. Muller, L. Flores-Santos, P.X. García-Reynaldos, E. Martin, A. Aghmiz, M. Giménez, M. Diéguez, C. Claver, A.M. Masdeu-Bultó, M.A. Maestro, J. Mahía, to be published.
[58] A. Pfaltz, Acc. Chem. Res. 26 (1993) 339.
[59] M. Gómez, S. Jansat, G. Muller, M.A. Maestro, J. Mahía, Organometallics 21 (2002) 1077.

[60] M.A. Pericàs, C. Puigjaner, A. Riera, A. Vidal-Ferran, M. Gómez, F. Jimenez, G. Muller, M. Rocamora, Chem. Eur. J. 8 (2002) 4164.
[61] K. Boog-Wick, P.S. Pregosin, M. Wörle, A. Albinati, Helv. Chim. Acta 81 (1998) 1622.
[62] J. Christoffers, A. Mann, J. Pickardt, Tetrahedron 55 (1999) 5377.
[63] N. New, in: T. Hayashi, A. Togni (Eds.), Ferrocenes, VCH, Weinheim, 1995.
[64] C.J. Richards, A.J. Locke, Tetrahedron: Asymmetry 9 (1998) 2377.
[65] A. Togni, Angew. Chem. Int. Ed. Engl. 35 (1996) 1475.
[66] B. Koning, A. Meetsma, R.M. Kellogg, J. Org. Chem. 63 (1998) 5533.
[67] H. Adams, J.C. Anderson, R. Cubbon, D.S. James, J.P. Mathias, J. Org. Chem. 64 (1999) 8256.
[68] S. Gladiali, S. Medici, G. Pirri, S. Pulacchini, D. Fabbri, Can. J. Chem. 79 (2001) 670.
[69] D. Enders, R. Peters, R. Lochtman, G. Raabe, Angew. Chem. Int. Ed. 38 (1999) 2421.
[70] D. Enders, R. Peters, J. Runsink, J.W. Bats, Org. Lett. 1 (1999) 1863.
[71] D. Enders, R. Peters, R. Lochtman, G. Raabe, J. Runsink, J.W. Bats, Eur. J. Org. Chem. (2000) 3399.
[72] A. Albinati, P.S. Pregosin, K. Wick, Organometallics 15 (1996) 2419.
[73] J. Herrmann, P.S. Pregosin, R. Salzmann, A. Albinati, Organometallics 14 (1995) 3311.
[74] A. Albinati, J. Eckert, P.S. Pregosin, H. Rüegger, R. Salzmann, C. Stössel, Organometallics 16 (1997) 579.
[75] P. Barbaro, A. Currao, J. Herrmann, R. Nesper, P.S. Pregosin, R. Salzmann, Organometallics 15 (1996) 1879.
[76] M. Tschoerner, G. Trabesinger, A. Albinati, P.S. Pregosin, Organometallics 16 (1997) 3447.
[77] E. Hauptman, P.J. Fagan, W. Marshall, Organometallics 18 (1999) 2061.
[78] A. Borwitzky, T. Schareina, E. Paetzold, G. Oehme, Phosphorus, Sulfur, Silicon, Relat. Elem. 114 (1996) 115.
[79] X. Verdaguer, A. Moyano, M.A. Pericàs, A. Riera, M.A. Maestro, J. Mahía, J. Am. Chem. Soc. 122 (2000) 10242.
[80] M. Diéguez, A. Ruiz, C. Claver, J. Org. Chem. 67 (2002) 3796.
[81] O. Pàmies, M. Diéguez, G. Net, A. Ruiz, C. Claver, Organometallics 19 (2000) 1488.
[82] M. Valentini, K. Selvakumar, M. Wörle, P.S. Pregosin, J. Organomet. Chem. 587 (1999) 244.
[83] K. Selvakumar, M. Valentini, P.S. Pregosin, Organometallics 18 (1999) 4591.
[84] D.A. Evans, K.R. Campos, J.R. Tedrow, F.E. Michael, M.R. Gagné, J. Am. Chem. Soc. 122 (2000) 7905.
[85] E. Hauptman, R. Shapiro, W. Marshall, Organometallics 17 (1998) 4976.
[86] P.-H. Leung, S.-K. Loh, K.F. Mok, A.J.P. White, D.J. Williams, J. Chem. Soc. Dalton Trans. (1996) 4443.
[87] P. Barbaro, C. Bianchini, A. Togni, Organometallics 16 (1997) 3004.
[88] J.W. Faller, N. Zhang, K.J. Chase, W.K. Musker, A.R. Amaro, C.M. Semko, J. Organomet. Chem. 468 (1994) 175.
[89] T. Ueda, T. Adachi, K. Sumiya, T. Yoshida, J. Chem. Soc. Chem. Commun. (1995) 935.
[90] A.A.H. van der Zeijden, J. Jimenez, C. Mattheis, C. Wagner, K. Merzweiler, Eur. J. Inorg. Chem. (1999) 1919.
[91] X. Verdaguer, J. Vázquez, G. Fuster, V. Bernardes-Génisson, A.E. Greene, A. Moyano, M.A. Pericàs, A. Riera, J. Org. Chem. 63 (1998) 7037.
[92] A. Pfaltz, M. Lautens, in: E.N. Jacobsen, A. Pfaltz, H. Yamamoto (Eds.), Comprehensive Asymmetric Catalysis, vol. 2, Springer, Berlin, 1999, pp. 833–884.
[93] H. Steinhagen, M. Reggelin, G. Helmchen, Angew. Chem. Int. Ed. Engl. 36 (1997) 2108.
[94] B.M. Trost, D.L. van Vranken, Chem. Rev. 96 (1996) 395.
[95] A.K. Ghosh, P. Mathivanan, J. Cappiello, Tetrahedron: Asymmetry 9 (1998) 1.
[96] P. Braunstein, F. Naud, Angew. Chem. Int. Ed. 40 (2001) 680.
[97] G. Helmchen, A. Pfaltz, Acc. Chem. Res. 33 (2000) 336.
[98] M. Peer, J.C. de Jong, M. Kiefer, T. Langer, H. Rieck, H. Schell, P. Sennhennm, J. Sprinz, H. Steinhagen, B. Wiese, G. Helmchen, Tetrahedron 52 (1996) 7547.
[99] S.-L. Ypu, X.-L. Hou, L.-X. Dai, Tetrahedron: Asymmetry 11 (2000) 1495.
[100] X.-L. Hou, X.-W. Wu, L.-X. Dai, B.-X. Cao, J. Sun, Chem. Commun. (2000) 1195.
[101] K. Hiroi, Y. Suzuki, I. Abe, Tetrahedron: Asymmetry 10 (1999) 1173.
[102] T. Hayashi, M. Kawatsura, Y. Uozumi, J. Am. Chem. Soc. 120 (1998) 1681.
[103] L. Acemoglu, J.M.J. Williams, Adv. Synth. Catal. 343 (2001) 75.
[104] M. Cavazzini, G. Pozzi, S. Quici, D. Maillard, D. Sinou, Chem. Commun. (2001) 1220.
[105] Y. Hamada, K. Sakaguchi, K. Hatano, O. Hara, Tetrahedron Lett. 42 (2001) 1297.
[106] K. Fuji, H. Ohnishi, S. Moriyama, K. Tanaka, T. Kawabata, K. Tsubaki, Synlett (2000) 351.
[107] R. Takeuchi, M. Kashio, J. Am. Chem. Soc. 120 (1998) 8647.
[108] B.M. Trost, K. Dogra, I. Hachiya, T. Emura, D.L. Hughes, S. Krska, R.A. Reamer, M. Palucki, N. Yasuda, P.J. Reider, Angew. Chem. Int. Ed. 41 (2002) 1929.
[109] B.M. Trost, P.L. Fraisse, Z.T. Ball, Angew. Chem. Int. Ed. 41 (2002) 1059.
[110] B. Bartels, G. Helmchen, Chem. Commun. (1999) 741.
[111] G.C. Fu, Acc. Chem. Res. 33 (2000) 412.
[112] Y. Donde, L.E. Overman, J. Am. Chem. Soc. 121 (1999) 2933.
[113] A. Chesney, M.R. Bryce, R.W.J. Chubb, A.S. Batsanov, J.A. Howard, Tetrahedron: Asymmetry 8 (1997) 2337.
[114] S.-L. You, Y.-G. Zhou, X.-L. Hou, L.-X. Dai, Chem. Commun. (1998) 2765.
[115] J. Park, Z. Quan, S. Lee, K.H. Ahn, C.-W. Cho, J. Organomet. Chem. 584 (1999) 140.
[116] Y. Imai, W. Zhang, T. Kida, Y. Nakatsuji, I. Ikeda, Synlett (1999) 1319.
[117] G. Chelucci, M.A. Cabras, Tetrahedron: Asymmetry 7 (1996) 965.
[118] G. Chelucci, N. Culeddu, A. Saba, R. Valenti, Tetrahedron: Asymmetry 10 (1999) 3537.
[119] G. Chelucci, A. Bacchi, D. Fabbri, A. Saba, F. Ulgheri, Tetrahedron Lett. 40 (1999) 553.
[120] J.C. Anderson, D.S. James, J.P. Mathias, Tetrahedron: Asymmetry 9 (1998) 753.
[121] G.A. Rassias, P.C. Bulman Page, S. Reignier, S.D.R. Christie, Synlett (2000) 379.
[122] K. Hiroi, Y. Suzuki, I. Abe, Chem. Lett. (1999) 149.
[123] H. Nakano, Y. Okuyama, M. Yanagida, H. Hongo, J. Org. Chem. 66 (2001) 620.
[124] R.J. Gillespie, J.N. Spencer, R.S. Mogg, J. Chem. Educ. 73 (1996) 622.
[125] P. Barbaro, P.S. Pregosin, R. Salzmann, A. Albinati, R. Kunz, Organometallics 14 (1995) 5160.
[126] P.S. Pregosin, R. Salzmann, A. Togni, Organometallics 14 (1995) 842.
[127] T.G. Appleton, H.C. Clark, L.E. Manzer, Coord. Chem. Rev. 10 (1973) 355.
[128] B.M. Trost, R.C. Bunt, J. Am. Chem. Soc. 116 (1994) 4089.
[129] R. Noyori, Asymmetric Catalysis in Organic Synthesis, Wiley, New York, 1994.

[130] I. Ojima (Ed.), Catalytic Asymmetric Synthesis, Wiley, New York, 2000.
[131] E.N. Jacobsen, A. Pfaltz, H.H. Yamamoto (Eds.), Comprehensive Asymmetric Catalysis, vol. 1, Springer, Berlin, 1999, pp. 121–247.
[132] W. Li, J.P. Waldkirch, X. Zhang, J. Org. Chem. 67 (2002) 7618.
[133] A. Togni, C. Breutel, A. Schayder, F. Spindler, H. Landert, A. Tijani, J. Am. Chem. Soc. 116 (1994) 4062.
[134] O. Pàmies, J.-E. Bäckvall, Chem. Eur. J. 7 (2001) 5052.
[135] G. Zassinovich, G. Mestroni, S. Gladiali, Chem. Rev. 92 (1992) 1051.
[136] K.-J. Haack, S. Hashiguchi, A. Fujii, T. Ikariya, R. Noyori, Angew. Chem. Int. Ed. Engl. 36 (1997) 285.
[137] M. Bernard, V. Guiral, F. Delbecq, F. Fache, P. Sautet, M. Lemaire, J. Am. Chem. Soc. 120 (1998) 1441.
[138] S. Gladiali, A. Dore, D. Fabri, Tetrahedron: Asymmetry 5 (1994) 1143.
[139] D.G.I. Petra, P.C.J. Kamer, A.L. Spek, H.E. Schoemaker, P.W.N.M. van Leeuwen, J. Org. Chem. 65 (2000) 3010.
[140] H. Nishiyama, in: E.N. Jacobsen, A. Pfaltz, H. Yamamoto (Eds.), Comprehensive Asymmetric Catalysis, vol. 1, Springer, Berlin, 1999, pp. 267–289.
[141] J. Christoffers, Eur. J. Org. Chem. (1998) 1259.
[142] J. Christoffers, U. Rößler, Tetrahedron: Asymmetry 10 (1999) 1207.
[143] J. Christoffers, U. Rößler, Tetrahedron: Asymmetry 9 (1998) 2349.
[144] J. Christoffers, A. Mann, Eur. J. Org. Chem. (1999) 1475.
[145] P. Perlmutter, Conjugate Addition Reactions in Organic Synthesis, Pergamon, Oxford, 1992.
[146] S. Woodward, Chem. Soc. Rev. 29 (2000) 393.
[147] S. Woodward, Tetrahedron 58 (2002) 1017.
[148] A.H.M. de Vries, R.P. Hof, D. Staal, R.M. Kellogg, B.L. Feringa, Tetrahedron: Asymmetry 8 (1997) 1539.
[149] S.M.W. Bennett, S.M. Brown, A. Cunningham, M.R. Dennis, J.P. Muxworthy, M.A. Oakley, S. Woodward, Tetrahedron 56 (2000) 2847.
[150] C. Börner, M.R. Dennis, E. Sinn, S. Woodward, Eur. J. Org. Chem. (2001) 2435.
[151] C. Börner, W.A. König, S. Woodward, Tetrahedron Lett. 42 (2001) 327.
[152] C. Börner, J. Gimeno, S. Gladiali, P.J. Goldsmith, D. Ramazzotti, S. Woodward, Chem. Commun. (2000) 2433.
[153] O. Pàmies, G. Net, A. Ruiz, C. Claver, S. Woodward, Tetrahedron: Asymmetry 11 (2000) 871.
[154] A. Alexakis, C. Benhaim, Tetrahedron: Asymmetry 12 (2001) 1151.
[155] J.C. Anderson, R. Cubbon, M. Harding, D.S. James, Tetrahedron: Asymmetry 9 (1998) 3461.
[156] E. Drent, P.H.M. Budzelaar, Chem. Rev. 96 (1996) 663.
[157] (a) J.A. van Doorn, E. Drent, Eur. Pat. Appl. 345 (1989) 847; (b) J.A. van Doorn, E. Drent, Chem. Abst. 112 (1990) 3009.
[158] B.M. Trost, D.J. Murphy, Organometallics 4 (1985) 1143.
[159] P.S. Pregosin, H. Rüegger, R. Salzmann, A. Albinati, F. Lianza, R.W. Kunz, Organometallics 13 (1994) 83.